

University of Louisville

ThinkIR: The University of Louisville's Institutional Repository

Electronic Theses and Dissertations

1-2022

Lysosomal evasion of legionella pneumophila the effector.

Bethany Vaughn
University of Louisville

Follow this and additional works at: <https://ir.library.louisville.edu/etd>



Part of the [Pathogenic Microbiology Commons](#)

Recommended Citation

Vaughn, Bethany, "Lysosomal evasion of legionella pneumophila the effector." (2022). *Electronic Theses and Dissertations*. Paper 3833.

<https://doi.org/10.18297/etd/3833>

This Doctoral Dissertation is brought to you for free and open access by ThinkIR: The University of Louisville's Institutional Repository. It has been accepted for inclusion in Electronic Theses and Dissertations by an authorized administrator of ThinkIR: The University of Louisville's Institutional Repository. This title appears here courtesy of the author, who has retained all other copyrights. For more information, please contact thinkir@louisville.edu.

LYSOSOMAL EVASION OF *LEGIONELLA PNEUMOPHILIA* BY THE EFFECTOR

MAVE

By

Bethany Vaughn
B.A., Thomas More College, 2011
HTL, American Society for Clinical Pathology, 2016
M.S., University of Louisville, 2018

A Dissertation
Submitted to the Faculty of the
School of Medicine of the University of Louisville
In Partial Fulfillment of the Requirements
For the Degree of

Doctor of Philosophy
In Microbiology and Immunology

Department of Microbiology and Immunology
University of Louisville
Louisville, Kentucky

May 2022

Copyright 2022 by Bethany Vaughn

All rights reserved

LYSOSOMAL EVASION OF *LEGIONELLA PNEUMOPHILIA* BY THE EFFECTOR

MAVE

By

Bethany Vaughn
B.A., Thomas More College, 2011
HTL, American Society for Clinical Pathology, 2016
M.S., University of Louisville, 2018

A Dissertation Approved on

April 22, 2022

By the following Dissertation Committee:

Dissertation Director, Dr. Yousef Abu Kwaik

Dr. Matthew Lawrenz

Dr. Kevin Sokoloski

Dr. Richard Lamont

Dr. Silvia Uriarte

Dr. Brian Ceresa

DEDICATION

This dissertation is dedicated to my parents, who have always been supportive and encouraging, and to my children, Joey, Jack, and Amelia, for always keeping me on my toes and who I am so very proud of.

ACKNOWLEDGMENTS

I would first like to thank my mentor, Dr. Yousef Abu Kwaik, for taking a chance and letting me join the microbiology program through your lab. I would also like to thank my committee members: Dr. Matthew Lawrenz, Dr. Kevin Sokoloski, Dr. Richard Lamont, Dr. Silvia Uriarte, and Dr. Brian Ceresa. Your insight, guidance, and encouragement are very appreciated, and I cannot thank you enough.

I would like to thank my fellow Abu Kwaik lab members of past and present, particularly Dr. Chris Price, Snake Jones, and Dr. Juanita Von Dwingelo, I would have never made it this far without your help, your ability to put up with my loud personality, or your expertise. To Hannah Hanford, I am glad you joined our lab, for always making me laugh either with you or at you haha, and for being my ear; and (Peter) Cheon Jee Shin, your addition to our lab has definitely “rounded” us out, mainly because you have my same personality, so we keep Hannah and Chris in check haha. I am grateful to call you all my friends.

I would like to thank Dr. Robin Bideau for encouraging me to further my education and buying all my course textbooks. I really appreciate the conversations we have shared and your generosity. To Dr. Matthew Thompson, thank you for giving me the opportunity to delve into the world of placentas and for listening to me ramble on about my research. I would also like to thank Shanna Brotzge Pollock for making me take that first step to joining the program, who knows how long I would have put it off.

ABSTRACT

LYSOSOMAL EVASION OF *LEGIONELLA PNEUMOPHILA* BY THE EFFECTOR MAVE

Bethany Vaughn

April 22, 2022

Legionella pneumophila is a Gram-negative facultative intracellular bacterium found in freshwater environments that has co-evolved to survive and proliferate in various amoeba and protozoan species, which serve as the natural host for the bacterium. Humans are an accidental host of *L. pneumophila*, where infection occurs upon inhalation of aerosolized water droplets that contain the bacteria. Intracellular proliferation of *L. pneumophila* in alveolar macrophages is essential for manifestation of pneumonia, designated as Legionnaires' Disease. Biogenesis of the legionella containing vacuole (LCV) occurs via interception of ER-Golgi vesicle trafficking and avoids the default endosomal/lysosomal degradation pathway. Intracellular proliferation of *L. pneumophila* within protozoa and macrophages is dependent on the Dot/Icm type IV secretion system (T4SS) apparatus, which is comprised of 27 proteins and is responsible for translocating over 350 different effector proteins into the host cell. Many of these effector proteins contain eukaryotic-like domains and motifs, which have been acquired through interkingdom horizontal gene transfer from various aquatic eukaryotic hosts. While *L. pneumophila* contains the largest repertoire of effector proteins, known for an intracellular pathogen, most of which are not required for survival and proliferation in mammalian macrophages. It is more likely that the large repertoire of effector proteins constitutes a toolbox utilized by *L. pneumophila* to survive and replicate within various protozoan species. The diversion of the *L. pneumophila*-containing

vacuole (LCV) from the host endosomal-lysosomal degradation pathway is one of the main virulence features essential for disease manifestation. Many of the ~350 Dot/Icm-injected effectors identified in *L. pneumophila* have been shown to interfere with various host pathways and processes; but no *L. pneumophila* effector has ever been identified to be indispensable for lysosomal evasion.

While most effector mutants of *L. pneumophila* do not exhibit a defective phenotype within macrophages, we show that the MavE effector is essential for intracellular growth of *L. pneumophila* in human monocyte-derived macrophages (hMDMs), amoebae and for intrapulmonary proliferation in mice. This is shown by both single cell analysis during confocal microscopy and by quantifying colony forming units (CFUs). We have shown the *mavE* null mutant fails to remodel the LCV with ER-derived vesicles and is trafficked to the lysosomes where it is degraded, similar to formalin-killed bacteria. Importantly, during infection of hMDMs, the MavE effector localizes to the poles of the LCV membrane.

The crystal structure of MavE (39-172) was resolved to 1.8 Å, revealing a eukaryotic NPxY motif that binds with phosphotyrosine-binding domains present on signaling and adaptor eukaryotic proteins. We show that point mutations within the NPxY motif results in attenuation of *L. pneumophila* in both hMDMs and amoeba, and the substitution defects of P⁷⁸ and D⁶⁴ results in fusion of the LCV to the lysosomes, with no remodeling by the ER, leading to bacterial degradation.

Following ectopic expression of MavE, a proximity-dependent biotin identification (BioID) strategy was used to screen for MavE-interacting proteins in mammalian cells. These data show that MavE interacts with a host protein, acyl-CoA binding domain containing 3 (ACBD3), which co-localizes with the LCV. ACBD3 plays an essential role in the sorting and

modification of proteins exported from the endoplasmic reticulum through its interaction with the integral membrane protein giantin. We have shown the *mavE* null mutant-containing LCV fails to colocalize with ACBD3, similar to the Dot/Icm translocation-defective mutant. There are areas of homology of ACBD3 with proteins found in Amoebozoa, indicative of a possible conserved binding motif. We conclude that the MavE effector of *L. pneumophila* is indispensable for phagosome biogenesis and lysosomal evasion by interacting with the host protein ACBD3, which is involved in ER-Golgi vesicle trafficking and is likely conserved throughout evolution.

TABLE OF CONTENTS

| | |
|---|----|
| ACKNOWLEDGMENTS | iv |
| ABSTRACT..... | v |
| LIST OF FIGURES | xi |
| CHAPTER 1: | 1 |
| INTRODUCTION..... | 2 |
| Discovery of Legionnaires' Disease and Etiological Aspects | 2 |
| Clinical Manifestations of <i>L. pneumophila</i> | 3 |
| Epidemiology of <i>L. pneumophila</i> | 6 |
| Molecular Ecology of <i>L. pneumophila</i> and its Intracellular Lifecycle within Protozoa . | 8 |
| Intracellular Lifecycle of <i>L.pneumophila</i> within Macrophages | 10 |
| The Type II Secretion System (T2SS) | 11 |
| The Dot/Icm Type IV Secretion System (T4SS) | 15 |
| Core Effectors of <i>L. pneumophila</i> | 20 |
| Evolution and Phylogeny of Legionellae | 20 |
| Effectors Involved in Vacuolar Biogenesis..... | 22 |
| SPECIFIC AIMS | 26 |
| CHAPTER 2: | 29 |
| AN INDISPENSABLE ROLE FOR THE MAVE EFFECTOR OF <i>LEGIONELLA</i> <i>PNEUMOPHILA</i> IN LYSOSOMAL EVASION | 29 |
| Summary | 30 |
| Importance..... | 31 |

| | |
|--|----|
| Introduction..... | 32 |
| Results | 35 |
| Subcellular Localization of MavE..... | 35 |
| The role of MavE in intracellular replication | 39 |
| Role of MavE in ER-mediated remodeling and lysosomal evasion by the LCV | 44 |
| Crystal Structure of MavE..... | 47 |
| Structure-based Functional Analysis of MavE..... | 50 |
| Discussion | 58 |
| Materials and Methods | 63 |
| Bacterial strains and cell lines | 63 |
| DNA manipulations..... | 65 |
| Intracellular replication in hMDMs and Amoeba..... | 65 |
| Transfection of HEK293T cells (ATCC) | 66 |
| Mouse Model..... | 66 |
| Confocal microscopy..... | 67 |
| Cloning of recombinant MavE | 69 |
| Protein Expression and Purification | 70 |
| Crystallization..... | 71 |
| Data Collection and Structure Solution..... | 71 |
| Statistical analysis..... | 72 |
| CHAPTER 3: | 73 |
| MAVE INTERACTION WITH HOST PROTEIN ACBD3 | 73 |
| Introduction | 74 |
| Results | 76 |
| Identification of the MavE-interacting Host Proteins..... | 76 |
| Co-localization of ACBD3 with the <i>Legionella</i> containing vacuole in hMDMs | 80 |
| ACBD3 gene silencing in HEK293T and hMDMs | 80 |
| Co-localization of ACBD3 during siRNA knockdown | 83 |
| Role of MavE on intracellular replication of <i>L. pneumophila</i> in HEK293T cells..... | 86 |
| Discussion | 87 |
| Materials and Methods | 91 |

| | |
|---|-----|
| Cell lines | 91 |
| To identify the Protein:Protein interactions of the MavE protein | 91 |
| Streptavidin-Biotinylated protein purification..... | 92 |
| Identification of MavE Interactions by Mass Spectrometry..... | 93 |
| Cleanup with C18 PROTO™, 300Å Ultra MicroSpin Column | 93 |
| Liquid Chromatography | 94 |
| Data Acquisition | 95 |
| Data Analysis with Proteome Discover v2.4.0.305 and Scaffold Q+S v5.1.0 | 95 |
| Transfection of HEK293T cells (ATCC) | 96 |
| Antibodies and western blot analysis | 96 |
| Intracellular replication in HEK293T..... | 97 |
| RNAi Knockdown | 98 |
| Confocal microscopy..... | 99 |
| Statistical analysis..... | 100 |
| CHAPTER 4: | 101 |
| CONCLUSIONS AND FUTURE DIRECTIONS..... | 101 |
| REFERENCES | 102 |
| CURRICULUM VITAE..... | 132 |

LIST OF FIGURES

| | |
|---|----|
| Figure 1-1: Architectural model of the T2SS | 14 |
| Figure 1-2: Schematic of the periplasmic portion of the <i>Legionella</i> Dot/Icm Type IV secretion system | 19 |
| Figure 1-3: Model for the regulation of Rab1 activity by <i>Legionella</i> proteins..... | 25 |
| Figure 1-4: A working model of the response of hMDMs to <i>L. pneumophila</i> infection.. | 28 |
| Figure 2-1: Localization of MavE during ectopic expression and during infection of hMDMs | 37 |
| Figure 2-2: Localization of MavE during infection of hMDMs without digitonin | 38 |
| Figure 2-3: Growth of substitution mutants <i>in vitro</i> and expression and stability of the variant MavE proteins | 40 |
| Figure 2-4: MavE is essential for intracellular replication in hMDMs and <i>A. polyphaga</i> | 41 |
| Figure 2-5: The MavE effector is essential for intrapulmonary replication <i>in vivo</i> | 43 |
| Figure 2-6: Fusion of the vacuoles containing the <i>mavE</i> mutant with the lysosome | 45 |
| Figure 2-7: An essential role for MavE in bacterial viability within the LCVs of hMDMs | 46 |
| Figure 2-8: Crystal structure of MavE (39-172) | 49 |
| Figure 2-9: The role of the NPxY motif in biological function of MavE in hMDMs and <i>A. polyphaga</i> | 51 |
| Figure 2-10: The role of the NPxY motif in biological function of MavE in hMDMs and <i>A. polyphaga</i> | 52 |
| Figure 2-11: Remodeling of the vacuoles with the ER..... | 55 |
| Figure 2-12: Fusion of the vacuoles containing the <i>mavE</i> substitution mutants with the late endosomes/lysosomes..... | 56 |
| Figure 2-13: Fusion of the vacuoles containing the <i>mavE</i> substitution mutants with the lysosomes | 57 |

| | |
|--|----|
| Figure 3-1: MavE interacts with host protein ACBD3 | 79 |
| Figure 3-2: MavE interacts with host protein ACBD3 during ectopic expression | 79 |
| Figure 3-3: Localization of ACBD3 to the LCV during infection of hMDMs..... | 81 |
| Figure 3-4: Western Blot Analysis of Silencing of host protein ACBD3 in hMDMs..... | 82 |
| Figure 3-5: Silencing of host protein ACBD3 in HEK293T cells | 82 |
| Figure 3-6: Localization of ACBD3 to the LCV during infection of HEK293T cells 1- hour post infection..... | 84 |
| Figure 3-7: Localization of ACBD3 to the LCV during infection of HEK293T cells 10- hours post infection | 85 |
| Figure 3-8: The <i>mavE</i> mutant is not attenuated within HEK293T cells..... | 86 |
| Figure 3-9: Working model of MavE-ACBD3 interaction in macrophages..... | 90 |

CHAPTER 1:
INTRODUCTION

INTRODUCTION

Discovery of Legionnaires' Disease and Etiological Aspects

In the summer of 1976, approximately 4,000 American Legion delegates attended the 58th annual American Legion Convention in Philadelphia, Pennsylvania. Within 2 weeks of the convention, 180 attendees suffered from pneumonia-like symptoms of which 29 had succumbed to the atypical pneumonia. Most of the victims had visited the Bellevue Stratford, a grand hotel on Broad Street that had hosted the convention on July 21–24. However, a bus driver and several pedestrians passing by the hotel were part of the same outbreak. Nicknamed the “Philly Killer,” a total of 34 persons were confirmed to have died from the illness and a total of 221 had become ill [1, 2].

Initially, a physician in Philadelphia telephoned the Centers for Disease Control and Prevention (CDC), fearing that this disease was caused by a new strain of influenza identified just 6 months prior. However, within days of arriving at the Bellevue hotel, the CDC ruled out influenza as the causative agent. The investigation of the unidentified infectious agent lasted close to six months and was worked on by multiple teams of parasitologists, virologists, epidemiologists, bacteriologists, and toxicologists. In January 1977, the causative agent was identified by Joseph McDade while examining smears of liver sections from guinea pigs inoculated with lung tissue from Legionnaires' patients. McDade noticed occasional clusters of peculiar rod-shaped bacteria; these were called Legionnaires' Disease bacterium until April 1979. Then the bacteria were given the name, *Legionella pneumophila* representing the disease caused as well as those who were affected by the first documented outbreak, the attendees of the American Legion Convention [2-4]. It was later suspected that the Stratford hotel air conditioning was

contaminated with *Legionella pneumophila* as the specific source for the 1976 outbreak, however, environmental tests for *Legionella* were not yet developed, so the exact source remains unknown [5].

L. pneumophila is a global pathogen and existed prior to the 1976 outbreak. The number of cases has been on the rise since early 2000's with nearly 10,000 cases of Legionnaires' disease reported in the United States alone in 2018 [6]. Bacteria of the genus *Legionella* comprises 65 species with the primary causative agent of Legionnaires' disease being *L. pneumophila*. However, largely reported cases of disease in Australia and New Zealand are attributable to *Legionella longbeachae* [7]. The species *L. pneumophila* can be subdivided into 16 serogroups and confirmed human infection is caused primarily by serogroup 1 but infections with other serogroups, including 3, 4, and 6 have been reported [7-11]. Serogroup 1 is the most virulent strain causing 80-90% of laboratory confirmed legionellosis cases [12]. Legionellosis occurs most commonly when bacilli from the genus *Legionella* is present in a contaminated water source is aerosolized and inhaled [13]. Such contaminated water sources include but are not limited to air conditioning cooling towers, grocery misters, decorative fountains, and hot tubs.

Clinical Manifestations of *L. pneumophila*

Once *Legionella* reaches the lung, clinical presentation of the infection results in two distinct disorders, Legionnaires' disease or Pontiac Fever [13]. Legionnaires' disease is a severe, often fatal pneumonia associated with fever, chills, cough, lethargy, headache, muscle aches, sometimes with extrapulmonary manifestations such as renal

failure, encephalopathy, and pericarditis. [13]. Pontiac Fever, named after the 1968 outbreak in Pontiac, Michigan, is a febrile flu-like illness which usually resolves in 2 to 5 days with no pneumonia or mortality and does not benefit from any treatment with antibiotics [13]. Both Pontiac fever and the more severe Legionnaire's disease may be caused by the same bacteria and serogroups, but Pontiac fever resembles acute influenza with no pneumonia [14, 15]. Why Pontiac fever has less severe manifestations than Legionnaires' disease is not yet understood.

Legionnaires' disease can be very serious with a 10-15% mortality rate and can reach as much as 25-50% in immunocompromised and immunosuppressed patients [16]. Older people, immune compromised individuals, smokers, and people with underlying lung disease are more susceptible to Legionnaires' disease. While healthy individuals are also at risk for contracting the disease, they might not have any symptoms or only experience a mild illness [13, 16-18]. Community-acquired pneumonia (CAP) is an acute infection of the pulmonary parenchyma that develops in persons outside of a hospital/healthcare facility [19]. CAP is the leading cause of morbidity and mortality in high- and low-income countries [20]. Recently, studies have identified *Legionella* species as being among the top 3 microbial causes of hospitalization due to CAP [21]. However, the exact incidence of Legionnaires' disease is unknown due to the difference in surveillance, reporting, and diagnostic methods [20, 21]. In more than 50% of cases of pneumonia, the causative organism is not known [22].

Symptoms of Legionnaires' disease usually appear within 2 to 10 days after exposure, with an average of onset 5 to 6 days after exposure [23]. Symptoms usually appear much sooner for Pontiac fever, appearing in just 5 to 72 hours [24]. Patients with

a more severe form of the disease may show gastrointestinal symptoms including diarrhea, bloody sputum, vomiting, and abdominal pain [25-27]. Patients that succumb to the disease generally die as result of multi organ failure or respiratory shock [28]. No vaccines exist to protect from Legionnaires' disease, but instead can be treated with recommended classes of antibiotics including fluoroquinolones, macrolides, and rifampin [29-31]. However, macrolides are not recommended to treat immunocompromised patients as they can interfere with immunosuppressant agents. Also, treatment with penicillin and β -lactams is not recommended due to *L. pneumophila* being resistant to these antibiotics [32-34].

Legionnaires' disease is substantially underdiagnosed and under-reported in many countries because of a lack of diagnostics and surveillance systems [35-37]. Data from the USA indicated a 249% increase in estimated national incidence of Legionnaires' disease from 2000 to 2011 [25, 38]. The yearly incidence of Legionnaires' disease seems to be associated with climate changes and subject to seasonal variations with humidity and rainfall resulting in increased aerosol transmission, with 62% of cases occurring during summer and early autumn [39, 40]. Often when patients present with pneumonia, antibiotics are used, and no lab diagnostic tests are performed to determine the causative agent of the pneumonia. However, the German Competence Network for Community-Acquired Pneumonia has set out to standardize microbiology protocols for extensive testing to diagnose *Legionella* pneumonia [41]. The study reported a prevalence of 180-360 cases per million inhabitants and extrapolating this data to the numbers reported in the USA, cases of Legionnaires' disease reported to the CDC most likely represent less than 5% of actual cases [41]. Highly sensitive urine-ELISA assays are commonly being

used to detect all *Legionella* species, yielding isolates for additional characterization [42-44]. However, only sequence-based schemes have the necessary resolution to speciate or recognize potentially novel strains of *Legionella* [45]. Without consistent patient testing that is subject to skill, experience, and procedural rigor of the laboratory, it is difficult to confirm the number of Legionnaires' disease cases annually. Importantly, proper diagnosis is needed for treatment worldwide and the rates reported likely underestimate the actual disease burden of legionellosis.

Epidemiology of *L. pneumophila*

Outbreaks of *L. pneumophila* first emerged in the 20th century as a result of human alterations to the environment such as cooling towers or plumbing in large buildings [10]. *L. pneumophila* are an important public health problem as they are ubiquitous in globally distributed aquatic habitats and water distribution systems. Legionellae would be an extremely rare cause of human disease if left in their natural state, however inhalation of contaminated aerosolized water droplets often are traced to human-made aquatic environments [10, 46-49]. A single exception to this is *Legionella longbeachae*, a frequent isolate from potting soil [10, 50]. While *L. pneumophila* is typically an environmental pathogen, person-to-person transmission does not occur in most cases with the exception of one rare, reported case in 2014 [51]. The very close contact that occurred between patient 0 (a smoker that had worked at an industrial cooling tower complex) and patient 1 (an elderly woman that cared for patient 0 in a nonventilated room before being transported to the hospital) most likely attributed to the transmission [51-53].

Members of the *Legionella* species have been detected by Polymerase Chain Reaction (PCR) in up to 80% of freshwater environments worldwide and has become the most identified drinking water pathogen [10, 54]. Species of *Legionella* are ubiquitous to many freshwater environments and man-made water systems around the world. *L. pneumophila* multiplies at temperatures between 25-42°C, and thermally altered aquatic environments can result in rapid multiplication of the bacteria [55]. *L. pneumophila* can be controlled in water handling systems with proper maintenance, however some municipal drinking water systems have summertime water temperatures that favor *Legionella* growth [50]. For eradication, continual water treatment is required, although monitoring for *Legionella* in potable water systems is not required by any state or federal regulations [50]. Control measures to prevent bacterial intrusion, growth, and transmission include monitoring temperature, maintaining hot water tanks at temperatures above 60°C, disinfecting with either monochloramine, chlorine dioxides, or copper-silver ions and checking pH frequently [56-58]. Remediation however is generally tailored to the circumstances of the risk of *Legionella* growth and transmission. Therefore, treatment of contaminated water sources includes biocides, boiling water, UV irradiation, and using 0.2-micron biological point-of-use (POU) filters. However, these methods provide temporal solutions and are not successful for eradicating the bacteria from water sources [56, 57, 59-61]. The protection of *L. pneumophila* within biofilms and amoeba contributes to the bacterial survival, allowing for re-colonization within months of disinfection [62].

Molecular Ecology of *L. pneumophila* and its Intracellular Life Cycle within Protozoa

While Legionellae can survive in aquatic and moist soil environments, protozoa are an important reservoir for supporting growth of legionellae in aquatic environments [63]. Remarkably, *L. pneumophila* resist digestion by amoebae that are natural microbial predators in the environment. *L. pneumophila* is a facultative intracellular parasite of 17 known species of amoebae and 7 species of non-amoebal protozoa [64-78]. When *Legionella* invades amoebae, it forms a unique protective single-membrane replicative vacuole that does not mature through the default endosomal-lysosomal degradation pathway [10, 79-81]. This association of Legionellae with protozoa is a major factor in bacterial amplification and persistence in the environment, ultimately enhancing its pathogenicity [82, 83].

The relationship between *L. pneumophila* and amoebae plays an important role in the persistence of bacterium in the environment and contributes to resistance in bacterial eradication. Under harmful and/or unfavorable environments, the trophozoite form of protozoa can differentiate into a spore-like dormant cyst to ensure their survival, but the cyst restricts intracellular growth of *L. pneumophila* [84]. However, *Legionella spp.* have developed the ability to resist and survive within an amoebic cyst for at least 6 months [85-88]. Interestingly, *L. pneumophila* has evolved to subvert amoebal encystation by secreting the effector protein LamA, an amylase, which degrades host cell glycogen, which is the main resource for synthesis of the cellulose double-wall of the cyst [89].

Another supportive finding that amoeba plays a key role in the ecology and pathogenesis of *L. pneumophila* is discovery of *Legionella*-like amoebal pathogens

(LLAPs) [90, 91]. LLAPs are phylogenetically related to *Legionella* and have been associated with Legionnaires' disease, playing a role in CAP [92-94]. While LLAP rRNA shows a 95% similarity to *L. pneumophila* rRNA, LLAPs cannot be cultured *in vitro* on artificial media but are readily isolated by coculture with protozoa, highlighting the importance protozoa play in the transmission of *Legionella* species [92, 95].

Transcriptional analysis of *L. pneumophila* during infection of *Acanthamoeba castellanii* showed that there are two phenotypic bacterial phases existing both *in vivo* and *in vitro* [96]. One morphological form of *L. pneumophila* is a replicative rod-shaped form, and the second, a motile coccoid-shaped Mature Intracellular Form (MIF) developed upon egress from the spent protozoan host [97-99]. The MIF form features a distinct thickened cell wall, multilayer membrane laminations and Poly-3-Hydroxybutyrate [PHB] inclusions ideal for long-term survival between protozoan hosts [100]. Respirable sized vesicles containing *L. pneumophila* are released from protozoa and are highly resistant to biocides, sonication, and freezing [101]. When released from a protozoan host, *L. pneumophila* exhibits an enhanced ability to infect mammalian cells compared to agar grown bacteria [102]. The biochemical and physiological change observed in protozoan grown *L. pneumophila* has promoted its ability to infect human macrophages [103-105]. The progeny that escapes from lysed amoebae are highly motile with an increase in uptake by phagocytosis with increased resistance to antibiotics, biocides, and disinfectants [103-105]. The co-evolution of *Legionella* within protozoa have facilitated survival and proliferation of *L. pneumophila* within the evolutionary distant human macrophage.

Protozoa play a crucial role in the lifecycle of *Legionella* colonization and persistence in its natural environment and are associated with biofilm formation. Biofilm formation promotes the survival of *L. pneumophila* [106]. Interestingly, several amoeba species are associated with biofilm communities, and the amount of *L. pneumophila* in biofilms is directly correlated with the biomass of protozoa [107, 108]. The biofilm structure or its association with amoeba make *L. pneumophila* containing biofilms extremely resilient to treatment with biocides [109]. Legionellae exposed to environmental stresses and/or found within biofilms are also able to enter a Viable But Non Culturable cell state (VBNC) [110]. VBNC *Legionella* show low metabolic activity but can be resuscitated within amoebae after co-culture [111]. The VBNC state allows survival and adaptation of *Legionella* to commonly used preventative and control practices of water sources such as chlorination [110].

Intracellular Life Cycle of *L. pneumophila* within Macrophages

Protozoa are the natural host for *L. pneumophila* while humans are considered an accidental host. The ability of *L. pneumophila* to infect human macrophages is hypothesized to be a consequence of prior adaptation to an intracellular life within its natural protozoan hosts [112]. Accidental infection of humans occurs when an individual inhales water contaminated with *Legionella* spp. [10, 80]. Once *L. pneumophila* infects a human host it enters through conventional or coiling phagocytosis into alveolar macrophages where the intracellular life cycle is strikingly similar to the life cycle observed when amoebae engulf *L. pneumophila* [10, 80, 113, 114]. Once inside the host cell, the bacteria can be found inside a unique single-membrane replicative vacuole [81].

The vacuole differs from the vacuolar compartment of avirulent bacteria in that it does not acidify and evades the endosomal-lysosomal degradation pathway [115]. The vacuole intercepts ER-to-Golgi vesicle traffic to become an ER-derived vacuole [10, 116-118]. This vacuole is termed the *L. pneumophila* Containing Vacuole (LCV). After a 4-hour lag phase, *L. pneumophila* undergoes exponential growth within the LCV, with a doubling growth rate of 60 minutes. By 16 to 18-hours post infection, the bacteria are released into the host cell cytosol where another 1-2 rounds of replication occur [119-122]. This is known as the post-exponential transmissive phase when the bacteria become virulent, flagellated, and cytotoxic [112, 122, 123]. The final stage in the *L. pneumophila* intracellular lifecycle is culminated by lysis of the host cell and the release of the bacteria [124-126]. When a neighboring cell is infected, this cycle is repeated. The successful intracellular lifestyle of *Legionella* within protozoa and macrophages is only possible because of the export of bacterial protein effectors through the Type II (T2SS) and Type IV (T4SS) secretion systems [127-129].

The Type II Secretion System (T2SS)

The Type II secretion system (T2SS) exists in many Gram-negative bacteria, including both plant and animal pathogens, but are mainly distributed among the genera of *Proteobacteria* [130]. The T2SS is composed of 12 core proteins making up 4 subcomplexes (T2S C, D, E, F, G, H, I, J, K, L, M and O) [130]. The first subcomplex is a multimer of T2S D proteins that provide the ultimate portal for transit across the outer membrane (OM) and out of the cell known as “secretin”, second is an inner membrane (IM) platform which provides a periplasm-spanning channel connection to the secretin, comprised of T2S F, L and M [130]. The OM-associated subcomplex and the IM-

associated subcomplexes are coupled by the IM-associated “clamp protein” T2S C and the third subcomplex is a periplasm-spanning pseudopilus, consisting of the major pseudopilin T2S G and minor pseudopilins T2S H, I, J, and K, believed to act in a “piston” or “screw-like” fashion [127, 130-133]. The fourth subcomplex is a hexamer of T2S E, a cytoplasmic ATPase that is recruited to the IM to “power” the secretion process, where T2S O protein is an IM-prepilin peptidase that cleaves and methylates the pseudopilins as a prelude to their incorporation into the pseudopilus (Figure 1-1) [127, 130-133]. The T2S consists of a two-step process where proteins to be secreted are first trafficked into the periplasm, folding into tertiary conformation, across the inner membrane of the bacteria by the Sec translocon or the Tat pathway [131]. The second step is responsible for secreting proteins that are recognized by the secretion apparatus to the extracellular milieu via an outer membrane pore [131].

The *L. pneumophila* T2SS is important for intracellular infection of amoebae and host cells, biofilm formation, planktonic survival, as well as growth in mouse models of disease [134-138]. Nearly all pathogens that express the T2SS system exist within aquatic and soil environments in addition to their higher organism hosts [131]. The T2SS system functions at a temperature range of 22-37°C, temperatures commonly associated with aquatic niches [136]. The intrapulmonary role of *L. pneumophila*'s T2SS involves intracellular infection of macrophages by facilitating the onset of bacterial replication at 4 to 8 h post entry and the capacity to grow to large numbers at 12 h [138].

To date, the T2SS exports at least 27 proteins with 20 enzymatic activities, some of which are responsible for degrading proteins and lipids [131, 139-142]. The effector substrates of the T2SS system increase the likelihood of infection of amoebae with *L.*

pneumophila. Secreted exoproteins have striking similarity to eukaryotic proteins. These effectors include the acyltransferase PlaC, ribonuclease SrnA, metalloprotease ProA, and two novel proteins – NttA and NttC [75, 133, 134, 143]. Each effector is important for infection, and their importance varies depending on the species of amoebae. In addition to amoebal infection, the secreted chitinase ChiA has been linked to bacterial persistence in the lung [140]. Thus, the repertoire of *L. pneumophila* effectors secreted by the T2SS system has evolved to enable adaptation to a broad host range [133].

Various studies have considered the importance of the T2SS system in relation to its ability to survive in aquatic environments [106, 111-115]. One study from Söderberg *et al.* has shown that T2SS mutants show a decreased ability to survive extracellularly at a temperature range of 4-25°C, suggesting there are effectors secreted by the T2SS that facilitate survival in low temperatures [136, 144]. It has also been shown that mutants lacking the T2SS Lcl protein, an immunogenic GlycosAminoGlycans (GAG) binding adhesion, are not able to form biofilms as efficiently as bacteria containing a functional T2SS system [145, 146]. T2SS systems mutants have impaired gliding motility which is likely the result of an inability to secrete a novel surfactant, TolC [147-150]. T2SS promotes infection of alveolar macrophages in the lungs by dampening the host cytokine response and releasing damaging enzymes which could aid in prolonged bacterial growth [135, 140, 151, 152]. The intracellular localization of many T2SS substrates is unknown, however a recent study by Truchan *et al.* elucidated the cellular localization of ProA and ChiA, which are secreted outside the LCV and then form a ring-like pattern around the LCV membrane in the host cell cytosol [153, 154].

The T2SS promotes the growth, ecology and virulence of *L. pneumophila*, with mutants lacking the T2SS being severely impaired for infection of the natural hosts, *Acanthamoeba castellanii* and *Hartmannella vermiformis*, indicating that proteins secreted via T2SS are required for infection of protozoan hosts in addition to mammals [133].

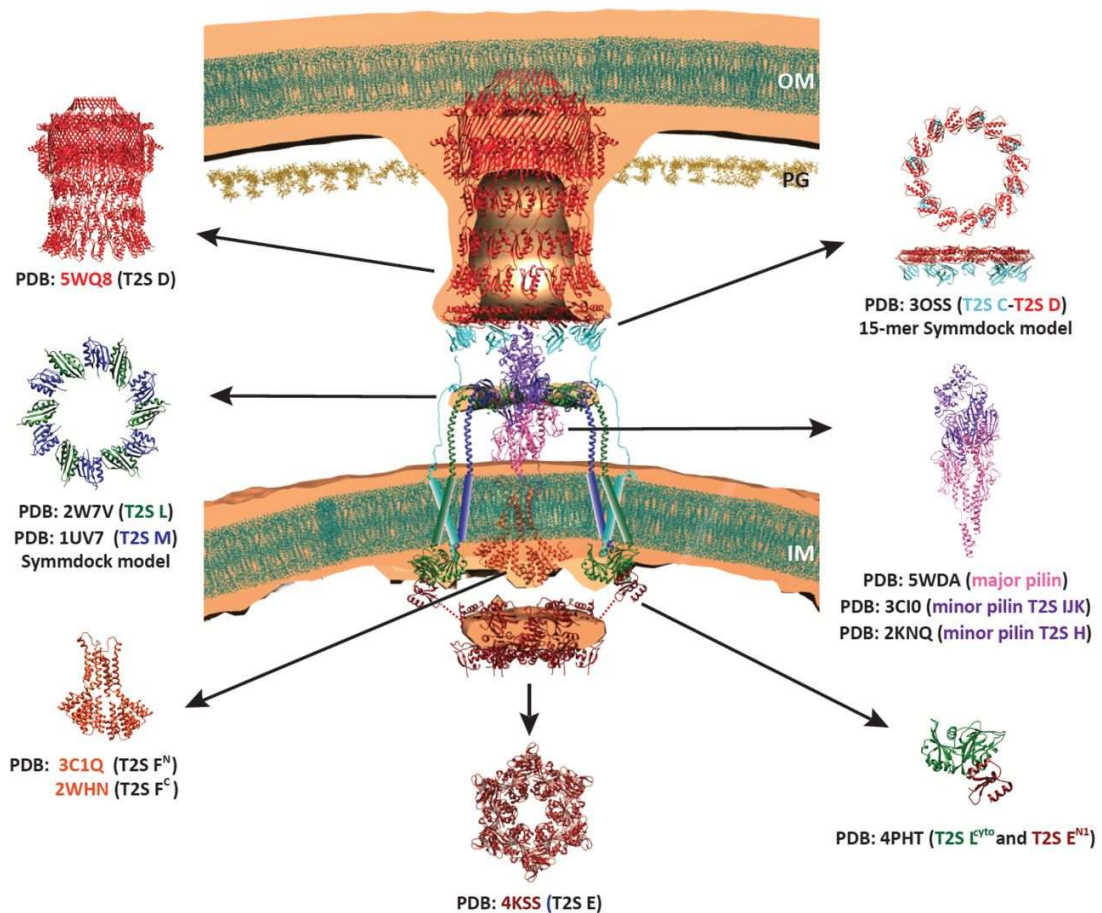


Figure 1-1 Architectural model of the T2SS.

Atomic models of T2SS components are superimposed on the central slice of the T2SS Transmembrane domains of the IM proteins are shown as cylinders. Linkers between N1E domain and N2E/CTE domains of T2S E are represented by dotted lines. OM = outer membrane, IM = inner membrane, PG = peptidoglycan. Lipids are shown in dark cyan and peptidoglycan dark yellow. Adapted from Figure 3: *In vivo structure of the Legionella type II secretion system by electron cryotomography*[130].

The Dot/Icm Type IV Secretion System (T4SS)

The Dot/Icm system is currently one of the most intensively studied T4SS systems. The secretion system is an important virulence system involved in almost all aspects of the intracellular biology of *L. pneumophila*, since bacteria lacking the secretion system are not pathogenic and cannot replicate within host cells [155]. The T4SS is specialized macromolecular delivery machines that are classified as T4ASS or T4BSS [156]. The genes encoding the Dot/Icm system consists of a set of 27 genes that were named *dot* (defective in organelle trafficking) or *icm* (intracellular multiplication) [157-163]. The T4BSS of *L. pneumophila* is composed of 27 proteins that form a “Wi-Fi” like structure, acting as a nano syringe and translocating approximately 350 effector proteins from the bacterium’s cytoplasm across the LVC membrane into the host cell cytosol (Figure 1-2) [164-172]

The T4BSS apparatus localizes to the pole of the LCV within macrophages and polar secretion of substrates is crucial for the establishment of the LCV [173]. Two of the Dot/Icm proteins, DotU and IcmF, target assembly of the T4SS apparatus to the cell poles independently of other Dot/Icm proteins [156]. With the help of a secretion system coupling complex comprised of DotL, DotM, and DotN, in association with three chaperone proteins, IcmW, IcmS and LvgA, protein substrates in the bacterial cytoplasm are delivered to the translocation channel in the inner membrane [164, 174-178]. The DotC, DotD, DotF (IcmG), DotG (IcmE) and DotH (IcmK) proteins constitute a core transmembrane complex, DotL (IcmO) is a type IV coupling protein that consists of a conserved Nucleotide-Binding Domain (NBD) and an All α -helical Domain (AAD) [174, 179-181]. DotL appears to form a multiprotein type IV coupling protein complex with

four other proteins, DotM (IcmP), DotN (IcmJ), IcmS and IcmW. The functions of these four putative subunits are elusive, and how they interact with DotL remains unknown [174, 179-181].

L. pneumophila injects >350 effectors, which constitutes the largest repertoire of effector proteins translocated by bacterial pathogens into host cells, which accounts for more than 11% of its genome coding capacity. The next closest is *Coxiella burnetii*, which harbors ~100 putative effector proteins [182-186]. The translocated effectors have a translocation signal, commonly found in the C-terminus that consists of a 20-35 amino acid sequence that directs them to the T4SS and can include an E-Block motif encompassing several glutamic acid residues [185, 187-190]. *L. pneumophila* also codes for many metaeffectors, which are “effectors of effectors” that regulate the function of other effectors injected within the host cell [191, 192]. Translocation of some effectors appears to occur rapidly upon attachment of *L. pneumophila* to host cell plasma membrane and phagocytosis of *L. pneumophila*, but not all effectors are simultaneously translocated into the host cell at the onset of infection, resulting in a temporal control of effector transcription and metaeffector activity [96, 187, 193, 194].

The T4SS is active in effector translocation for at least 8 hours after bacterial uptake [195]. Expression and translocation of effectors is quite diverse. The SidM/DrrA and SidE family of effectors can be detected early in infections but then disappear at later stages [196-198], while LepB displays increased co-localization with the LCV during the entire course of infection [196-198]. The temporal presence/control of some effectors has been shown to be consistent with their biological function [196-198]. An example of this is the set of effectors SidM, LepB and SidD that target Rab1 with antagonist

activities to temporally control its activation/deactivation on the LCV early in infection [197].

Metaeffectors regulate the function of other effectors through protein-protein interactions. In addition to post-transcriptional regulation of effector levels in the host cell by host proteasome or metaeffectors, effector activity is also achieved by control of their secretion upon contact with the host cell [96, 191, 192, 199]. Proteomics have shown control of effector synthesis impacting the timing of effector delivery. For example, the replicative phase-effector MvcA (Lpg2148) is detected in the cell 5 hours after injection of the transmissive phase effector MavC, allowing the deubiquitinase activity of MvcA to reverse MavC-mediated UBE2N ubiquitination [199, 200].

Allombert et.al revealed that Dot/Icm secretion is controlled by c-di-GMP signaling, as partial inactivation of c-di-GMP synthesizing diguanylate cyclase Lpl0780/Lpp0809, or partial overproduction of c-di-GMP degradation enzymes, results in significant changes in the rate and timing of some effector translocation [201].

The single deletion of effector proteins of *L. pneumophila* often does not result in an intracellular growth defect in macrophages due to functional redundancy of many effectors of *L. pneumophila* [202-206]. Even deletion of up to 31% of the effectors causes only marginal replication defects in mouse macrophages [205]. Functional redundancy may occur via different mechanisms including pathway redundancy, cellular process redundancy, target redundancy, molecular redundancy, and system redundancy [204]. Redundant effector proteins have been shown to perform the same function in host cells and interact with the same host cell targets. One well characterized example of this is the SidE family of effectors [202]. The SidE family consists of four effector proteins (SidE,

SdeA, B, and C) which function to catalyze the addition of ubiquitin moieties to the host proteins Reticulon 4 and Rab33b [207, 208]. When each of these effectors are individually deleted, there is no replication defect detected in macrophages, but when all four effector proteins are deleted, there is a significant decrease in intracellular replication of *L. pneumophila*, which can be restored with complementation of SdeA alone [208, 209].

Very few effector proteins have been shown to be vital for intracellular replication in macrophage infection by *L. pneumophila*, a likely result of functional redundancy among effector proteins as lack of a mammalian host target to the effector [202, 204, 205]. It is likely that over time *L. pneumophila* has accumulated a toolbox of effector proteins as a result of horizontal gene transfer during adaptation to many protozoan species. Different effectors are likely specific for infection of specific protozoan hosts.

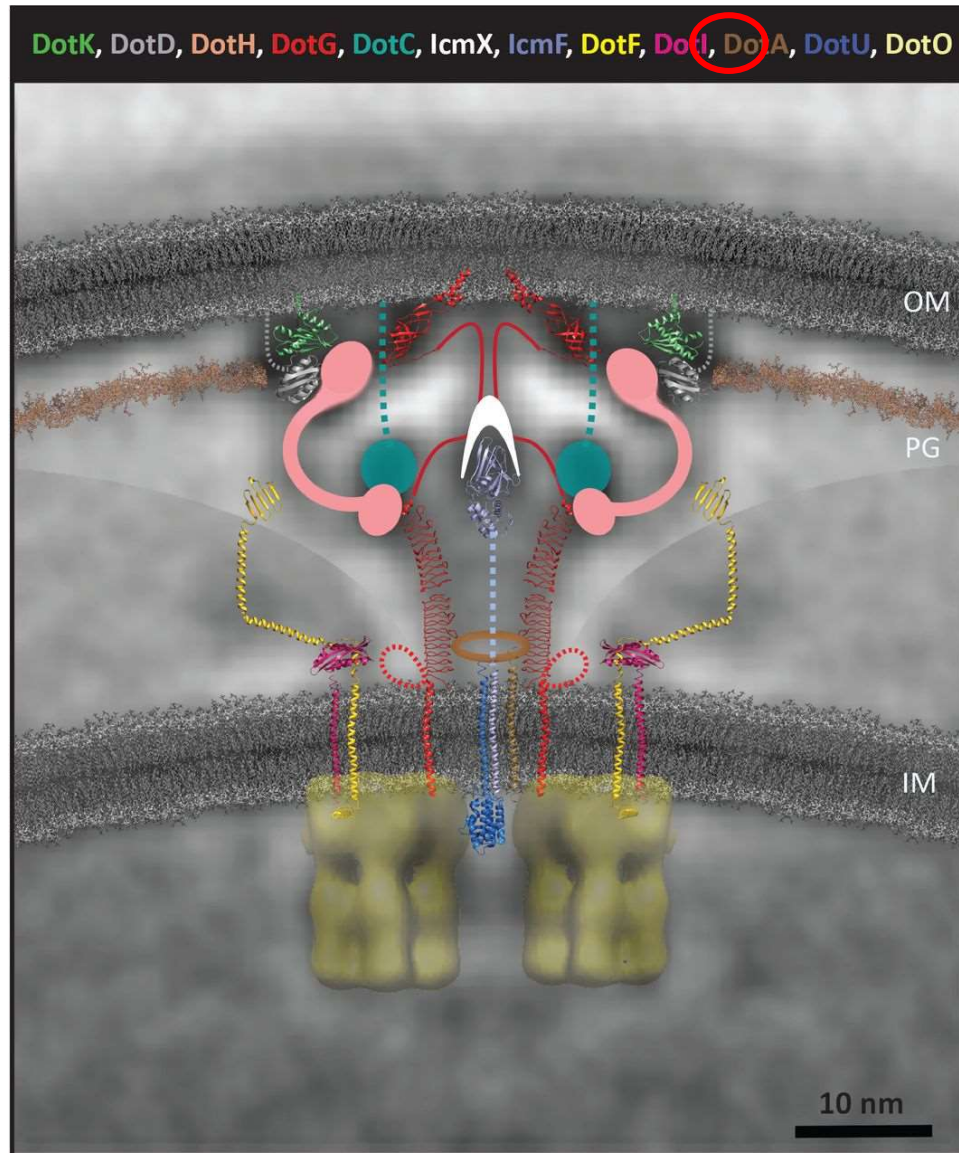


Figure 1-2 Schematic of the periplasmic portion of the Legionella Dot/Icm type IV secretion system.

Components whose structures are not known or are confidently predictable are depicted as circles (e.g., DotC) or as the shape of densities seen in the subtomogram averages or difference maps (e.g., DotH and IcmX). Polypeptide links to the outer membrane are shown as dotted lines. The sequences in DotG with unknown structure are shown as solid lines with a speculative path. A large number of transmembrane helices are not shown for inner membrane proteins (DotA, DotE, DotL, DotM, DotP, DotU, DotV, IcmV and IcmT). In addition, cytoplasmic components of the system are not shown. Lipids are shown in grey (OM is outer membrane and IM is inner membrane) and peptidoglycan in brown (PG). DotA is the T4SS mutant used in this study as a negative control (circled in red). Adapted from Figure 4: *Molecular architecture of the Legionella Dot/Icm type IV secretion system* [210].

Core Effectors of *L. pneumophila*

The vast number of effectors in the toolbox of *L. pneumophila* likely allows for its ability to infect a wide range of hosts as a “generalist” pathogen, while most pathogens tend to be specialized and are restricted to one host. *Legionella spp.* harbor more than 18,000 unique translocated effectors [211]. A large number of the effectors contain eukaryotic-like domains and motifs acquired from all domains of life [211]. Remarkably, only eight core effectors are conserved in all 58 analyzed *Legionella* genomes [183, 211]. These core effectors of *Legionella* are MavN, VipF, RavC, CetLp1, lpg2832, lpg3000, lpg1356/lpp1310, and Ankh/LegA3/Lpg2300 [183, 211]. One effector, MavN, has orthologs in all the sequenced *Legionella* as well as one other bacterium encoding the Dot/Icm T4SS, *Rickettsiella grylli* [137]. MavN a protein associated with the LCV membrane and required for efficient iron acquisition during intracellular growth, allowing microbial bypass of host iron restriction [212, 213]. Ankh/LegA3/Lpg2300, targets the host LARP7 component of the 7SK snRNP complex which interferes with host transcriptional elongation cite. The Ankh effector was the only core effector conserved across the *Legionella* genus and also present in other organisms containing the Dot/Icm T4SS such as *Coxiella burnetii* and *Rickettsiella grylli* [183, 211].

Evolution and Phylogeny of Legionellae

Plasticity is a qualitative trait of an organism providing a possible fitness advantage in response to different hosts [214]. The plasticity of the *L. pneumophila* genome is likely impacted by its co-evolution with numerous protozoan hosts. *L. pneumophila* is competent of natural transformation of DNA and is capable of

conjugation by the T4ASS [163, 215, 216]. Co-evolution and adaption of *L. pneumophila* to numerous protozoan hosts and inter-kingdom Horizontal Gene Transfer (HGT) may explain the genome plasticity, the large repertoire of effector proteins and their effector redundancy, and presence of effectors containing eukaryotic-like domains and motifs [217-219].

Pathogenic evolution and intracellular adaptation of *L. pneumophila* to a broad range of protozoan hosts has been shaped largely by intra-species, inter-species and inter-kingdom HGT, as well as intra-species recombination events [206, 211, 220-224]. In addition, some HGT of *L. pneumophila* has likely come from protozoan endosymbionts and intra-protozoan bacteria [217-219]. It may not be surprising that recent phylogenetic studies have indicated that the Dot/Icm translocation system and two of its translocated core effectors (AnkH and MavN) [224], present in all *Legionella* species as well as *Coxiella* and *Rickettsia*, have been acquired by the bacterium during very early events of its evolution and protozoan host adaptation [225]. It is thought that the key events in host adaptation events in *L. pneumophila* have taken place very early in its evolution of the last *Legionella* common ancestors (LLCA) in the deep-branching gammaproteobacterial order Legionellales, which contains among others *Coxiella*, *Rickettsia*, and *Legionella* [225]. It is estimated that LLCA diverged approximately 1.89 billion years ago. This implies that the protozoan hosts adaptation events in Legionellales have occurred between 2.12 and 1.75 Ga [225]. Early evolution of *Legionella*-protozoan host interaction has played a major role in subsequent transmission and pathogenesis of *L. pneumophila* to the accidental human host.

Effectors Involved in Vacuolar Biogenesis

Phagocytosis is a form of endocytosis that refers to cellular uptake of large particles and is initiated by the interaction of surface receptors with their cognate ligand [226, 227]. Upon phagocytosis, the nascent phagosome undergoes a complex sequence of maturation events governed by regulators of the endosomal-lysosomal degradation pathway that yields an acidic degradative compartment designated as the phagolysosome [226, 228]. Phagocytic cells are equipped with a variety of receptors that recognize foreign material and particles permitting them to internalize the particles into a plasma-membrane derived vacuole that follows a maturation process that ultimately yields a phagolysosome [226]. Additionally, non-immune cells are equipped with receptors utilized by bacterial pathogens such as *Chlamydia* to enter by receptor-mediated endocytosis [229]. Therefore, successful evolution of intra-vacuolar pathogens is dependent on their capacity to evade innate immune pathways and modulate biogenesis of their vacuole and adaptation to the unique micro-environment within the vacuole [230]. Depending on the phagocytosed bacterial pathogen, the default maturation of the phagosome along the endosomal-lysosomal pathway is overridden by specific pathogen-produced factors that interfere with the fate of the pathogen-containing vacuole [231]. All intra-vacuolar pathogens possess specialized secretion systems (T3SS-T7SS) that inject effector proteins into the host cell cytosol to modulate a variety of host cell processes and remodel their vacuoles into proliferative niches [232]. Although intravacuolar pathogens utilize similar secretion systems to interfere with their vacuole biogenesis, each pathogen has evolved a unique toolbox of protein effectors injected into the host cell to interact with, and modulate, biogenesis of the vacuole. The interference

and divergence of the pathogen-containing vacuole from the default endosomal-lysosomal pathway is at the crux of the successful evolution to the intra-vacuolar microenvironment and inflict pathology and disease [233-235]. Despite being an accidental human pathogen, *Legionella* utilize the same lysosomal evasion mechanisms to avoid killing by its natural amoeba hosts and human macrophages [232, 236, 237].

Within alveolar macrophages and the amoeba hosts, the LCV evades fusion with vesicles of the endosome-lysosomal pathway [117] and intercepts ER-to-Golgi vesicle traffic regulated by Rab1A/Rab1B [238, 239], Rab2 [240], at least one SNARE complex composed of one v-SNARE (Sec22b), and three cognate t-SNAREs (syntaxin 5, membrin, and Bet1) (Figure 1-3) [241, 242]. Both Rab1 and Arf1 have been found to be localized to the LCV by 30 min post infection [243-245]. In addition, Sar1 and Arf1, two small GTPases, regulate the formation of COPII and COPI-coated vesicles and are required for the production of early secretory vesicles [246-248]. The expression of dominant interfering mutants in the three small GTPases (Sar1, Rab1, and Arf1) inhibits biogenesis of the LCV and decreases intracellular survival of *L. pneumophila* [244, 245, 249].

The function of most Dot/Icm-injected effectors is still to be determined. However, few effectors have shown to be involved in LCV biogenesis. The RalF effector functions as a GEF to recruit the ADP-ribosylation factor 1 (Arf1) to the LCV [243]. This enables the GEF-like RalF effector to modulate membrane transport in the secretory pathway [250]. Additionally, the DrrA/SidM effector preferentially recruits Rab1 and tethers ER-derived vesicles to the LCV, mediated by another *L. pneumophila* effector, LidA [166]. DrrA/SidM may compete with endogenous guanine nucleotide exchange

factors (GEFs) to redirect Rab1 from its normal secretory intracellular localization to plasma membrane-derived vesicles [251]. The LepB effector accumulates on the LCV as DrrA/SidM and Rab1 cycle off and has been shown to function as a GTPase activating protein (GAP) for Rab1 (Figure 1-3) [196, 252]. While LidA binds several Rab GTPases including Rab1, it may sequester Rab proteins or tether ER-derived vesicles with the LCV to facilitate SNARE-mediated fusion [252]. The VipD effector belongs to a family of bacterial effectors that contain the N-terminal lipase domain and a C-terminal domain [253]. VipD localizes to early endosomes via the C-terminal domain and interferes with endosomal trafficking through blocking interaction of Rab5 and Rab22 with EEA1 [253]. VipD binds to the endosomal regulator Rab5 and triggers the hydrolytic phospholipase A1 activity of VipD, causing the removal of the lipid phosphatidylinositol 3-phosphate facilitating endosomal lysosomal evasion by *L. pneumophila* [254]. The SidE family of effector proteins (SidE, SdeA, SdeB, and SdeC) have been found to catalyze the non-canonical ubiquitination of Rab small GTPases, leading to a potential role in vesicular trafficking [255].

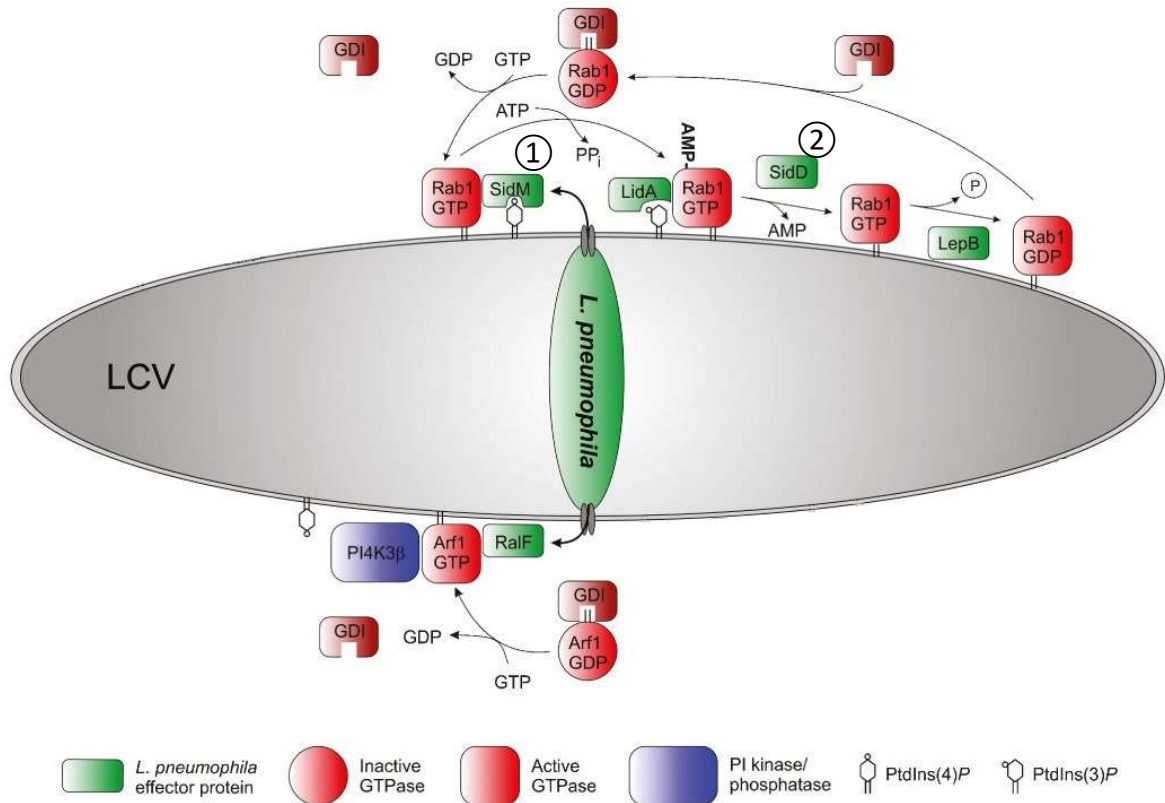


Figure 1-3 Model for the regulation of Rab1 activity by *Legionella* proteins.

(A) SidM associated with the LCV membrane extracts Rab1 from the Rab1-GDI complex and subsequently activates Rab1 by its GEF and AMPylation activity. AMPylated Rab1 becomes inaccessible to GAP proteins such as LepB and TBC1D20, thereby is locked into its active state. (B) The deAMPylase SidD removes the AMP moiety from Rab1, making it accessible to LepB, which stimulates its GTPase activity, leading to the extraction of the inactive Rab1 from the bacterial phagosome by an unknown GDI. The time frame for each event occurring during infection is indicated as ①: First 2 hours of infection. ②: After 2 hours of infection. The LCV is formed by type IV-secreted effector proteins that bind to PI lipids (PtdIns (3)P or PtdIns (4)P), recruit PI-modifying host enzymes (PI4KIII β or OCRL1) or modify small GTPases (Rab1 or Arf1). *L. pneumophila* effectors show activity as GEF (SidM and RalF), GAP (LepB), AMPylase (SidM), de-AMPylase (SidD), LidA binds to activated Rab1 and other GTPases. GDI, GDP dissociation inhibitor. Adapted from Figure 3: *Secretive Bacterial Pathogens and the Secretory Pathway*[256] and Figure 1: *Take it and release it: The use of the Rab1 small GTPase at a bacterium's will* [257]

SPECIFIC AIMS

Manifestation of Legionnaires' disease is totally dependent on the intracellular proliferation of *L. pneumophila* in alveolar macrophages within the *Legionella*-containing vacuole (LCV), which is trafficked through a unique pathway controlled by the pathogen. The LCV intercepts endoplasmic reticulum (ER)-derived vesicles and evades lysosomal fusion [116, 258]. Biogenesis of the LCV and subsequent proliferation of *L. pneumophila* within the LCV is dependent on the Dot/Icm type IV translocation system [117, 244], which directly translocates ~350 effector proteins from the bacterial cytoplasm into the host cell [190, 259-262]. Although many Dot/Icm-translocated effectors have been shown to directly regulate the early secretory system of the host cell, with the exception of VipD, no *L. pneumophila* effector has ever been shown to be indispensable for evasion of the endosomal-lysosomal degradation pathway, which continues to be a major gap in our knowledge of evasion of degradation of *L. pneumophila* by macrophages [190, 263-265]. Importantly, evasion of the endosomal-lysosomal degradation pathway by intracellular bacterial pathogens in general is not well understood. However, the effector VipD localizes to early endosomes and interferes with endosomal trafficking by blocking interaction of Rab5 and Rab22 with EEA1. VipD binds the endosomal regulator Rab5 subsequently causing the removal of the lipid phosphatidylinositol 3-phosphate, facilitating endosomal lysosomal evasion by *L. pneumophila* [253, 254].

A gene fusion strategy has allowed the identification of carboxyl terminal translocation signals of previously unidentified effector proteins in *Legionella* [190]. The effectors were identified as either Rav (Regions Allowing Vacuole colocalization) or

Mav (More regions Allowing Vacuole colocalization) [190]. This study revealed the translocated effector protein MavE (lpg2344). MavE contains a C-terminal transmembrane domain but lacks the E-block motif needed for injection of many Dot/Icm translocated substrates [190]. A Basic Local Alignment Search Tool (BLAST) search revealed MavE is widely conserved throughout the *Legionella* genus. Through high-throughput screening in yeast, a direct interaction of MavE and the effector YlfA/LegC7 was discovered [191]. YlfA/LegC7, along with two other effectors (LegC2 & LegC3), assembles in a complex on the LCV and interact with ER-derived vesicles to initiate membrane fusion [190, 191, 266-268]. However, whether the LegC7/LegC2/LegC3 complex interacts with MavE is not known. In addition, the subcellular localization of MavE during infection is not known and determining the role of MavE during infection will further explain LCV biogenesis and lysosomal evasion of *L. pneumophila*.

The structure of MavE harbors with a eukaryotic NPxY motif involved in binding to phosphotyrosine-binding (PTB) adaptor proteins involved in fusion of early secretory vesicles [269]. Here I show an essential role for MavE in intracellular proliferation of *L. pneumophila* within hMDMs and amoeba. Our central **hypothesis** is *L. pneumophila* utilizes the MavE effector to bypass the endosomal-lysosomal degradation pathway. To test the **hypothesis**, our specific aims are:

Specific Aim 1: *Temporal role for MavE in bypassing lysosomal degradation by L. pneumophila*

Specific Aim 2: *The role of the NPxY motif of MavE in lysosomal evasion*

Specific Aim 3: *Identification of MavE-interacting proteins on the LCV Membrane*

When these studies are completed, we expect the following response of hMDMs to *L. pneumophila*. We know MavE is translocated by the T4SS and suspect the NPxY motif to interact with host adaptor proteins involved in endosomal-lysosomal fusion, facilitating lysosomal evasion by the LCV (Figure 1-4).

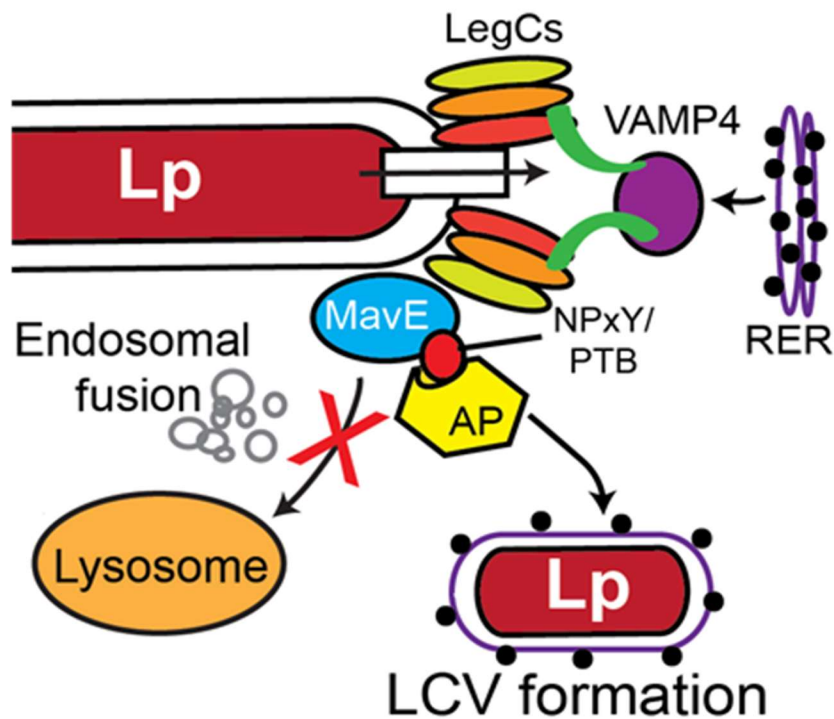


Figure 1-4: A working model of the response of hMDMs to *L. pneumophila* infection. A working model for the role of MavE in lysosomal evasion by the LCV. MavE is translocated by the T4SS and the NPxY motif of MavE interacts with host adaptor proteins involved in endosomal-lysosomal fusion. The LegC2, 3, 7 complex interacts with MavE.

CHAPTER 2:

AN INDESPENSIBLE ROLE FOR THE MavE EFFECTOR OF *LEGIONELLA*
PNEUMOPHILA IN LYSOSOMAL EVASION*

* Vaughn B, Voth K, Price CT, Jones S, Ozanic M, Santic M, Cygler M, Abu Kwaik Y. An Indispensable Role for the MavE Effector of *Legionella pneumophila* in Lysosomal Evasion. *mBio*. 2021 Feb 9;12(1): e03458-20. doi: 10.1128/mBio.03458-20.

Summary

Diversion of the *Legionella pneumophila*-containing vacuole (LCV) from the host endosomal-lysosomal degradation pathway is one of its main virulence features essential for manifestation of Legionnaires' pneumonia. Many of the ~350 Dot/Icm-injected effectors identified in *L. pneumophila* have been shown to interfere with various host pathways and processes; but no *L. pneumophila* effector has ever been identified to be indispensable for lysosomal evasion. While most single effector mutants of *L. pneumophila* do not exhibit a defective phenotype within macrophages, we show that the MavE effector is essential for intracellular growth of *L. pneumophila* in human monocyte-derived macrophages (hMDMs), amoebae and for intrapulmonary proliferation in mice. The *mavE* null mutant fails to remodel the LCV with ER-derived vesicles and is trafficked to the lysosomes where it is degraded, similar to formalin-killed bacteria. During infection of hMDMs, the MavE effector localizes to the poles of the LCV membrane. The crystal structure of MavE resolved to 1.8 Å, reveals a C-terminal transmembrane helix, three copies of tyrosine-based sorting motifs, and an NPxY eukaryotic motif, which binds phosphotyrosine binding domains present on signaling and adaptor eukaryotic proteins. Two-point mutations within the NPxY motif results in attenuation of *L. pneumophila* in both hMDMs and amoeba, and the substitution defects of P⁷⁸ and D⁶⁴ are associated with failure of vacuoles harboring the mutant to be remodeled by the ER and in fusion of the vacuole to the lysosomes leading to bacterial degradation. Therefore, the MavE effector of *L. pneumophila* is indispensable for phagosome biogenesis and lysosomal evasion.

Importance

Intracellular proliferation of *Legionella pneumophila* within a vacuole in human alveolar macrophages is essential for manifestation of Legionnaires' pneumonia. Intra-vacuolar growth of the pathogen is totally dependent on remodeling the *L. pneumophila*-containing vacuole (LCV) by the ER and on its evasion of the endosomal-lysosomal degradation pathway. The pathogen has evolved to inject ~350 protein effectors into the host cell where they modulate various host processes; but no *L. pneumophila* effector has ever been identified to be indispensable for lysosomal evasion. We show that the MavE effector localizes to the poles of the LCV membrane and is essential for lysosomal evasion and intracellular growth of *L. pneumophila* and for intrapulmonary proliferation in mice. The crystal structure of MavE show an NPxY eukaryotic motif essential for ER-mediated remodeling and lysosomal evasion by the LCV. Therefore, the MavE effector of *L. pneumophila* is indispensable for phagosome biogenesis and lysosomal evasion.

Introduction

Intracellular pathogens that reside in vacuoles within macrophages have evolved with mechanisms to evade the endosomal lysosomal degradation [235, 270] and autophagy pathways [271] as well as other innate defense pathways [272, 273]. Cytosolic pathogens have also evolved with mechanisms to cytosolic detection by the innate defense processes of macrophages [274].

Legionella pneumophila is a Gram-negative environmental bacterium, naturally infecting amoebae in water sources [206]. The bacterium evades lysosomal degradation by amoebae and proliferates intracellularly [206]. *L. pneumophila* can become aerosolized allowing for environmental transmission to human hosts. Once inhaled into the lungs, *L. pneumophila* infects resident alveolar macrophages, causing a severe pneumonia known as Legionnaires' disease [10, 275, 276]. Within macrophages, *L. pneumophila* grows in a membrane-bound vesicle known as the *Legionella* containing vacuole (LCV) [203, 259]. The LCV fuses with endoplasmic reticulum (ER)- derived vesicles and evades lysosomal fusion [116]. Proliferation of *L. pneumophila* within the LCV is dependent on the Dot/Icm type IV secretion system (T4SS) [117, 244], which translocates ~350 effector proteins into the host cell [190, 259-262]. These injected effectors have evolved to manipulate various host cell processes in order to remodel the host cell into a proliferative niche for pathogen proliferation [118, 203]. The loss of function of this secretion system causes defective phagosome biogenesis in terms of recruitment of ER-derived vesicles to the LCV and in rapid fusion to of the LCV to the lysosomes [117, 203, 277].

The ability of the LCV to be remodeled into an ER-derived vacuole and evade degradation through the endosomal-lysosomal pathway is a key virulence determinant of

L. pneumophila [203, 207, 278]. However, the mechanism *L. pneumophila* employs to evade lysosomal fusion is still unclear, but it is regulated at various levels [279]. Multiple Dot/Icm translocated effectors directly regulate vesicular traffic associated with the early secretory system [190, 263-265]. Few of the T4SS effector proteins, such as DrrA/SidM, LidA, VipD, and LepB have been shown to be partially required for lysosomal evasion [264, 280, 281]. Many of these effectors interact with small host GTPases and/or Rab proteins, which are prominent targets of *L. pneumophila* effector proteins [282-285]. However, to date, no known effector has proven to be indispensable for evasion of the endosomal-lysosomal degradation pathway. The prevalence of functional redundancy among the 350 *L. pneumophila* effectors suggests key host pathways are targeted by *L. pneumophila* [286], and many of these pathways are highly conserved through evolution from unicellular eukaryotes, such as amoeba, to mammals [287, 288]. Redundancy of effectors occurs in many different manners, including molecular mimicry, targets, pathways, cellular processes, and system redundancy [204]. However, the redundancy of effectors likely represents a toolbox for *L. pneumophila* to replicate within diverse environmental hosts; having specific effectors for certain hosts and some of the amoebae-adapted effectors may have unpredicted paradoxical effects on human macrophages [202-206].

The MavE (Lpg2344) effector was first identified in a screen aimed at identification of new translocated substrates based on the presence of glutamate-rich motif found in more than half of *L. pneumophila* effectors [190]. While the amino acid sequence of MavE has no homology to known proteins, a BLAST search revealed MavE is widely distributed throughout the *Legionella* genus, but its role in the infection remains unknown [289, 290].

Recently, a yeast two-hybrid screen revealed that MavE has a direct interaction with another effector protein, a metaeffector, YlfA/LegC7 [190, 191]. YlfA/LegC7 modulates ER vesicle trafficking events [267]. YlfA/LegC7 along with two other effectors, YlfB/LegC2 and LegC3 assemble as a complex on the LCV that interacts with ER-derived vesicles to initiate membrane fusion [266-268]. Single *ylfA* and *ylfB* mutants and an *ylfA-ylfB* double mutant replicate similar to the WT strain in macrophages [291]. However, in single cell assays, the *YlfA-YlfB* double mutant exhibits ~30% reduction in ER-mediated remodeling and formation of replicative LCVs [292]. However, the *ylfA-ylfB* double mutant is similar to the WT strain in lysosomal evasion, indicating that ER-mediated remodeling and lysosomal evasion of the LCV are two independent events [292]. However, the role of this LegC7/LegC2/LegC3 complex in association with MavE in intracellular proliferation and lysosomal evasion by *L. pneumophila* is not known.

The combination of the eukaryotic motifs in MavE and metaeffector activity of YlfA/LegC7 suggests the MavE effector is likely involved in governing biogenesis of the nascent LCV [190]. Here we demonstrate that the MavE effector is the first effector identified to be indispensable for diverting the LCV from the endosomal-lysosomal pathway and is essential for intracellular replication in human macrophages, amoebae, as well as for intrapulmonary proliferation in mice. MavE is localized to the LCV pole, which is consistent with localization of the Dot/Icm translocation apparatus. The crystal structure of MavE shows a single-pass transmembrane domain at its C-terminus, an NPxY eukaryotic motif, and three copies of the tyrosine-based sorting motifs [293-295]. Our data show the NPxY eukaryotic motif, and the P and the upstream D residue of MavE are

required its function in ER-mediated remodeling of the LCV and lysosomal evasion, both of which are essential for intracellular proliferation.

Results

Subcellular Localization of MavE

Since pathogenic effectors injected into host cells have distinct sub-cellular localization where they interact with specific targets, the sub-cellular localization of MavE during infection was determined by transiently transfecting HEK293T cells with a construct encoding 3X-FLAG tagged MavE to enhance expression and detection of MavE. Following 24h, the cells were infected with wild type *L. pneumophila*, a translocation-deficient ($\Delta T4SS$) *dotA* mutant, or the *mavE* mutant for 2h. Ectopic expression of MavE exhibited distinct punctate distribution throughout the cell, indicative of vesicular localization (Figure 2-1A). Remarkably, 3X-FLAG tagged MavE was trafficked to 90% of wild type strain-containing LCVs and this co-localization is Dot/Icm-dependent since the $\Delta T4SS$ mutant vacuoles exhibited less than 5% co-localization. In cells infected with the *mavE* mutant, MavE was trafficked to 10% of LCVs only. These data suggest that other Dot/Icm-injected effectors may be required during infection, and injection of various effectors is required for proper localization of MavE to the LCV membrane.

To examine sub-cellular localization of MavE during infection of macrophages, we constructed *L. pneumophila* strains that express 4HA-tagged MavE fusions and infected human monocyte-derived macrophages (hMDMs) for 1hr. Following fixation, the plasma membranes of infected hMDMs were differentially permeabilized using digitonin to detect if MavE was exposed to the cytosol. The 4HA-MavE translocated by wild type bacteria was spatially and exclusively localized to the cytosolic side of 80% of the LCVs (Figure

2-1B). Interestingly, MavE was concentrated at the LCV poles, which is consistent with the localization of the Dot/Icm translocation system to the bacterial poles [296]. MavE was not detected on LCVs harboring the $\Delta T4SS$ mutant (Figure 2-1B). To exclude potential effect of digitonin on co-localization to the LCV, methanol fixation was utilized after the infection but digitonin was excluded. The data showed that the 4HA-tagged MavE was consistently concentrated at the LCV poles in WT infected hMDMs in a Dot/Icm-dependent manner (Figure 2-2).

The detection of MavE on wild type strain-containing LCVs decreased rapidly and significantly over time, with only 30% of LCVs decorated with MavE at 3h post-infection. As the HA tagged MavE used was IPTG-inducible, the MavE was synthesized by the bacteria prior to infection. To determine if the loss of MavE was due to host proteasomal degradation, MG132 was used to inhibit the proteasomes [297]. We have shown previously that inhibition of proteasomal degradation blocks replication of *L. pneumophila* within hMDMs due to the lack of sufficient amino acids but has no detectable effect on phagosome trafficking and is totally reversible upon supplementation of amino acids [297]. The data showed that upon inhibition of the proteasomes, MavE was retained on the LCVs, suggesting that MavE is degraded by the host proteasomes (Figure 2-1C).

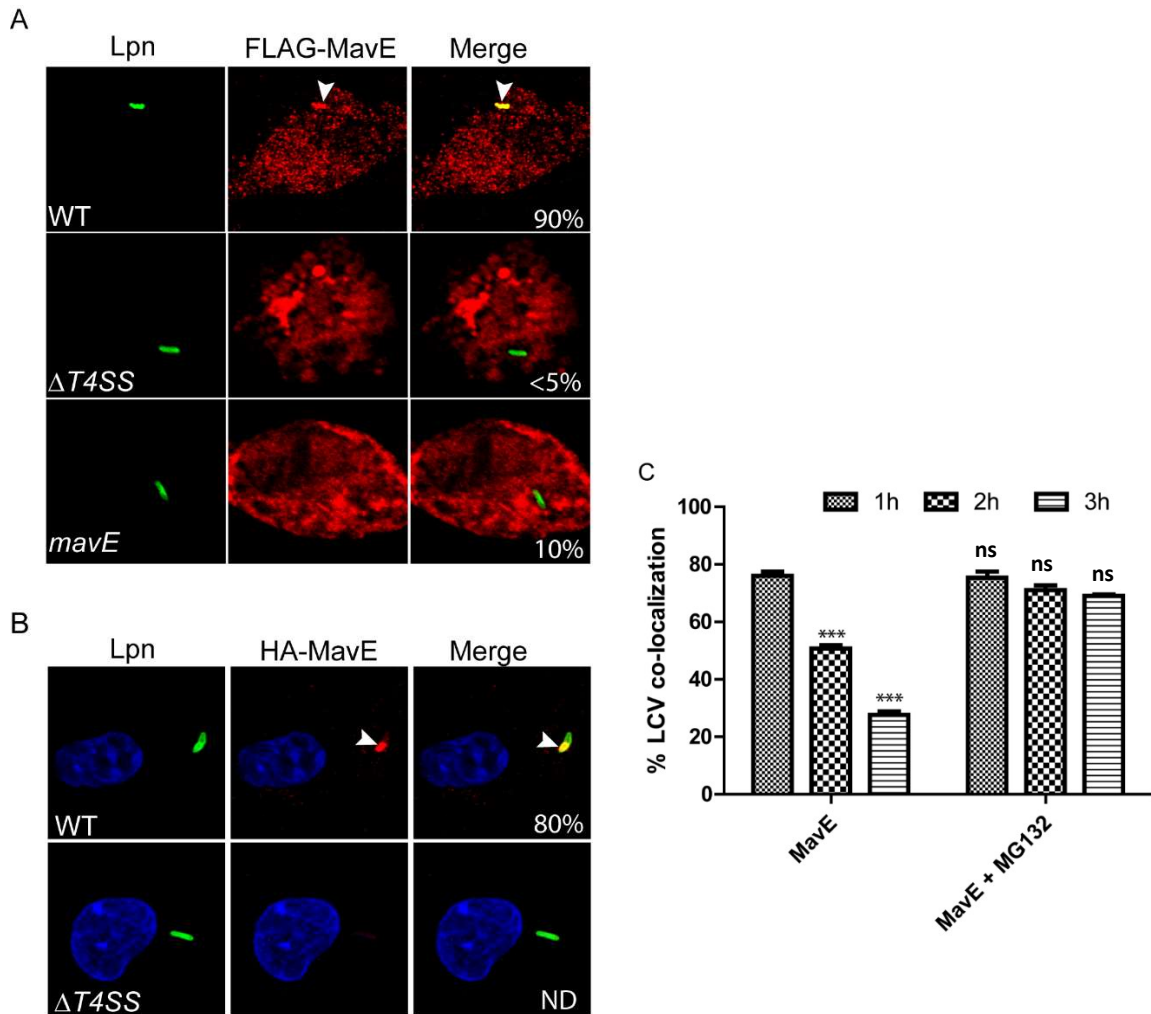


Figure 2-1: Localization of MavE during ectopic expression and during infection of hMDMs. (A) Representative confocal microscopy images of transfected HEK293T cells with 3X-FLAG tagged MavE. Cells were infected for 2hrs, in triplicate, using wild type *L. pneumophila*, the $\Delta T4SS$ mutant, or the *mavE* mutant (green). Ectopic expression of MavE exhibited distinct punctate distribution throughout the cell (red). Quantification of co-localization of MavE with the LCV (indicated by arrowheads-yellow) is shown in merged images. (B) Representative confocal microscopy images of 4HA-tagged MavE (red) constructs in both wild type and *T4SS L. pneumophila* (green), following 1hr infection in hMDMs. Quantification of co-localization of MavE with the LCV (indicated by arrowheads-yellow) is shown in merged images. ND indicates not detectable. (C) The presence of MavE on wild type LCVs decreased from 1hr-3hr post infection. The proteasome inhibitor, MG132, blocked the loss of MavE (Student *t*-test, * $p \leq 0.05$; ** $p \leq 0.01$; *** $p \leq 0.001$, ns indicates not significant)

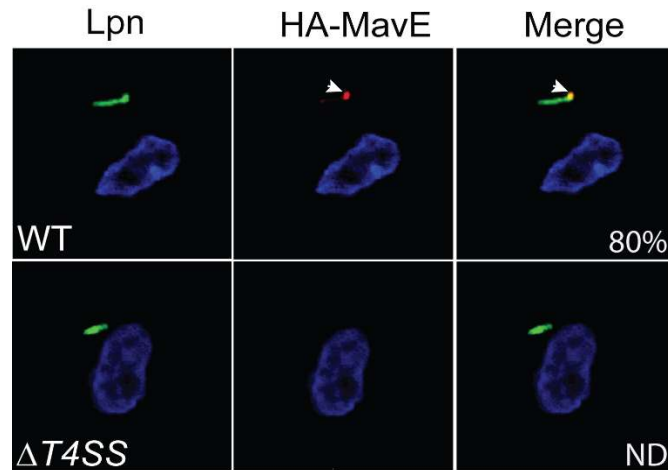


Figure 2-2: Localization of MavE during infection of hMDMs without digitonin treatment. (A) Representative confocal microscopy images of 4HA-tagged MavE (red) constructs in both wild type and $\Delta T4SS$ mutant of *L. pneumophila* (green), following 1hr infection in hMDMs followed by methanol fixation without digitonin treatment. ND indicates, not detected. Quantification of co-localization with the LCV (indicated by arrowheads-yellow) is shown in merged images. Infected monolayers were fixed in -20°C methanol for 5 mins. The results are representative of three independent experiments performed in triplicate. A total of 100 infected cells for each replicate were counted for presence or absence of localization.

The role of MavE in intracellular replication

With few exceptions, most single effector mutants in *L. pneumophila* do not exhibit a defective phenotype in macrophages [206]. To further examine the function of MavE, we determined if MavE was required for intracellular replication. An isogenic mutant was generated and used to infect hMDMs. Growth of the *mavE* mutant during *in vitro* broth culture was identical to the wild type strain (Figure 2-3A). The data showed that the *mavE* mutant failed to replicate in hMDMs, similar to the translocation-deficient *T4SS* mutant (Figure 2-4A). Complementation of the *mavE* mutant (*mavE/C*) reversed the severe intracellular growth defect. Infection of *Acanthamoeba polyphaga*, a natural host of *L. pneumophila*, exhibited ~10-fold less *mavE* mutant bacteria recovered at 24 and 48hr post-infection compared to those infected with the wild type or the complemented mutant (*mavE/C*) (Figure 2-4B).

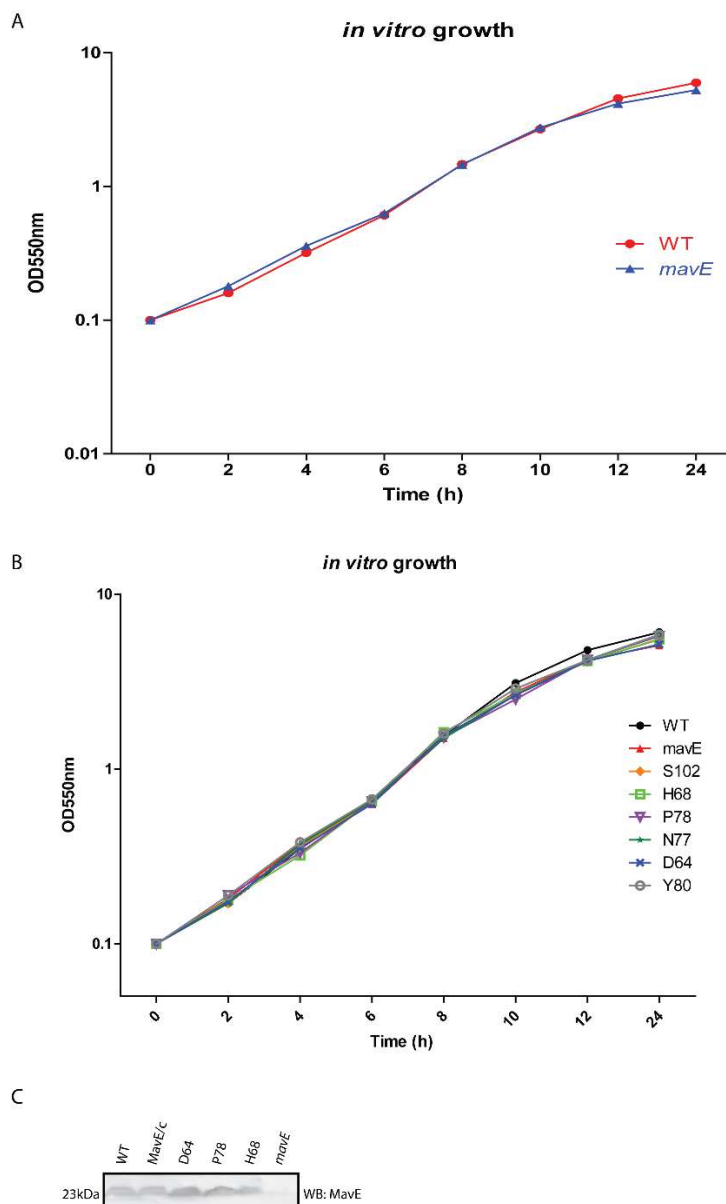


Figure 2-3: Growth of substitution mutants *in vitro* and expression and stability of the variant MavE proteins. (A) Overnight cultures of WT and $\Delta mavE$, in BYE broth were grown overnight at 37°C then diluted to OD₅₅₀ 0.05 and grown at 37°C for 24h. Growth rates were determined by measuring optical density at 550nm every two hours, for 12, then again at 24h post-inoculation. Data is representative of three independent experiments. (B) Overnight cultures of WT, $\Delta mavE$, and NPxY substitution mutants in BYE broth were grown overnight at 37°C then diluted to OD₅₅₀ 0.05 and grown at 37°C for 24h. Growth rates were determined by measuring optical density at 550nm every two hours, for 12, then again at 24h post-inoculation. Data is representative of three independent experiments. (C) Immunoblots of total bacterial lysates from WT *L. pneumophila* and each of the MavE substitution attenuated mutant strains. Cell lysates of equivalent number of bacteria were subjected to immunoblotting using rabbit anti-MavE antiserum [298, 299].

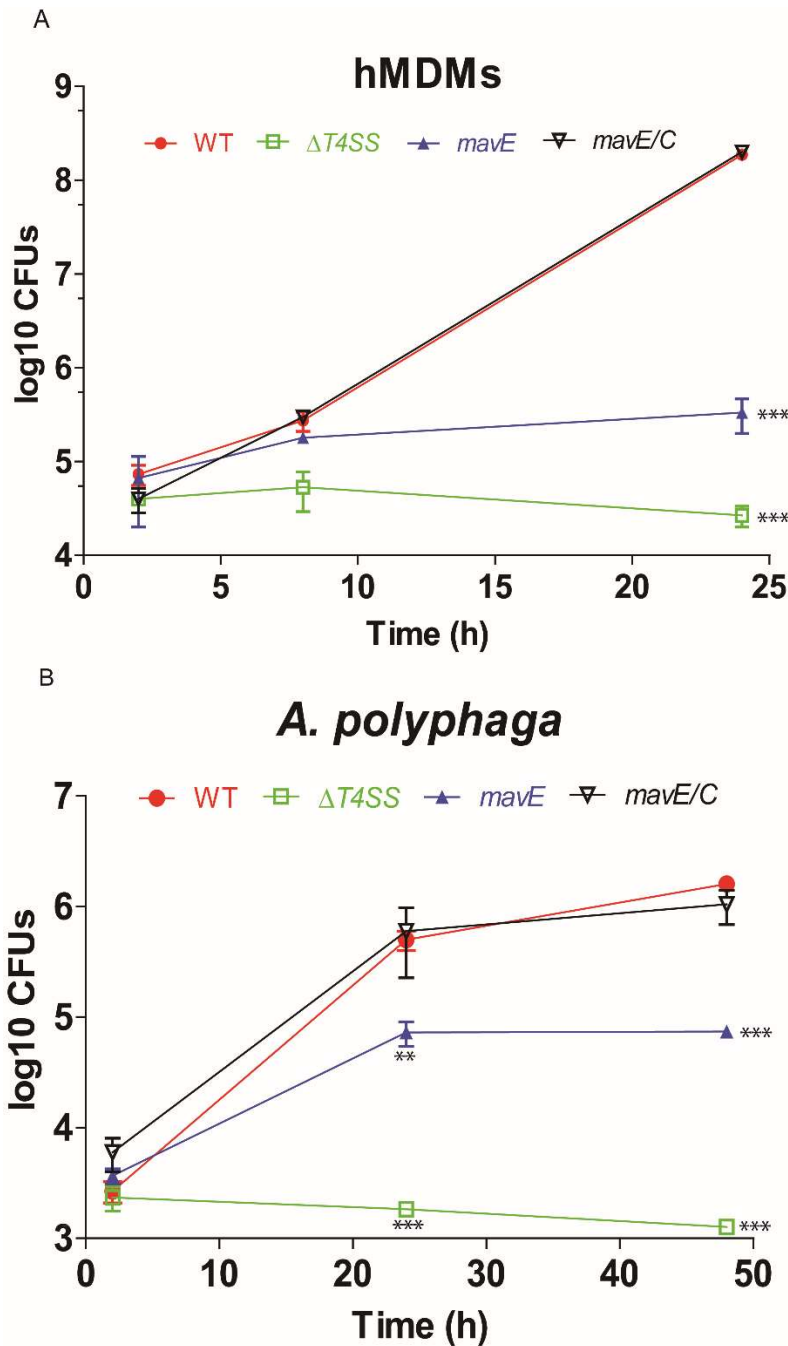


Figure 2-4: MavE is essential for intracellular replication in hMDMs and *A. polyphaga*. (A) To determine intracellular replication of the WT strain, the *T4SS* mutant, the *mavE* mutant, and complemented *mavE* mutant (*mavE/C*), hMDMs were infected and number of CFUs was determined at 2 and 24 h post-infection. Data points represent (mean CFUs \pm SD, n = 3) and are representative of three independent experiments. (B) To determine intracellular replication of the WT strain, the *T4SS* mutant, the *mavE* mutant, and complemented *mavE* mutant (*mavE/C*), *A. polyphaga* were infected and the number of CFUs was determined at 2, 24 and 48 h post-infection. Data points represent (mean CFUs \pm SD, n = 3) and are representative of three independent experiments. (Student *t*-test, * $p \leq 0.05$; ** $p \leq 0.01$; *** $p \leq 0.001$)

In the A/J mouse lethality model, using an intratracheal inoculation of 10^7 cfu (LD50), the *mavE* mutant was completely attenuated, with 100% animal survival at 10-days post-infection (Figure 2-5A). In contrast, both WT and the complemented *mavE* mutant showed 50% lethality (Figure 2-5A). To determine if the *mavE* mutant has a defect in intrapulmonary growth, A/J mice were intratracheally infected with 10^6 cfu to determine intrapulmonary proliferation. At 2, 6, 12, 24, 48 and 72 hours, the bacterial burden was determined in the lungs, spleen, and liver. Compared to the WT bacterial burden, a decrease of bacterial burden of the *mavE* mutant was observed in lung tissue at 72 hours post infection (Figure 2-5B). Following 24 hours post infection, a decrease in bacterial burden was found in both the spleen and liver for the *mavE* mutant bacterial strain (Figures 2-5C & D). The A/J mice intratracheally infected with the complemented *mavE* mutant was similar to infection by WT bacteria in bacterial burden in the lungs, spleen and liver. Taken together, the MavE effector is essential for intracellular growth in macrophages, amoeba, and contributes to intrapulmonary proliferation in mice.

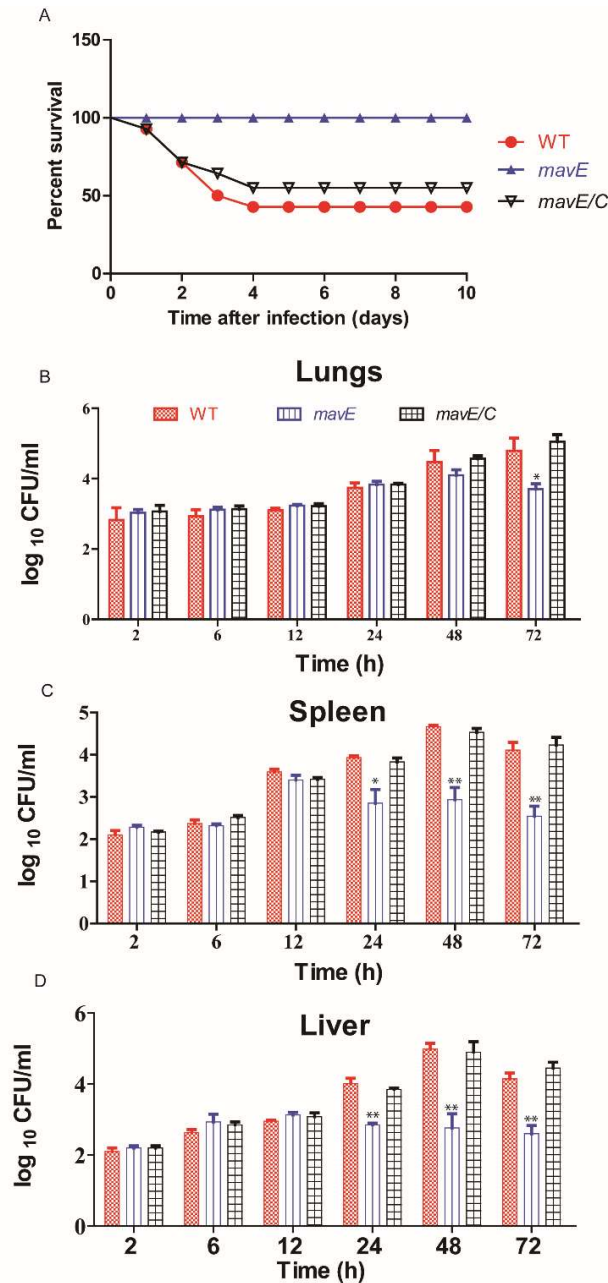


Figure 2-5: The MavE effector is essential for intrapulmonary replication *in vivo*. (A) Mouse lethality assay in which A/J mice were intratracheally infected with wild type, the *mavE* mutant, and complemented strains (*mavE/C*) at 10^7 CFU and monitored for 10 days. (B) Lung CFUs were determined in A/J mice at 2, 6, 12-, 24-, 48- and 72-hours post inoculation. The CFUs in the *mavE* mutant intratracheally infected mice compared to both the wild type and complemented strains (*mavE/C*) are shown. (C) Spleen CFUs were determined of wild type, *mavE* mutant and complemented strain (*mavE/C*) determined in intratracheally infected A/J mice at 2, 6, 12-, 24-, 48- and 72-hours post inoculation. (D) Liver CFUs were determined in intratracheally infected A/J mice at 2, 6, 12-, 24-, 48- and 72-hours post inoculation for the wild type, *mavE* mutant and complemented strain (*mavE/C*). (Student *t*-test, * $p \leq 0.05$; ** $p \leq 0.01$; *** $p \leq 0.001$, n=18)

Role of MavE in ER-mediated remodeling and lysosomal evasion by the LCV

Since the *mavE* mutant is defective for intracellular growth, we determined if trafficking of the vacuole harboring the mutant was altered. To determine if the *mavE* mutant failed to create an ER- derived vacuole, we utilized confocal microscopy to determine co-localization of the LCV with the ER marker, KDEL. The data showed that over 90% of LCVs harboring wild type bacteria co-localized with KDEL, while only 15% and 8% of the *mavE* mutant and formalin killed WT (FK-WT)-containing vacuoles, respectively, co-localized with the ER marker (Figure 2-6A). Much like WT-containing LCVs, 87% of the complemented mutant (*mavE/C*) containing LCVs co-localized with KDEL.

To examine co-localization with late endosomes/lysosomes, the late endosome/lysosomal marker, LAMP1, was utilized. Our data showed that only 5% of the wild type containing LCVs co-localized with the LAMP1 marker. In contrast, 88% of LCVs harboring the *mavE* mutant co-localized with LAMP1 (Figure 2-6B). The defect of the mutant was restored upon complementation where only 15% of the vacuoles harboring the complemented *mavE* mutant co-localized with LAMP1. For the LCVs containing FK-WT bacteria as a control, ~90% of the vacuoles co-localized with the LAMP1 marker.

Importantly, 70% of LCVs harboring the *mavE* mutant co-localized with the lysosomal marker, Cathepsin D, similar to formalin-killed bacteria, while only 9% of LCVs harboring the wild type strain localized with Cathepsin D (Figure 2-6C). Importantly, in contrast to the bacilli shape of WT bacteria, the majority of the *mavE* mutant bacteria exhibited altered morphology that included rounding and blebbing, indicative of bacterial degradation, which is consistent with fusion of the LCV to the lysosome (Figure 2-7).

Taken together, MavE is the first effector of *L. pneumophila* shown to be indispensable for biogenesis of the LCV and lysosomal evasion.

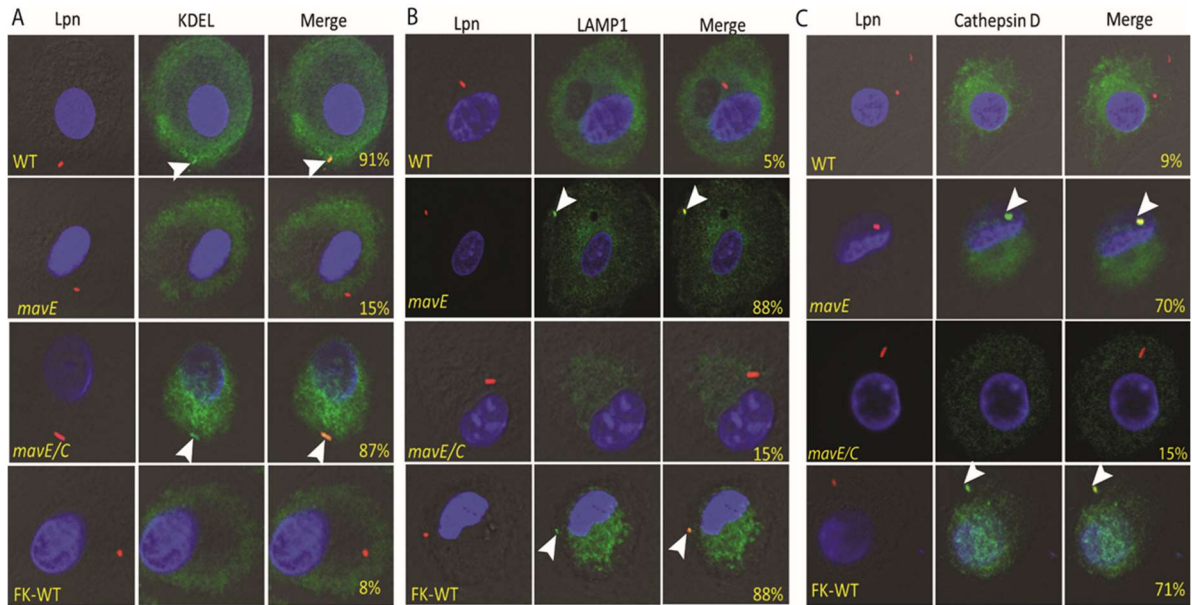


Figure 2-6: Fusion of the vacuoles containing the *mavE* mutant with the lysosome
(A) Co-localization of the LCVs containing wild type, formalin-killed (FK) *L. pneumophila*, *mavE* mutant, or the complemented strain (*mavE/C*) labeled with the ER marker, KDEL (green), DAPI (blue) and anti-*Legionella* (red). Quantification of co-localization with the LCV (indicated by arrowheads-yellow) is shown in merged images.
(B) Co-localization of the LCVs containing wild type, formalin-killed (FK) *L. pneumophila*, *mavE* mutant, or the complemented strain (*mavE/C*) stained with the late endosome/early lysosomal marker, LAMP1 (green), DAPI (blue) and anti-*Legionella* (red). Quantification of co-localization with the LCV (indicated by arrowheads-yellow) is shown in merged images.
(C) Co-localization of the LCVs containing wild type, formalin-killed *L. pneumophila*, *mavE* mutant, or the complemented strain (*mavE/C*) stained with the lysosomal marker, Cathepsin D (green), DAPI (blue) and anti-*Legionella* (red). Quantification of co-localization with the LCV (indicated by arrowheads-yellow) is shown in merged images. All analyses were performed on 100 infected cells analyzed from multiple cover slips. The results are representative of three independent experiments performed in triplicate.

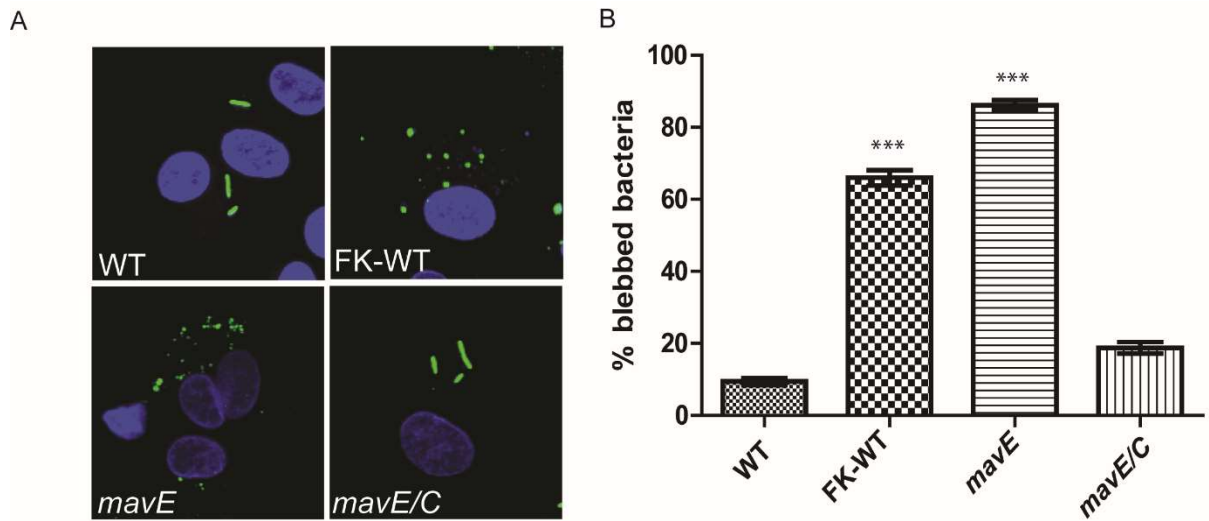


Figure 2-7: An essential role for MavE in bacterial viability within the LCVs of hMDMs (A) Representative confocal microscopy images of wild type, formalin killed-wild type, *mavE* mutant and the translocation deficient *T4SS* mutant *L. pneumophila*, following 1hr infection in hMDMs. The cells were fixed and stained with anti-*Legionella* (green) and DAPI (blue). All analyses were performed on 100 infected cells analyzed from multiple cover slips. The results are representative of three independent experiments performed in triplicate, and error bars represent standard deviation. (Student *t*-test, * $p \leq 0.05$; ** $p \leq 0.01$; *** $p \leq 0.001$)

Crystal Structure of MavE

MavE contains a predicted transmembrane helix at the C-terminus (aa 183-206). This region was excluded from the constructs submitted to crystallization to assure protein solubility. We succeeded in crystallizing construct MavE (39-172). Its crystal structure was solved by single anomalous dispersion (SAD) and refined to a resolution of 1.8 Å. There are three molecules in the asymmetric unit, designated *A*, *B* and *C*. Molecules *B* and *C* are related by twofold symmetry, and molecule *A* is also related by a twofold axis to a *B* chain in a neighboring unit cell (Figure 2-8A). This organization results in two layers of *B* and *C* molecules being sandwiched between a single layer of *A* molecules (Figure 2-8A). MavE (39-172) is comprised of five α -helices, which are designated from N- to C-terminus as A, B, C, D, and E. The N- and C-terminal residues of MavE are near one another, with helices A and E making contacts *via* Arg155 and Arg162 guanidinium nitrogen atoms in E (Arg155/162) forming hydrogen bonds to Leu57 carbonyl oxygen and Glu54 side chain oxygen atoms in A, respectively. Helices B and C are connected by a long (22 residue) loop, with the first ~10 residues (Gln72-Arg79) having poorly defined electron density. The N⁷⁷PxY⁸⁰ motif, which is disordered in the structure, is located within this loop, and stretches across helices C and D which, in turn, lie diagonally ovetop helices A and E. Thus, helices A and E act as a narrow scaffold upon which helices B, C and D are positioned, with the longest loop of the structure (between helices B and C) rendered solvent accessible.

Significant intermolecular contacts in the MavE crystal occur at the *AA* or *BC* dimer interfaces. Each ~1000 Å² interface is formed by N- and C-terminal residues, which

contact a kinked region of helix C in the symmetry-related molecule. Two centrally positioned citrate molecules strengthen the *BC* dimer interaction using a water-mediated hydrogen bond network. Residues contributing to this interaction are Ala38, Glu42, Gln125 and Ser128 of each chain. The difference electron density map ($mF_o - DF_c$) indicates the presence of another stabilizing element at the *A-A* interface, although the identity of this small molecule remains unclear.

To gain insight into MavE function, we searched for proteins with a similar fold. To this end, we submitted MavE (39-172) coordinates to the DALI server [300]. The most interesting result in our search for homologues was a core domain of the grass pollen allergen, Phlp 5b (PDB id 1L3P, Z-score = 7.1). This domain is comprised of a four-helix bundle [301]. Helices A, B, C and D of MavE (39-172) align well with the Phlp 5b core domain (Figure 2-8B), but helix E has no counterpart in Phlp 5b. Two 35-residue helix-turn-helix motifs are present in Phlp 5b and they share 37% sequence identity with one another. These motifs adopt remarkably similar helix termination and chain reversal strategies. As such, Phlp 5b was described as a twinned two-helix bundle. The corresponding helix-turn-helix motifs in MavE also share several residues, with some stabilizing the core architecture. Based on these observations, MavE can be said to have a similar core domain to that of Phlp5b. Interestingly, the extended loop between helices B and E in MavE is not present in Phlp5b and constitutes an insertion into this fold. This insertion contains not only the NPxY motif but also a triad Asp64-His68-Ser102 that is reminiscent of the catalytic triad of serine proteases. Two of these residues are located within the insertion loop. While these sidechains in the crystal structure are not connected by hydrogen bonds (as they are in the catalytic triad of proteases), they could be brought

into such interactions by simple rotation of the sidechains (Figure 2-8), suggesting a possibility that MavE possesses catalytic activity.

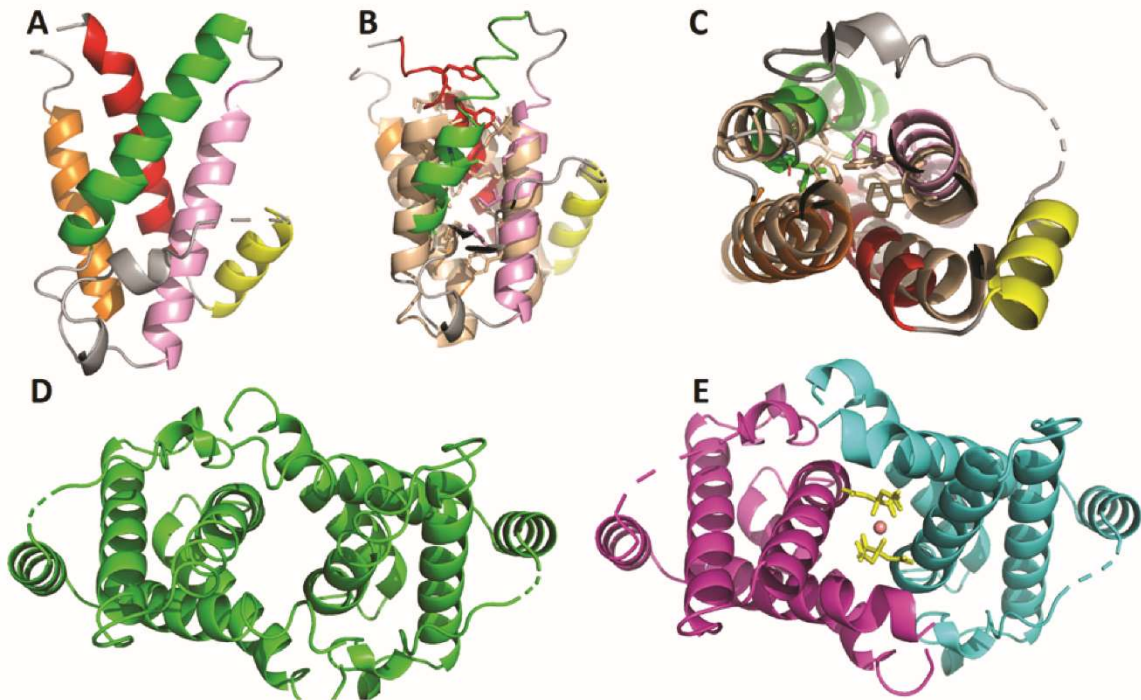


Figure 2-8: Crystal structure of MavE (39-172). (A) Overall structure of a single MavE chain. Helices A, B, C, D and E are colored red, yellow, pink, green and orange, respectively. Loops are shown in grey. (B) Overlay of MavE (39-172) and the grass pollen allergen Phlp 5b. MavE is colored as in A and the grass pollen allergen is colored wheat. Hydrophobic core residues are depicted as sticks. (C) View of the overlay shown in B from below. Note that helix E and the loop connecting it to B are absent in Phlp 5b. The dimer interface for AA and BC chains is depicted in (D) and (E), respectively.

Structure-based Functional Analysis of MavE

To determine the role the NPxY motif has in the function of the MavE effector during infection, six-point mutations were made in the critical domains predicted to contribute to the biochemical function of MavE. Three residues in the NPxY motif (N77A, P78A and Y80A) were targeted for substitution. They are located on the insertion loop, are exposed on the MavE surface and show high mobility/flexibility (poor electron density). Three other residues (D64-H68-S102), which constituted a potential catalytic triad reminiscent of the catalytic triad of serine proteases, were also targeted for substitution mutagenesis. Growth of the *mavE* substitution mutants during *in vitro* broth culture grew identical to the wild type strain (Figure 2-3B). The *L. pneumophila* expressing *mavE* variants were used to infect hMDMs to evaluate intracellular growth kinetics (Figure 2-10). Two of the substitution mutants, D64A and P78A, were found to be attenuated (Figure 2-9A). Similar results were observed in *A. polyphaga*. An additional substitution mutant, H68A, also showed attenuation in *A. polyphaga* (Figure 2-9B). Using immunoblots of total bacterial lysates, there was no major differences in the expression and stability of the variant proteins in the *L. pneumophila* variants with defective phenotypes (Figure 2-3C). Thus, the structure of the MavE protein harbors several functional motifs including an NPxY eukaryotic motif, and these motifs are required for the function of MavE in intracellular proliferation of *L. pneumophila*.

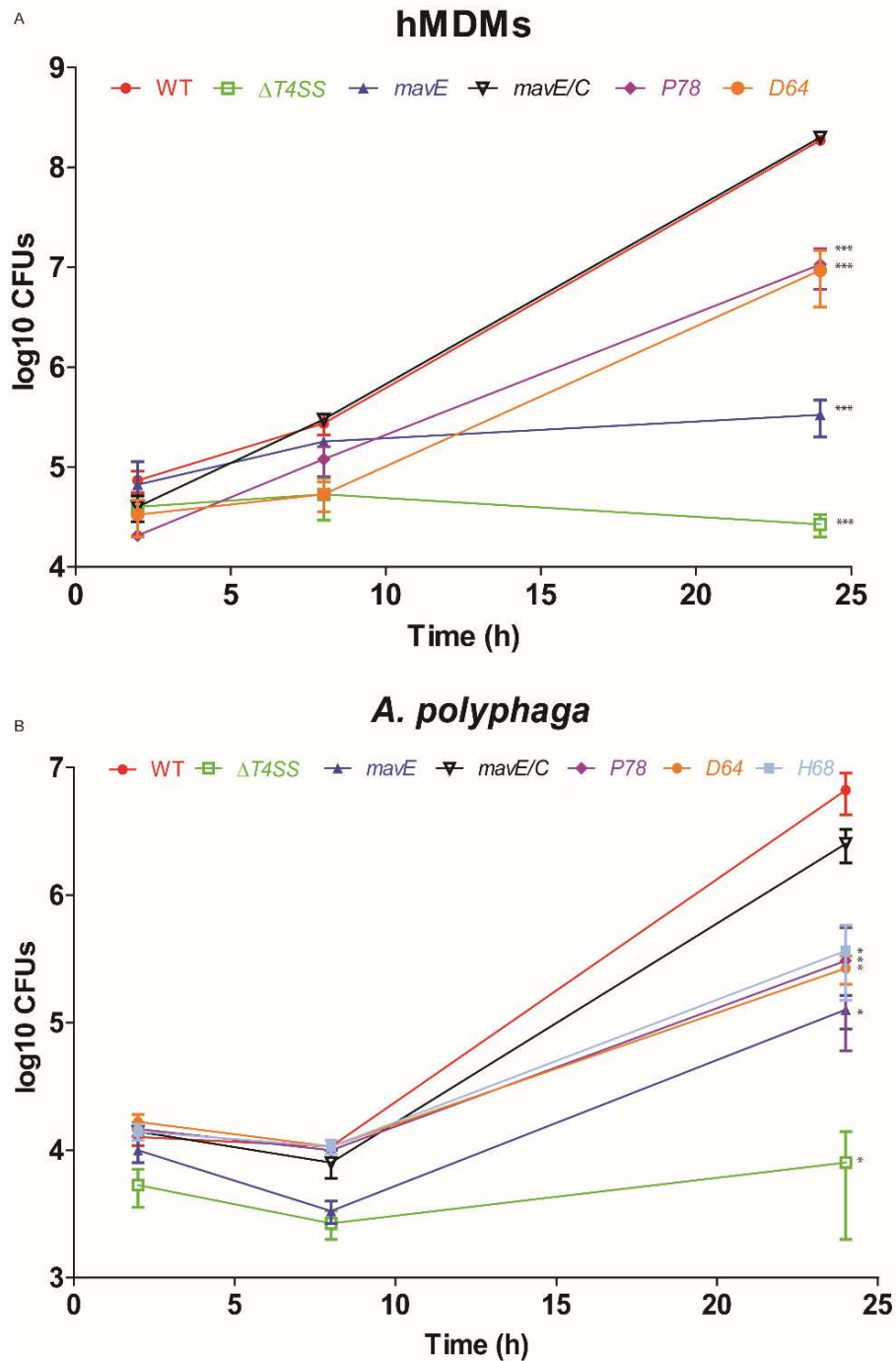


Figure 2-9: The role of the NPxY motif in biological function of MavE in hMDMs and *A. polyphaga*. (A) hMDMs and (B) *A. polyphaga* were infected with the WT strain, the *T4SS* mutant, the *mavE* mutant, NPxY substitution mutants (D64A and P78A), and complemented *mavE* mutant (*mavE/C*), and number of CFUs were determined at 2, 8, and 24 h post-infection. Data points represent (mean CFUs \pm SD, n = 3) and are representative of three independent experiments. Data points represent (mean CFUs \pm SD, n = 3) and are representative of three independent experiments. (Student *t*-test, * $p \leq 0.05$; ** $p \leq 0.01$; *** $p \leq 0.001$)

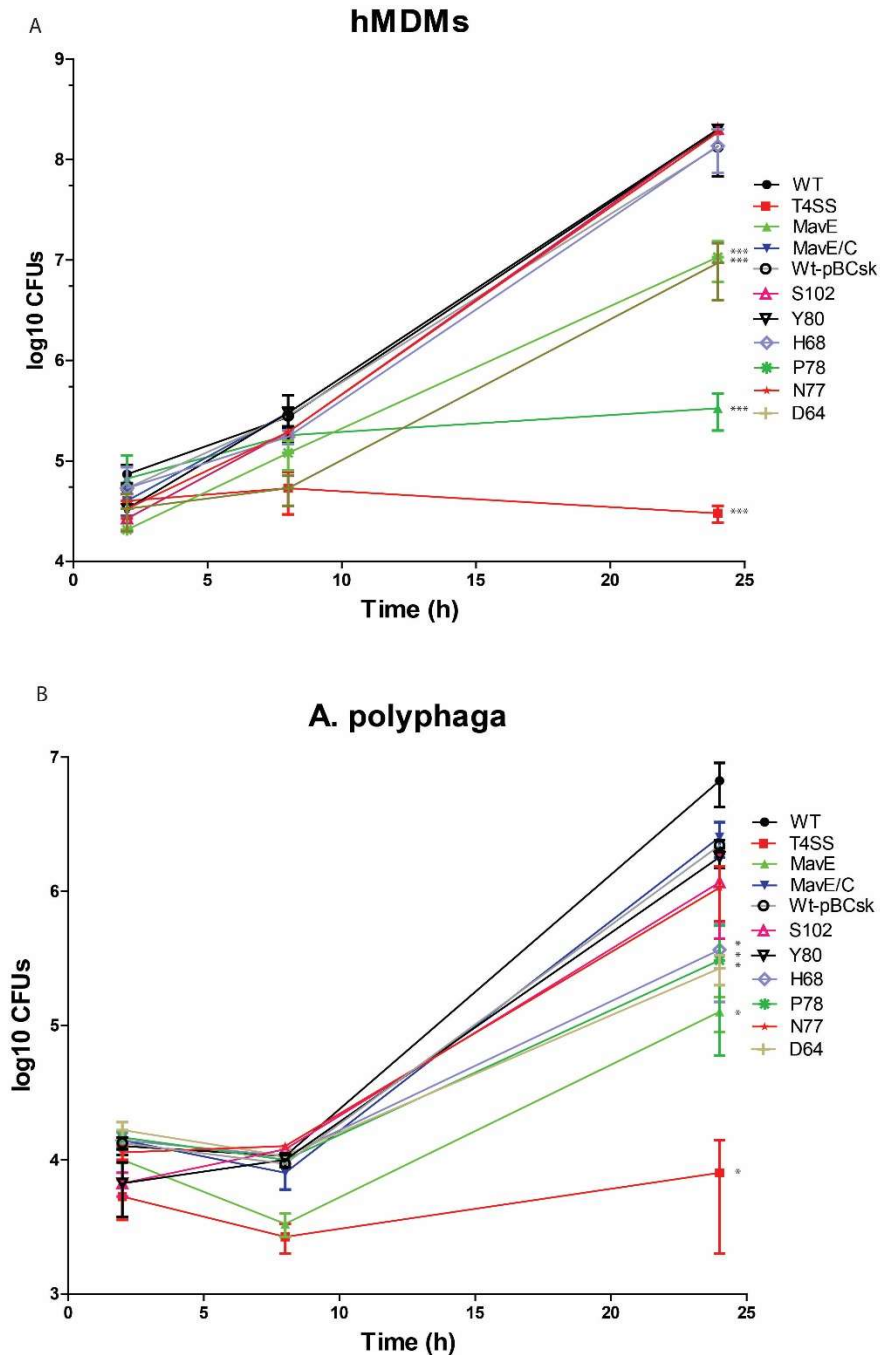


Figure 2-10: The role of the NPxY motif in biological function of MavE in hMDMs and *A. polyphaga*. Showing all point mutations (A) hMDMs and (B) *A. polyphaga* were infected to determine intracellular replication of the WT strain, the $\Delta T4SS$ mutant, the *mavE* mutant, NPxY substitution mutants (D64A, P78A, S102A, Y80A, H68A and N77A), the WT strain harboring the pBCsk vector, and complemented *mavE* mutant (*mavE/C*), hMDMs. The number of CFUs was determined at 2, 8, and 24 h post-infection. Data points represent (mean CFUs \pm SD, n = 3) and are representative of three independent experiments done in triplicate. (Student *t*-test, * indicates $p \leq 0.05$; ** $p \leq 0.01$; *** $p \leq 0.001$).

To determine if the *mavE* substitution mutants shown essential for intracellular replication in hMDMs also exhibit altered phagosome biogenesis, we utilized confocal microscopy to determine co-localization of the LCV with the ER marker, KDEL (Figure 2-11). The additional substitution mutant, H68A, shown to be attenuated in *A. polyphaga* and substitution mutant, S102A, which did not show attenuation, were used as controls. The data showed that 92% of LCVs harboring wild type bacteria co-localized with KDEL, while only 12% of the *mavE* mutant strain-containing vacuoles co-localized with the marker (Figure 2-11). Much like the *mavE* mutant strain-containing LCVs, 14% of the D64A substitution mutant LCVs and 11% of the P78A substitution mutant LCVs co-localized with KDEL. For the controls, 87% of the H68A substitution mutant and 90% of the S102A substitution mutant containing LCVs co-localized with the ER marker KDEL.

Importantly, ~90% of the LCVs containing the P78A and the D64A substitution mutants' bacteria co-localized with the LAMP1 marker, similar to the *mavE* mutant, while only 7% of the wild type containing LCVs co-localized with the marker (Figure 2-12). The controls, S102 and the H68A substitution mutants' LCVs showed 5-9% co-localization with LAMP1.

Our data showed that the D64A substitution mutant showed 70-75% co-localization with Cathepsin D, similar to the *mavE* mutant (Figure 2-13). Importantly, 66% of the P78A containing LCVs co-localized with Cathepsin D, similar to the *mavE* null mutant (Figure 2-13). Only 8% of LCVs harboring the wild type strain localized with the lysosomal marker Cathepsin D. Only 10-13% of the LCVs containing the H68A

and S102A substitution mutants co-localized with Cathepsin D. Importantly, similar to the *mavE* mutant, the majority of the P78A and D64A substitution mutant bacteria exhibited altered morphology with exaggerated rounding and blebbing, indicative of bacterial degradation and consistent with fusion of the LCV to the lysosomes. Taken together, the two substitution mutants, D64A and P78A, phenocopied the *mavE* null mutants in failure to create ER-derived vacuoles that bypass the lysosomal degradation pathway, and to proliferate in hMDMs. Thus, the P78 residue within the NPxY motif and the D64 residue are required for the function of MavE in phagosome biogenesis and lysosomal evasion.

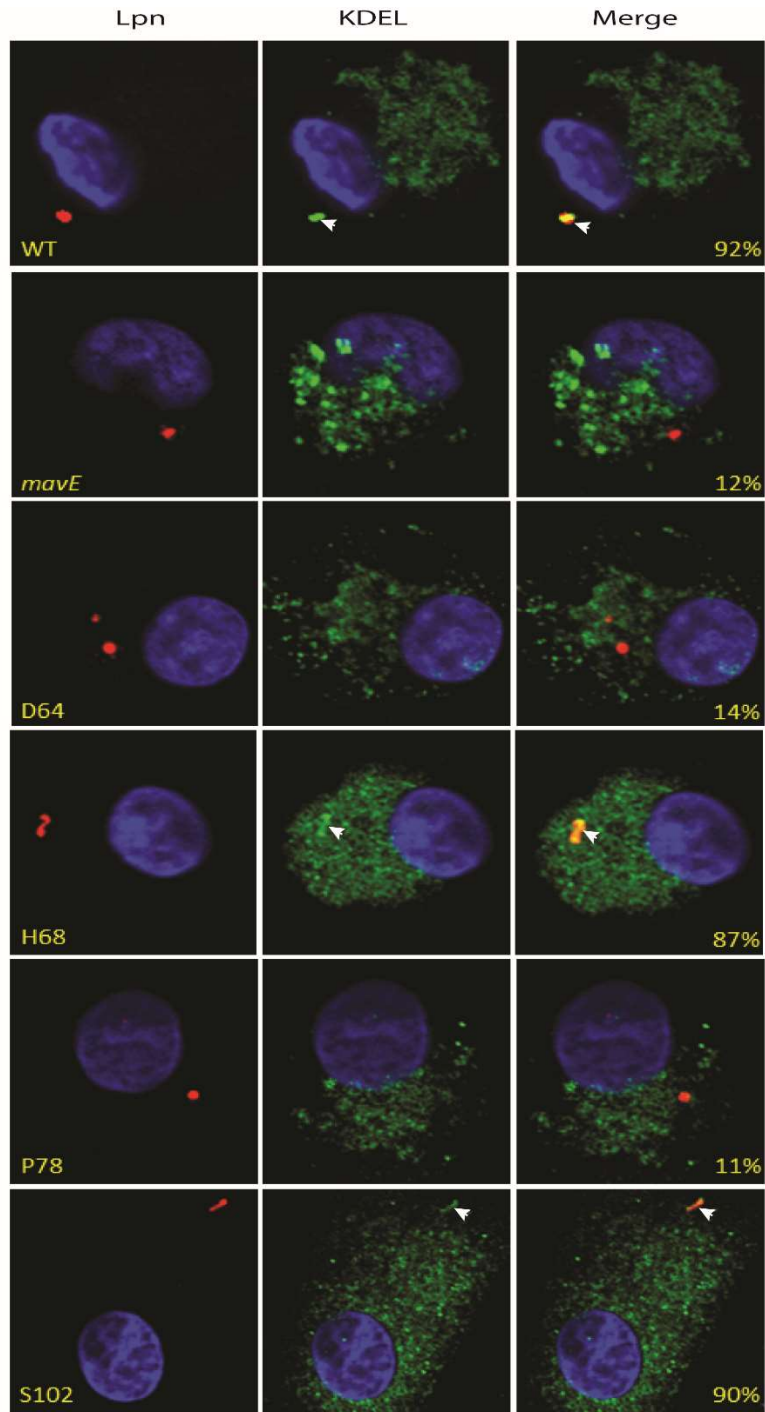


Figure 2-11: Remodeling of the vacuoles with the ER. Representative confocal microscopy images of co-localization of the LCVs containing wild type, *mavE* mutant, or NPxY substitution mutants; D64A, H68A, P78A, and S102A strains labeled with the ER marker, KDEL (green), DAPI (blue) and anti-*Legionella* (red). Quantification of co-localization with the LCV (indicated by arrowheads-yellow) is shown in merged images. All analyses were performed on 100 infected cells analyzed from multiple cover slips. The results are representative of three independent experiments performed in triplicate.

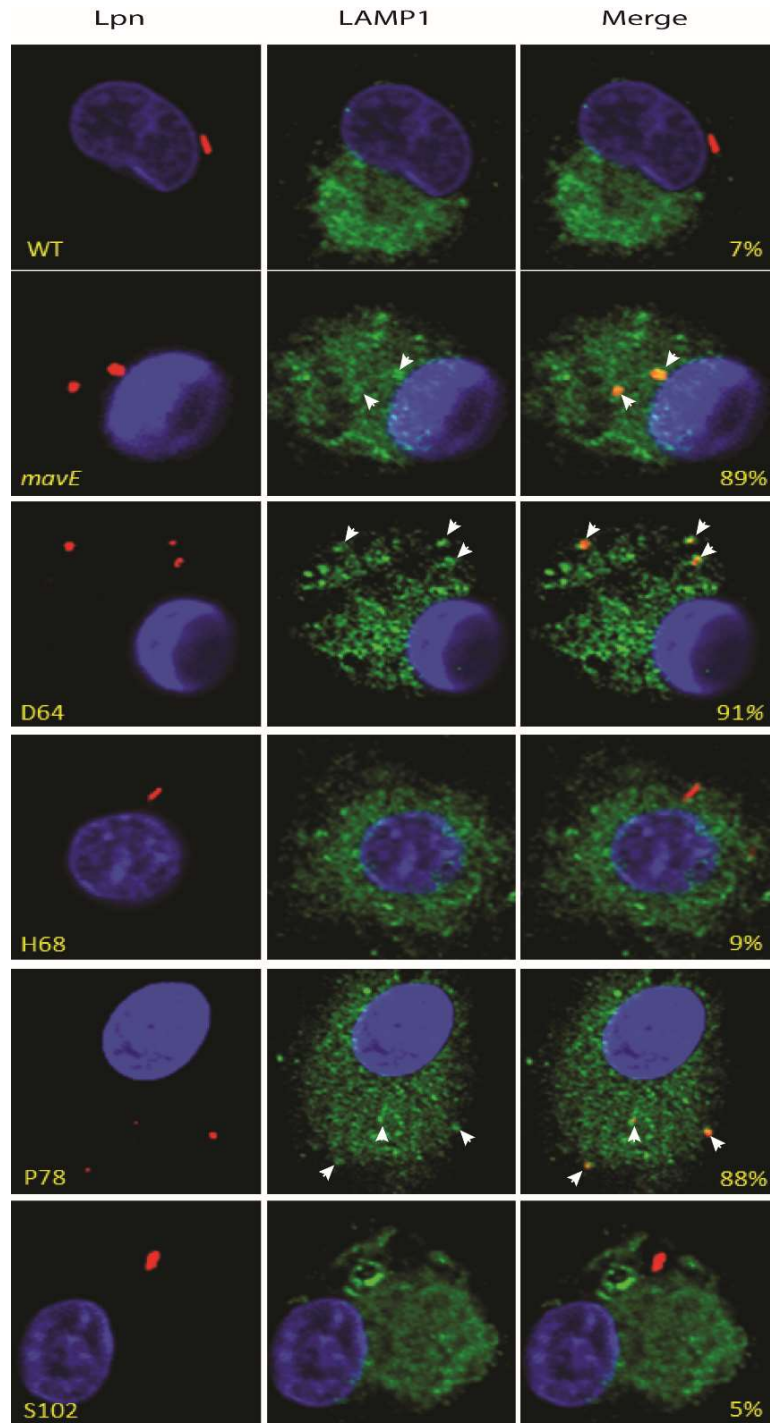


Figure 2-12: Fusion of the vacuoles containing the *mavE* substitution mutants with the late endosomes/lysosomes. Co-localization of the LCVs containing wild type, *mavE* mutant, or the NPxY substitution mutants; D64A, H68A, P78A, and S102A strains with the late endosome/ lysosomal marker, LAMP1 (green), DAPI (blue) and anti-*Legionella* (red). Quantification of co-localization with the LCV (indicated by arrowheads-yellow) is shown in merged images. All analyses were performed on 100 infected cells analyzed from multiple cover slips. The results are representative of three independent experiments performed in triplicate.

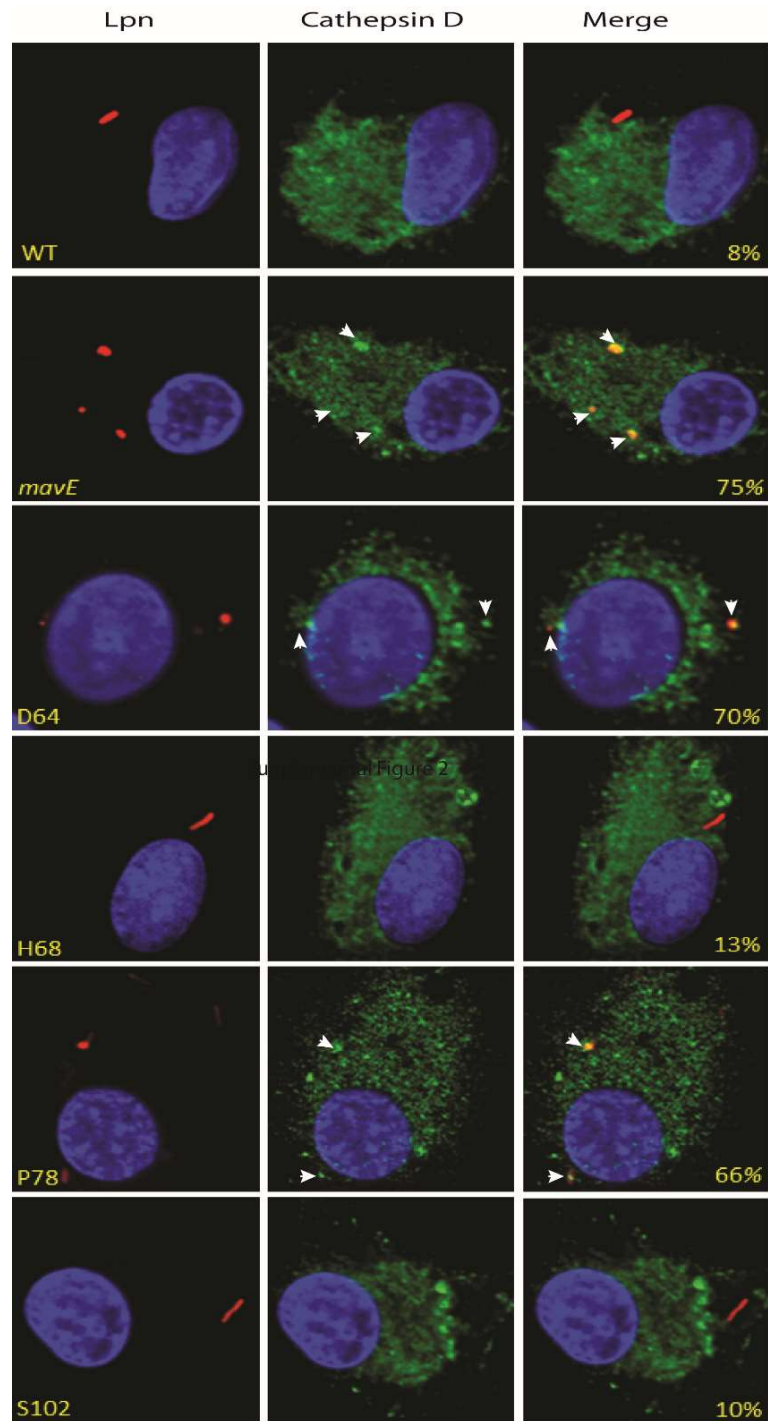


Figure 2-13: Fusion of the vacuoles containing the *mavE* substitution mutants with the lysosomes. Co-localization of the LCVs containing wild type, *mavE* mutant, or the NPxY substitution mutants; D64A, H68A, P78A, and S102A strains with the lysosomal marker, Cathepsin D (green), DAPI (blue) and anti-*Legionella* (red). Quantification of co-localization with the LCV (indicated by arrowheads-yellow) is shown in merged images. All analyses were performed on 100 infected cells analyzed from multiple cover slips. The results are representative of three independent experiments performed in triplicate.

Discussion

Intracellular pathogens, whether cytosolic or intra-vacuolar within macrophages have evolved with various idiosyncratic mechanisms to evade various innate defense processes to avoid degradation within macrophages [230, 302-304]. These pathogenic mechanisms involve the injection or secretion of pathogenic effectors into the host by various secretion or injections apparatuses designated type I-IX translocation system [305-308], and are present in extracellular pathogens, such as *Bordetella* [309], as well. These effectors modulate various cellular processes as well host metabolism to render the host cell suitable as a proliferative nutrient-rich niche [302, 310-316]. Cytosolic pathogens, such as *Rickettsia*, have evolved to evade the host cytosolic anti-microbial processes [317, 318]. Modulation of host metabolism is a general common theme among intracellular pathogens, leading to suitable nutritional niche for pathogen proliferation, and that has been well characterized for *Mycobacterium* [297, 311, 312, 319-321]. For intra-vacuolar pathogens, the crux of these host processes is evasion of the endosomal-lysosomal degradation pathway by most intra-vacuolar pathogens, such as *Mycobacterium*, *Chlamydia*, and *Salmonella* [235, 270]. Modulation of the macrophage autophagy [322] and M1 vs. M2 polarization by intracellular pathogens [89] is an emerging theme to modulate the host inflammatory response [323, 324]. The intra-vacuolar pathogen, *L. pneumophila* resides within the LCV that seems to be excluded from the endocytic pathway and is more of an ER-like compartment than a phagosome [203, 235]. While there are numerous studies on translocated effectors of *L. pneumophila* and few of them have a partial role in lysosomal evasion, none of the effectors are indispensable for lysosomal evasion [166, 203, 325]. With few exceptions, single effector deletions for most

characterized effectors of *L. pneumophila* do not exhibit a defective intracellular growth phenotype [326]. Redundancy among the *L. pneumophila* effectors occurs in different manners and deletion of redundant paralog effectors does not always impair intracellular growth [206-208]. Here, we show MavE is the first effector to be indispensable for both phagosome biogenesis and lysosomal evasion by *L. pneumophila*. The altered LCV biogenesis of ER remodeling in absence of MavE could be an indirect by-product of the altered lysosomal evasion. MavE is localized at the cytosolic side of the LCV poles and is likely functioning in subverting vesicular fusion with the endocytic pathway. It has been shown that polar localization is a key feature of virulence of *L. pneumophila*, and this polarity could result in an increased localized concentration of sub-domain of certain effectors at the LCV pole; possibly meeting a critical threshold concentration necessary for effector activity [173]. Although ER remodeling of the LCV and its lysosomal evasion are independent processes, it is not known which comes first [327]. LCVs communicate with and modulate the secretory vesicle trafficking pathway; however, little is known about the temporal aspect of ER remodeling and lysosomal evasion by the LCV [327].

The MavE structure contains a core domain reminiscent of the grass pollen allergen, Phlp 5b. Comparing to allergen Phlp 5b, MavE contains a long insertion loop located between helix B helix C. These insertions represent a region of functional significance to MavE, as their absence in Phlp 5b suggests it is dispensable for protein stability. It has been suggested that the compactness of the twinned two-helix core domain facilitates proteolytic resistance in Phlp 5b [301]. In accordance with this notion, MavE may have evolved this domain to act as a robust scaffold for displaying functional elements to binding partners. The fact that Phlp 5b retains allergenicity can further rationalize this claim, as *L.*

pneumophila effectors must resist innate immune defenses. This stability might be essential for effectors performing a critical function in virulence, especially those having no redundant counterpart.

Structural features outside the MavE core domain are of functional significance to this protein. The loop connecting helices B and C is the longest in our model and contains a region of conformational heterogeneity, as evidenced by high B-factors and the absence of clear electron density. Intriguingly, the B-C loop harbors an NPxY sequence, which is the canonical phosphotyrosine-binding (PTB)-domain interacting motif [328]. The presence of this motif on a flexible, solvent exposed loop in MavE may suggest a role for this protein in recruiting PTB-domains, which predominantly exist on adaptor or scaffold proteins [294]. The two substitution mutants, D64A and P78A, are essential for MavE function within hMDMs and *A. polyphaga*, with an additional mutant, H68A to be essential in amoebae. Neither the N77A nor Y80A variants significantly impede *L. pneumophila* replication within hMDMs, whereas all three NPxY motif variants are similarly attenuated in *A. polyphaga*. The attenuated replication of the D64A and H68A substitution mutants can be explained by disrupting the putative activity of MavE. However, it is plausible that certain substitution of residue (D/H) for a nonpolar one (A) may alter the structure due to differences in electronegativity. Our findings highlight the significance of the NPxY motif, and specifically P78, to the function of MavE and possible *L. pneumophila* divergence between human and amoebae hosts. The variation between essential MavE function within hMDMs and *A. polyphaga* of the substitution mutants may be due to the evolutionary distance between host cells. The evolution of amoeba host-specific effectors that modulate amoeba-specific cellular processes by *L. pneumophila*

may explain why only two substitution variants of MavE result in loss of its function in biogenesis of the LCV in hMDMs.

The proline residue within NPxY has been shown to form a β -turn structure that distinguishes this motif from the similar NxxY sequence, which is also recognized by adaptor proteins [329]. This structural distinction between NPxY and NxxY provides a source of specificity for adaptor proteins [330]. Our results suggest that the NPxY motif of MavE has a β -turn structure that is critical for its interaction with host adaptors as well as metaeffector(s). Further investigation of these host adaptors and other PTB-domain containing proteins that are selective for NPxY motifs will provide additional insight into the role of MavE.

The primary hosts of *L. pneumophila* are lower eukaryotes, such as free-living amoebae, which encode a small number of PTB-domain containing proteins [331]. Only two PTB-domain containing proteins are present in *Dictyostelium discoideum*, namely Talin A and B [294]. These proteins link the cytoplasmic domains of integrin β -subunits to actin filaments, and thereby promote the formation of cellular junctions with the extracellular matrix. *Acanthamoeba castellanii*, a natural host of *L. pneumophila*, also encodes a putative Talin protein [332]. Since Talin is the only PTB-domain containing protein found in the natural hosts of *Legionella*, MavE may interfere with host processes requiring functional Talin [294]. Specifically, the recruitment of Talin by MavE could disrupt the organization of host actin [333] and thus alter the standard progression of vacuolar biogenesis events. In this way, MavE may participate in evasion of LCV-lysosome fusion.

Helices B and C of MavE (39-172) contain S102, H68 and D64 in a negatively charged pocket on the protein surface. Although these residues do not conform to the hydrogen bond network characteristic of a serine protease catalytic triad [334], their divergence from this pattern may be an artifact of crystal packing. Indeed, conformational changes in the flexible loop connecting B and C may affect the orientation of these two helices relative to one another. In addition, the loop connecting C and D is unclear in the electron density, suggesting flexibility in this region. Since movement of this loop would affect the orientation of C, this too could contribute to structural changes required to form the canonical catalytic triad. It is possible that our C-terminal truncation produced conformational changes in the soluble domain of MavE, which widen the putative active site and render it non-catalytic. Alternatively, the catalytic triad containing Ser102, His68, and Asp64 found in MavE may not exhibit a protease catalytic activity. Further studies evaluating the proteolytic activity of MavE will be informative.

In summary, our data show that MavE is involved in the acquisition of ER-derived membranes by the LCV and in evasion of lysosomal fusion. It is likely that both functions depend on the NPxY motif located within a solvent exposed loop on the MavE structure. By mediating interactions with adaptor proteins, the NPxY motif of MavE may coordinate LCV trafficking through interaction with host adapter proteins and other *L. pneumophila* metaeffectors such as Y1fA/LegC7. Because of the unusually large repertoire of effectors, it is likely that additional *L. pneumophila* effectors also function to facilitate lysosomal evasion by the LCV [277, 292, 335]. These effectors are likely to function in concert with temporal coordination among the effectors to enable ER remodeling and lysosomal evasion of the LCV. Future studies identifying any key players that interact with MavE as a

complex and function with MavE in lysosomal evasion will generate a broader understanding of the main virulence strategy utilized by *L. pneumophila*.

Materials and Methods

Strains and cell lines

L. pneumophila strain AA100/130b (ATCC BAA-74), and the T4SS-deficient mutant (*lspG*) were grown on BCYE agar [261]. To generate an isogenic *mavE* deletion mutant, 2 kb of DNA flanking either side of the *mavE* gene was amplified using PCR using primers listed in Table 1 and cloned into the shuttle vector, pBCSK+ (StrateGene), resulting in pBCSK+*mavEKO1*. To delete the entire *mavE* gene within pBCSK-*mavEKO1*, inverse PCR was employed using primers listed in Table 1, resulting in a pBCSK+*mavEKO2*. The kanamycin resistance cassette from the Ez-Tn5 transposon was amplified using primers listed in Table 1 and the resulting PCR product was subcloned into pBCSK+*mavEKO2* in between the *mavE* flanking DNA regions using standard molecular biology procedures, resulting in pBCSK+*mavEKO3*. This plasmid was introduced into *L. pneumophila* AA100 via natural transformation, as described previously[216]. Following 3 days, natural transformants were recovered by plating on BCYE agar supplemented with 50 µg/ml kanamycin. To confirm deletion of the *mavE* gene in the transformants, PCR was used using the primers listed in Table 1. To complement the *mavE* mutant, PCR was used to amplify the *mavE* gene and its upstream promoter region using primers listed in Table 1, and subcloned into pBCSK+, generating pBCSK+*mavE/C*. This plasmid was introduced into the *mavE* mutant via electroporation as described previously[336]. Complemented *mavE* mutants were selected on BCYE plates supplemented with 5 µg/ml chloramphenicol, resulting in the complemented strain,

mavE/C. For infections of cell monolayers, *L. pneumophila* was grown in BCYE agar plates with appropriate antibiotic selection at 37°C for 3 days prior to use in infections, as described previously [337]. Human monocyte-derived macrophages (hMDMs) were isolated from healthy donors and cultured in RPMI 1640 (Corning Cellgro) as described previously [337, 338]. HEK293T cells (ATCC) were cultured in DMEM (Gibco) supplemented with 10% fetal bovine serum as previously described [337, 338]. All methods were carried out and approved in accordance with the University of Louisville Institutional Review Board guidelines and blood donors gave informed consent as required by the University of Louisville Institutional Review Board (IRB # 04.0358).

TABLE 1
Primers used in this study^a

| Primer ^b | Orientation ^c | Sequence |
|--|--------------------------|----------------------------------|
| Primers used to clone <i>mavE</i> and flanking DNA to generate the <i>mavE</i> mutant (pBCSK plasmid) | | |
| MavE KO | F | GTCGACAGGTAATTTCTGATAATGAAC |
| MavE KO | R | TCTAGAATAGAGCCGTTGGAAGAAAGT |
| Primers used for inverse PCR to delete <i>mavE</i> from the above fragment to make the <i>mavE</i> mutant | | |
| MavE KO | F | aaatttGTTTAAACGGAAGTGTTTACAGGATT |
| MavE KO | R | CCTGCAGGAGGTAGTGTTTTATACTAA |
| Primers used to clone into pBCSK to complement the <i>mavE</i> mutant | | |
| MavE/C | F | AAGCTTATTATATAATGATTTATCAATTT |
| MavE/C | R | GGATCCTATTTGGTCCATCTTGAAC |
| Primers used to confirm KO of <i>mavE</i> in <i>L. pneumophila</i> | | |
| MavE KO test | F | TTTTATATCTTTAGGTTTCATTCA |
| MavE KO test | R | CTTGAAACGACCGTATTTG |
| Primers used for cloning into the p3XFLAG vector for eukaryotic expression | | |
| 3XFLAG <i>mavE</i> | F | AAGCTTCTGACTCGATTCATAATGCTTT |
| 3XFLAG <i>mavE</i> | R | AGATCTTTATGGTTTGTGCCAAACAAC |
| Primers used for cloning into the 4HA vector for bacterial expression | | |
| HA MavE | F | ggatccCTGACTCGATTCATAATGC |
| HA MavE | R | aagcttTTATGGTTTGTGCCAAACA |

^aAll primers are 5'-phosphorylated.

^bKO, knockout.

^cF, forward; R, reverse.

DNA manipulations

DNA manipulations, generation of MavE substitutions, and restriction enzyme digestions were performed using standard procedures [338, 339]. *L. pneumophila* WT expression HA₄-PieE were obtained from MRC Centre for Molecular Bacteriology and Infection. The MavE construct replaced the PieE sequence using the same methods and restriction sites previously described [340]. Restriction enzymes and T4 DNA ligase were purchased from NEB (Madison, WI). Plasmid preparations were performed with the PureLink HiPure Plasmid Maxiprep kit (Invitrogen). Purification of DNA fragments from agarose gels for subcloning was carried out with the QIAquick gel purification kit (Qiagen Inc, Valencia, CA).

Intracellular replication in hMDMs and Amoeba

For infection of cell monolayers, *L. pneumophila* strains were grown in BYE broth with appropriate antibiotic selection, at 37 °C with shaking, to post-exponential phase (OD_{550nm} 2.1–2.2). *A. polyphaga* (ATCC) was cultured in PYG media at 22 °C, experiments were performed in PY media at 35 °C, as previously described [337]. Human monocyte-derived macrophages (hMDMs) were isolated from healthy donors and cultured in RPMI 1640, supplemented with 10% fetal bovine serum, as previously described [337, 338]. The wild type strain; the isogenic mutants, *T4SS* and *mavE*; and complements *mavE/C*, *mavE/Y80*, *mavE/H68*, *mavE/P78*, *mavE/N77*, *mavE/D64*, *mavE-pBCsk*, *mavE-4HA*, and *WT-pBCsk* were grown to post-exponential phase in BYE broth at 37 °C with shaking prior to infection and used to infect hMDMs and *A. polyphaga*, as previously described [337, 338]. A total of 1×10^5 host cells were plated in 96 well plates and infected with *L. pneumophila* at an MOI of 10. Plates were centrifuged at

200 × g (5 mins), to synchronize infection. After 1 h, cells were treated with gentamicin to kill extracellular bacteria, as previously described [337, 338]. Over a 24 h time course, host cells were lysed with sterile water (hMDMs) or 0.02% v/v Triton X-100 (*A. polyphaga*). *L. pneumophila* CFUs were determined by plating serial dilutions onto BCYE agar.

Transfection of HEK-293 cells (ATCC)

The *mavE* gene was cloned into the mammalian expression vector, p3XFlag-CMV-10 (Sigma). To generate the *mavE*^{-9L¹⁰P/AA} allele, the wild type p3XFlag-CMV-10 MavE plasmid was used as a template for PCR based site directed mutagenesis. HEK-293 cells (ATCC) were grown to 80% confluency and plated onto poly-L-lysine-treated coverslips in 24 well plates. Following 24 h of incubation, HEK293T cell monolayers were transfected with ~2 µg of plasmid DNA encoding 3X-FLAG MavE/well by using polyethylenimine (Polysciences) for 24 h, following the manufacturer's recommendations (Roche) as previously described [341, 342].

Mouse model

For testing the virulence of the *mavE* mutant, specific pathogen-free, 6–8 weeks old A/J mice (Jackson) were used, as previously described [338, 343]. Groups of 3 A/J mice, for each time point, were infected intratracheally with 1 × 10⁶ CFUs. The wild type strain: the isogenic mutant *mavE* and complemented *mavE/C strains*, were grown to post-exponential phase on BCYE plates at 37 °C for 72 hours prior to infection and used to infect A/J mice. At 2, 6, 12, 24, 48, and 72 h after infection mice were humanely sacrificed and lungs, liver, and spleen were harvested and homogenized in sterile saline (5 ml) followed by cell lysis in distilled water. To determine CFUs, serial 10-fold

dilutions were plated on BCYE agar and incubated at 37 °C for 72 hours and colonies were enumerated. The percent survival was recorded for groups of 5 A/J mice infected using an inoculation of 1×10^7 CFUs (LD50) for WT, *mavE*, and *mavE/C* strains from 0 to 10 days post-infection. All the experimental procedures were in accordance with National guidelines and were approved by the Institutional Animal Care and Use committee (IACUC) at Faculty of Medicine, University of Rijeka. To determine any level of difference between groups, a value of “E” (the degree of freedom of analysis of variance or ANOVA), which should lie between 10 and 20 was determined to be 12 based off our sample size. ($E = \text{total number of animals} - \text{total number of groups}$).

Confocal microscopy

Processing of infected cells for confocal microscopy was performed as we described previously [338]. 4HA-tagged MavE constructs in both wild type and *T4SS L. pneumophila* were analyzed for confocal following 1hr infection in hMDMs. Co-localization of the LCVs containing WT, FK-WT, *mavE*; and complements *mavE/C*, *mavE/Y80*, *mavE/H68*, *mavE/P78*, *mavE/N77*, *mavE/D64*, *mavE-pBCsk*, and *WT-pBCsk* were analyzed for confocal following 2hr infection in hMDMs. Cells were prepared using the same protocol for intracellular replication except 2×10^5 host cells were plated on coverslips in 24 well plates. The monolayers were infected with *L. pneumophila* at an MOI of 10. Plates were centrifuged at $200 \times g$ (5 mins), to synchronize infection. After 1 h, cells were treated with gentamicin to kill extracellular bacteria, as previously described [337, 338]. For 4HA-tagged MavE constructs, following fixation in 10%NBF, the plasma membranes of infected hMDMs were differentially permeabilized using digitonin at 1 mg/ml in KHM Buffer. Incubated for exactly 1 min at RT and immediately

washed all wells 3x with 0.5 ml of KHM Buffer [344]. For all other confocal experiments, cells were fixed in -20°C methanol for 5 minutes and rinsed 3x in 10% PBS. For antibody labeling for MavE, mouse anti-*L. pneumophila* was used at a dilution of 1:500 and detected by Alexa-Fluor 488-conjugated donkey anti-mouse IgG (1:1000) (Invitrogen, Carlsbad, CA) and rabbit anti-MavE (ThermoFisher Scientific) was used at a dilution of 1:500 and detected by Alexa-Fluor 555-conjugated donkey anti-rabbit IgG (1:1000) (Invitrogen, Carlsbad, CA). For antibody labeling for localization, rabbit anti-*L. pneumophila* was used at a dilution of 1:750 and detected by detected by Alexa-Fluor 555-conjugated donkey anti-mouse IgG (1:1000)(Invitrogen, Carlsbad, CA) mouse monoclonal anti-Cathepsin D (abcam) was used at a dilution of 1:200 and detected by Alexa-Fluor 488-conjugated donkey anti-mouse IgG (Invitrogen, Carlsbad, CA), mouse monoclonal anti-KDEL (enzo) was used at a dilution of 1:200 and detected by Alexa-Fluor 488-conjugated donkey anti-mouse IgG (Invitrogen, Carlsbad, CA) at a 1:1000 dilution, mouse monoclonal anti-Lamp 1 (abcam) was used at a dilution of 1:200 and detected by Alexa-Fluor 488-conjugated donkey anti-mouse IgG (Invitrogen, Carlsbad, CA) at a dilution of 1:1000. For detection of 3X-FLAG tagged proteins during transfection experiments, mouse monoclonal anti-FLAG (Sigma) antibodies were used followed by detection with Alexa-Fluor 555-conjugated donkey anti-mouse (Invitrogen, Carlsbad, CA) at a 1:1000 dilution. DAPI was used for all experiments at a 1:5000 dilution. An Olympus FV1000 laser scanning confocal microscope was used in house to examine cells as we described previously [298]. On average, 10–20 0.5 µm serial Z sections of each image were captured and stored for further analyses, using Adobe Photoshop CS3. A total of 100 infected cells for each replicate were manually counted

for presence or absence of localization and a percentage given. A total of 3 biological repeats were analyzed for the presence or absence of localization.

Cloning of recombinant MavE

The MavE (Lpg2344) gene was amplified from *Legionella pneumophila* (Philadelphia) genomic DNA by PCR. Residues 183 – 204 are predicted to comprise a transmembrane (TM) region (Program Phobius) [345]. To clone only the soluble domain of MavE, we amplified the DNA sequence encoding residues 2 – 172. This construct terminates just after the final hydrophilic helical stretch and excludes the following loop and TM region. The MavE (2-172) insert DNA sequence was placed into pMCSG7 and pRL652 vectors by ligation independent cloning (LIC), incorporating an N-terminal TEV-cleavable His6- or GST-tag, respectively [346, 347]. His6-MavE (2-172) expressed poorly in BL21 (DE3) pLysS (promega) and GST-MavE (2-172) did not readily bind the glutathione resin. Running PsiBLAST on MavE showed that most homologous proteins have start sites corresponding to residue M38. To explore the possibility of a misannotated start site, we amplified MavE (39-172) using the following primers:

Sense: 5'-

TACTTCCAATCCAATgccACTAGATTTGAAAGAAATTCCTGATTAATAGC-3'

Antisense: 5'-

TTATCCACTTCCAATgTTATTCGTCTTTGAGTTTGGCAATTAATTCTT-3'. As

previously described, the MavE (39-172) DNA insert was placed into pMCSG7 and pRL652 vectors via LIC using the extensions underlined above. This construct of MavE was used for expression, purification and crystallization trials.

Protein Expression and Purification

His⁻⁶-MavE (39-172) was transformed into chemically competent BL21 (DE3) pLysS cells and plated on LB agar containing ampicillin (100 µg/ml). A single transformant was inoculated into 20 ml of LB supplemented with ampicillin (100 µg/ml) and glucose (0.4%), and grown overnight at 37°C. This overnight culture was sub-cultured into 1 L of terrific broth (TB) supplemented with ampicillin (100 µg/ml) and grown at 37°C. Once the cell culture reached an optical density (A₆₀₀) of ~1.0, the temperature was reduced to 18°C, 1 mM of Isopropyl β-D thiogalactopyranoside (IPTG) was added to the culture to induce protein expression and the cells were incubated for approximately 16 more hours. Cells were pelleted at 6900 x g for 15 minutes in a Beckman JLA 8.1000 rotor and stored at -80°C until further processed. Approximately 10 grams of pellet was obtained from 1 L of culture. Cells were re-suspended in 30 ml of a lysis buffer (50 mM Tris, pH 8.0, 10% (v/v) glycerol, 0.1% (v/v) Triton X-100) and lysed two times at 35 kPsi in a cell disruptor (Constant Cell Disruption Systems, Kennesaw, Georgia). The lysate was spun at 21000 x g for 30 minutes in a Beckman JA25.50 rotor. Supernatant was added to 5 ml of Qiagen NiNTA beads pre-equilibrated with three column volumes of a standard buffer (20 mM Tris, pH 8.0, 50 mM NaCl) and the beads were washed with 50 ml of standard buffer. Protein was eluted with standard buffer supplemented with 100 mM imidazole. Purified protein was concentrated to 18 mg/ml in a 10 kDa molecular weight cut-off Millipore centrifugal filter at 4000 x g. The hexahistidine tag was cleaved by adding 100 µl TEV protease to 500 µl concentrated MavE and incubating overnight at room temperature. Untagged MavE was then loaded

onto a Biorad SEC70 or GE SEC75 column for buffer exchange and further purification. Peak fractions were collected and concentrated to 25mg/ml for crystallization.

A seleno-methionine derivative of MavE (38-172) was produced by inhibiting methionine biosynthesis immediately prior to induction. Specifically, 100 mg lysine, phenylalanine and threonine and 50 mg isoleucine, leucine and valine were added to 1 L of culture 15 minutes prior to induction. 60 mg L-seleno-methionine was also added to the culture, such that this version of methionine would be incorporated into overexpressed MavE during induction.

Crystallization

Both His⁶-MavE (39-172) and MavE (39-172) were screened for crystallization using Crystal Screen HT, Index (Hampton Research, Aliso Viejo, CA), JCSG Core II and Classics Suite (Qiagen, Toronto, Canada). His⁶-MavE (39-172) did not crystallize under any of the conditions tested, whereas MavE (39-172) produced crystals under several conditions. After optimization by the hanging drop vapor diffusion method, the best crystals were obtained at 20°C in drops containing 1 µl protein in 15 mM Tris-HCl, pH 8.0, 50 mM NaCl mixed with 1 µl of reservoir solution (10% PEG 20000, 0.1 M Citrate, pH 3.0) and suspended over 500 µl reservoir solution.

Data Collection and Structure Solution

The protein crystals were cryo-protected by transferring to 1 µl mother liquor containing 20%(v/v) ethylene glycol. Diffraction data was collected to 1.8Å at the Canadian Macromolecular Crystallography Facility (CMCF) 08ID beamline, Canadian Light Source, using a MAR300CCD Detector [348]. Integration and scaling was carried out using the XDS software package [349] (autoprocess). MavE (39-172) harbours only

one methionine at residue 51 and substitution of this residue for seleno-methionine produced sufficient anomalous signal to solve the structure by single anomalous dispersion (SAD) using the phenix. autosolve script. Refinement of the structure was carried out using phenix. refine [350].

Statistical analysis

All experiments were performed at least three independent biological repeats, and the data shown are representatives of one experiment. To analyze for statistically significant differences between three sets of data, the two-tailed Student's *t*-test was used, and the *p*-value was obtained. (* indicates $p \leq 0.05$; ** indicates $p \leq 0.01$; *** indicates $p \leq 0.001$)

CHAPTER 3:

MAVE INTERACTION WITH HOST PROTEIN ACBD3

Introduction

L. pneumophila has evolved with virulence strategies that use its T4SS secreted effectors to parasitize protozoa and confers the ability to replicate within human phagocytic cells [351]. *L. pneumophila* employs over 350 translocated effectors into the host cell cytosol by the T4SS [158, 186, 286], which are essential for the biogenesis of the LCV, intracellular replication, and prevention of lysosomal degradation. The *L. pneumophila* effectors constitutes the largest arsenal of translocated effectors proteins by any bacterial pathogen [211]. Equipped with these effectors, *L. pneumophila* proliferates to high numbers within its host. Comparative experiments with several infection models including its natural amoeba host and human macrophages have shown that the modulation of diverse host cell functions by the Dot/Icm-translocated effectors are a prerequisite for biogenesis of the LCV [352].

Remarkably, host responses upon contact with *L. pneumophila* starts as early as phagocytosis [155]. Mutants of *L. pneumophila* lacking the response regulator effector LetA are phagocytosed less efficiently by both *D. discoideum* and macrophages [353]. Once phagocytosis is complete, the development of an ER-associated LCV is initiated by several *L. pneumophila* Dot/Icm injected effector proteins. These effectors modulate biogenesis of the LCV by recruiting and altering the composition of phosphoinositides on the LCV membrane along with various GTPases of the Rab and Arf families (Figure 1-3) [352]. An example of this is the ubiquitination and recruitment of Rab10 to the LCV by the SidC/SdcA effector [354]. Manipulation of ER-to-Golgi transport machinery to recruit ER-derived vesicles to the LCV is vital to the biogenesis of the replicative LCV [129].

Therefore, it is likely *L. pneumophila* modulate ER-to-Golgi vesicle traffic by specific effectors.

One of the host regulators of ER-to-Golgi vesicle traffic is the Acyl-Coenzyme A Binding Domain Containing 3 (ACBD3). Other designations for this protein are: peripheral-type benzodiazepine receptor and cAMP-dependent protein kinase associated protein 7 (PAP7), Golgi complex-associated protein of 60kDa (GCP60), Golgi complex-associated protein 1 (GOCAP1), and Golgi phosphoprotein 1 (GOLPH1) [355]. Interestingly, two effector proteins of the intracellular pathogen *Salmonella*, SseF and SseG, interact with the host ACBD3 protein, tethering the *Salmonella* containing vacuole (SCV) to the Golgi [356].

ACBD3 is a Golgi-resident multifunctional protein involved in the maintenance of the Golgi apparatus and functions by recruiting the lipid kinase Phosphatidylinositol 4-kinase beta (PI4KB). Together with the PI4K2A enzyme, PI4KB synthesizes phosphatidylinositol-4-phosphate (PI4P) [355, 357-359]. ACBD3 consists of several domains and its Golgi dynamics (GOLD) domain is localized at the C-terminus and serves as a protein-binding site to most reported ACBD3-interacting proteins (giantin, TSPO, Rhes, PKARI α , and Golgin-160) [355, 357, 360]. Thus, ACBD3 functions as an adaptor protein and signaling center across diverse signaling pathways to regulate myriad of cellular processes including apoptosis, homeostasis, and lipid homeostasis [357]. PI4KB is a soluble cytosolic protein whose primary function is to phosphorylate membrane lipids and generate PI4P [358, 361]. PI4P is an essential lipid found in various membrane compartments including the Golgi, trans-Golgi network (TGN), plasma membrane, endocytic compartments, and the LCV [357, 362]. *L. pneumophila* exploits PI4P to anchor

other injected effector proteins to the LCV to subvert host cell phosphoinositides (PI) metabolism, which is essential for establishment of the replicative LCV [362].

The ACBD3 protein recruits the ER-resident transmembrane protein phosphatase (PPM1L) to ER-Golgi membrane contact sites [363], where PPM1L dephosphorylates the ceramide transport protein CERT and regulates ceramide transport [363]. Ceramide is hydrolyzed and phosphorylated yielding sphingolipids [364], which are membrane lipids involved in interaction of various bacterial pathogens with the host cell [364]. Bacterial pathogens that cannot synthesize sphingolipids, including *Mycobacteria*, *Pseudomonas*, *Neisseria*, *Helicobacter*, *Chlamydia*, and *Legionella*, have developed different strategies to manipulate host sphingolipids to promote their pathogenicity [365]. *L. pneumophila* modulates the host cell sphingolipid metabolism, affecting the level of sphingosine by secreting *LpSPL* that encodes sphingolipid lyase activity in both transfected cells and infected macrophages. [366]. *LpSPL* targets the host's sphingolipid metabolism and restrains starvation-induced autophagy during *L. pneumophila* infection to promote intracellular survival by acting on autophagosome biogenesis [366]. Given the importance of lipid metabolism modulation by *L. pneumophila* during infection, ACBD3 is an excellent candidate to further understand the biogenesis of the LCV.

Results

Identification of the MavE-interacting Host Proteins

To identify host proteins that interact with the *L. pneumophila* translocated effector protein MavE, the proximity-dependent biotin identification (BIOID) strategy was employed [367]. This method is based on proximity-dependent cellular biotinylation of

neighboring proteins (with a practical labeling radius of ~25nm) by a promiscuous bacterial biotin ligase fused to a bait protein (BioID2) to identify protein-protein interactions in living cells [367]. A fusion of BioID2 with MavE harboring a cMyc tag was generated (Figure 3-1A). Plasmids containing BioID2 alone (negative control) or MavE-BioID2 were used to transiently transfect human embryonic kidney (HEK293T) cells for 24 hours. The biotinylated proteins were then purified from the cellular lysates of two biological replicates and identified using mass spectrometry (Table 2). Among the proteins solely identified in the MavE-BioID2 samples was a peptide sequence fragment (MAAVLNAER) that is exclusive to host protein ACBD3 (Figure 3-1B). The biotinylated peptide represents a 98% probability for the presence of ACBD3 and for positive protein identification, the mascot score must be above a 95% confidence level [368].

To confirm interaction of MavE with host protein ACBD3, pacGFP1-C1-MavE and pacGFP1-C1 was constructed and used to transfect HEK293T cells. The MavE-interacting host proteins were purified using magnetic beads conjugated with anti-GFP antibody and subjected to immunoblot with anti-ACBD3 antibody. The immunoblot showed that ACBD3 was specifically pulled down when MavE was ectopically expressed (Figure 3-2). A small amount of background ACBD3 was observed in the GFP pulldown however this is likely indicative of spillover from the total cell lysate containing a high concentration of ACBD3.

TABLE 2

Biotinylated host-MavE interacting protein identified by Mass Spectrometry

| Protein | Identification Probability (Sample #1/ Sample #2) |
|--|--|
| Isoform 2 of Ras-related protein Rab-8A | 87% /13% |
| Function: The small GTPases Rab are key regulators of intracellular membrane trafficking, from the formation of transport vesicles to their fusion with membranes. | |
| AP-1 Complex subunit beta* | 100% |
| Function: Subunit of clathrin-associated adaptor protein complex 1 that plays a role in protein sorting in the late-Golgi/trans-Golgi network (TGN) and/or endosomes | |
| GCP60/ACBD3 | 98%/24% |
| Function: Involved in the maintenance of Golgi structure by interacting with giantin, affecting protein transport between the endoplasmic reticulum and Golgi | |
| Serine/threonine- protein phosphatase 2A* | 98% |
| Function: PP2A is the major phosphatase for microtubule-associated proteins (MAPs) | |
| Arfaptin-2* | 99% |
| Function: Plays a role in constitutive metalloproteinase (MMP) secretion from the trans Golgi network. May have important functions during vesicle biogenesis at certain cargo subdomains, which could be predominantly utilized by secreted MMPs, such as MMP7 and MMP2 | |
| Transmembrane emp24 domain- containing protein 5* | 92% |
| Function: Potential role in vesicular protein trafficking, mainly in the early secretory pathway. Required for the maintenance of the Golgi apparatus; involved in protein exchange between Golgi stacks during assembly. Probably not required for COPI-vesicle-mediated retrograde transport. | |
| Ras-related C3 botulinum toxin substrate* | 85% |
| Function: Plasma membrane-associated small GTPase which cycles between an active GTP-bound and inactive GDP-bound state. In active state binds to a variety of effector proteins to regulate cellular responses. | |

*Only identified in 1 of the MavE-BioID2 biological repeat samples

For positive protein identification probability must be above a 95% confidence level

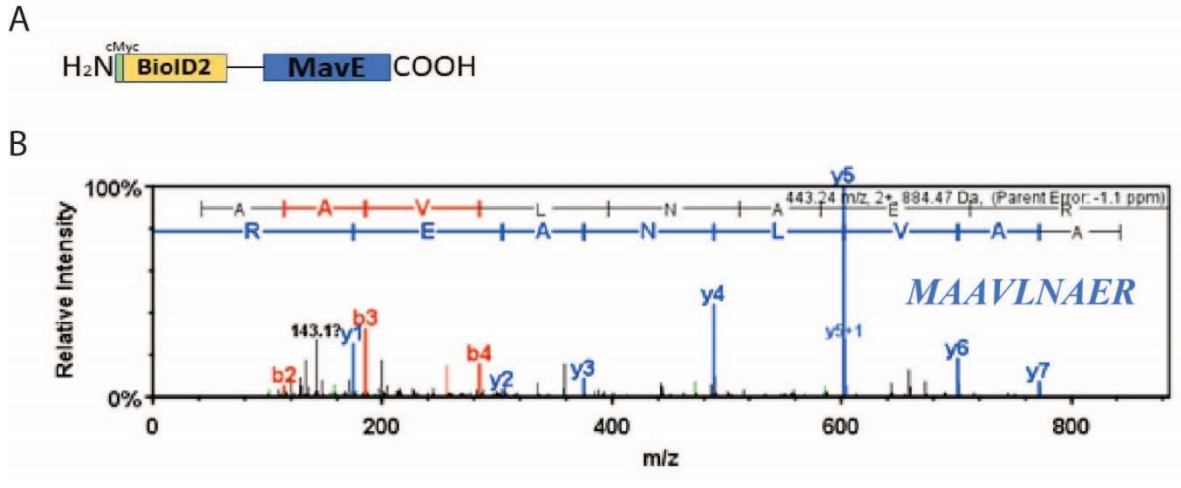


Figure 3-1: MavE interacts with host protein ACBD3. (A) Diagram of BioID2, in yellow, and fusion with MavE, in blue. The line represents a poly-glycine linker, and the green box represents a cMyc tag. (B) Mass spectrum of peptide sequence fragment captured from biotinylated proteins generated during ectopic expression of MavE-BioID2 and purified with streptavidin magnetic beads. This peptide sequence (MAAVLNAER) had a 98% probability in one biological repeat and is exclusive to ACBD3 also known as Golgi resident protein GCP60.

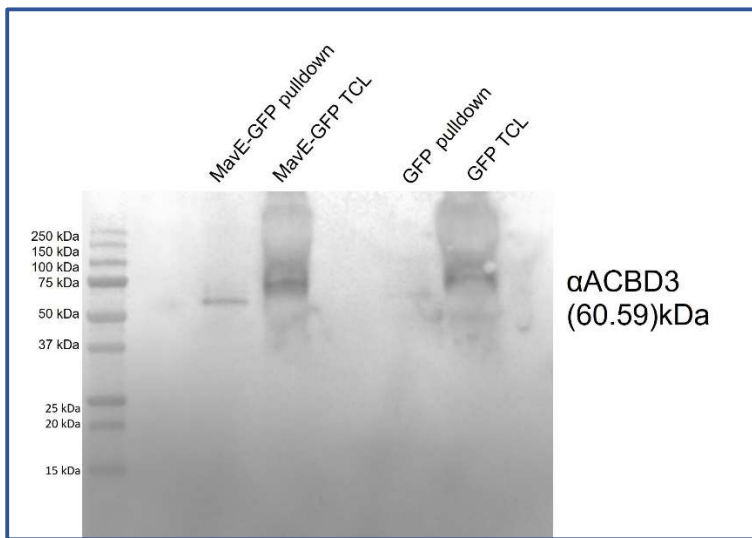


Figure 3-2: Western Blot Analysis of MavE interacts with host protein ACBD3 during ectopic expression. HEK293T cells were utilized to ectopically express MavE-GFP or GFP. Cell lysates were immunoprecipitated (IP) with magnetic anti-GFP beads and the IP was immunoblotted using anti-ACBD3 antibody to detect the presence of ACBD3 in the pulldown of MavE-GFP. TCL stands for total cell lysate. Results are representative of two independent experiments.

Co-localization of ACBD3 with the Legionella containing vacuole in hMDMs

The MavE effector is localized to the LCV membrane at the poles of the vacuole. Since ACBD3 interacts with MavE during ectopic expression, we determined if ACBD3 co-localizes with the LCV during infection using human monocyte derived macrophages (hMDMs). We utilized confocal microscopy to determine co-localization of the LCV with the ACBD3 at 1 hour post infection. The data showed that over 95% of LCVs harboring wild type bacteria co-localized with ACBD3, while only 16% and 11% of the *mavE* mutant and Δ T4SS-containing vacuoles, respectively, co-localized with the ACBD3 (Figure 3-3). Much like WT-containing LCVs, 86% of the complemented mutant (*mavE/C*) containing LCVs co-localized with ACBD3. We conclude that ACBD3 co-localizes with the LCV in a MavE-dependent manner.

ACBD3 gene silencing in HEK293T and hMDMs

MavE is indispensable for lysosomal evasion of the LCV and interacts with the host-ACBD3 protein. We wanted to determine the effect of silencing host protein ACBD3 on LCV biogenesis. We utilized an ON-TARGETplus Human ACBD3 siRNA pool and non-targeting pool to knockdown expression of ACBD3 in hMDMs (Table 4). Despite using high concentration of siRNA, there was no detectable knockdown of ACBD3 (Figure 3-4). This may not be a surprise as primary macrophages are particularly challenging to transfect as the transfection reagent and the transfected nucleic acid are often recognized and result in macrophage activation and degradation of the transfected nucleic acids [369]. Alternatively, we used the same siRNA pools to partially knockdown expression of ACBD3 in HEK293T (Figure 3-5). Optimization for DharmaFECT transfection reagent

was determined as recommended per manufacturer and the maximum recommended volume (μL) of reagent was needed to effectively silence ACBD3 in HEK293T cells.

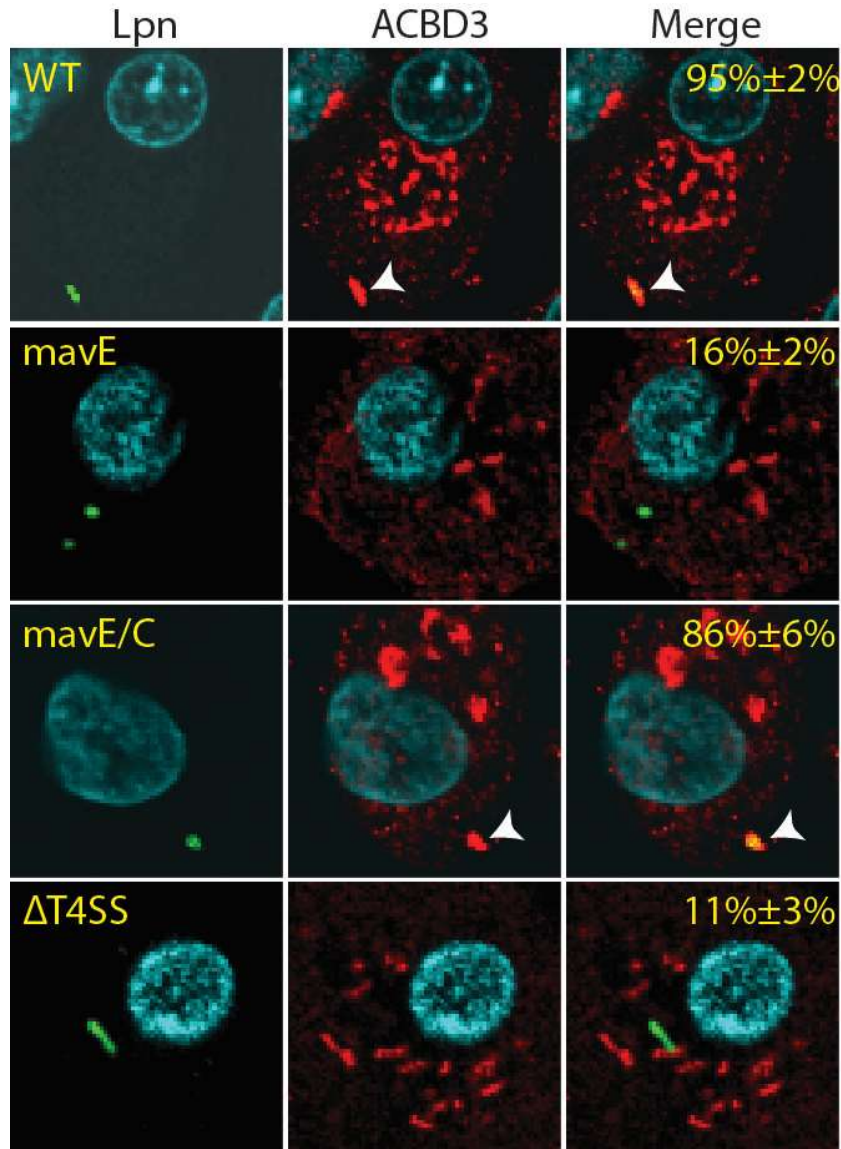


Figure 3-3: Localization of ACBD3 to the LCV during infection of hMDMs.

Representative confocal microscopy images of Co-localization of the LCVs containing wild type, ΔT4SS mutant, *mavE* mutant, or the complemented strain (*mavE/C*) labeled with anti-ACBD3 (red), DAPI (blue) and anti-*Legionella* (green). Quantification of co-localization with the LCV (indicated by arrowheads and yellow in color) is shown in merged images. The results are representative of three independent experiments performed in triplicate.

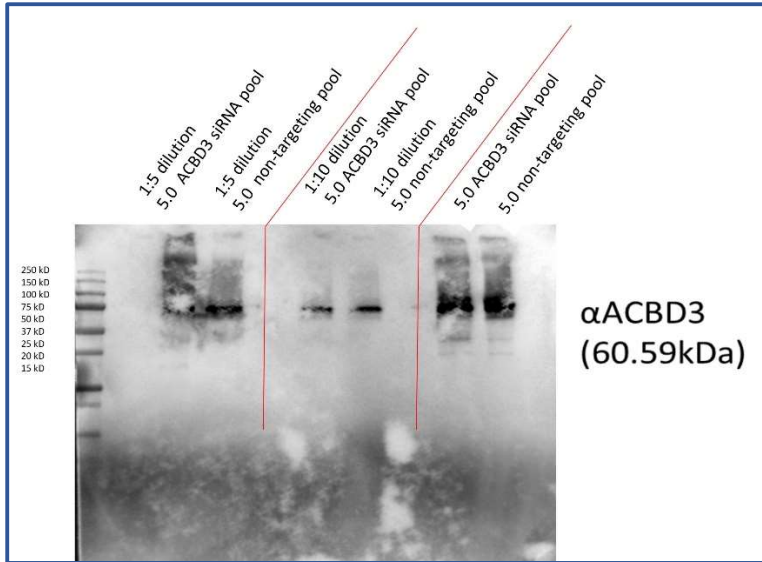


Figure 3-4: Western Blot Analysis of Silencing of host protein ACBD3 in hMDMs. Human monocyte derived macrophages were treated with ACBD3 RNAi for 24 hours. Knockdown was determined by immunoblotting of cellular lysates with anti-ACBD3 polyclonal antibody. Results are representative of three independent experiments.

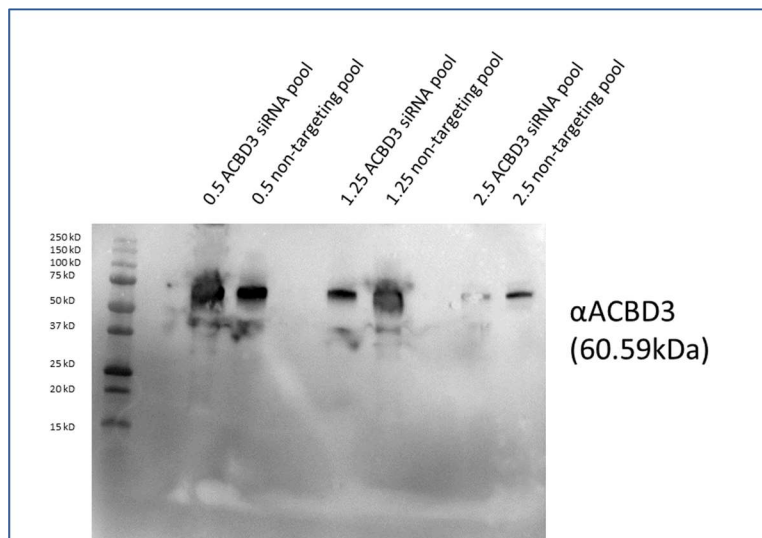


Figure 3-5: Western Blot Analysis of Silencing of host protein ACBD3 in HEK293T cells. HEK293T cells were treated with ACBD3 RNAi for 24 hours at varying volumes of DharmaFECT transfection reagent and maximum recommended siRNA volume. Knockdown was determined by immunoblotting of cellular lysates with anti-ACBD3 polyclonal antibody. Results are representative of three independent experiments. A total of 100 infected cells for each replicate were counted for presence or absence of localization.

Co-localization of ACBD3 during siRNA knockdown

We examined sub-cellular localization of ACBD3 in HEK293T cells. Consistent with localization of ACBD3 to the LCV in hMDMs, ACBD3 localized to the LCV harboring the WT strain of *L. pneumophila* and the complemented strain (*mavE/C*) at both 1-hour and 10-hour post infection in HEK293T cells (Figure 3-6). At 1-hour post infection, 93% of the LCVs harboring WT bacteria co-localized with ACBD3, while 19% of the *mavE* mutant containing LCVs co-localized with ACBD3 (Figure 3-6A). The defect of the *mavE* mutant was restored upon complementation where 87% of the vacuoles co-localized with ACBD3. Much like the *mavE* mutant strain-containing LCVs, 13% of the Δ T4SS mutant vacuoles co-localized with ACBD3 (Figure 3-6A). Similar results were observed 10-hours post infection in HEK293T cells. The data showed that in HEK293T cells, 97% of LCVs harboring wild type bacteria co-localized with ACBD3, while only 17% and 17% of the *mavE* mutant and Δ T4SS mutant-containing vacuoles, respectively, co-localized with the ACBD3 (Figure 3-7A). Much like WT-containing LCVs, 92% of the complemented mutant (*mavE/C*) containing LCVs co-localized with ACBD3. Thus, in both hMDMs and HEK293T cells, ACBD3 is co-localized with the LCV in a MavE-dependent manner.

HEK293T cells were transfected with either the optimized ON-TARGETplus Human ACBD3 siRNA pool or non-targeting pool 24 hours prior to WT, *mavE* mutant, *mavE/C*, and Δ T4SS bacterial infection to knockdown expression of ACBD3. Unfortunately, ACBD3 was not co-localized with the LCV in the scramble control or the siRNA knockdown at both 1-hour post infection or 10-hour post infection. Thus, there

was likely a side effect of the transfection reagent on co-localization of ACBD3 to the LCV (Figure 3-6B,C and 3-7B,C).

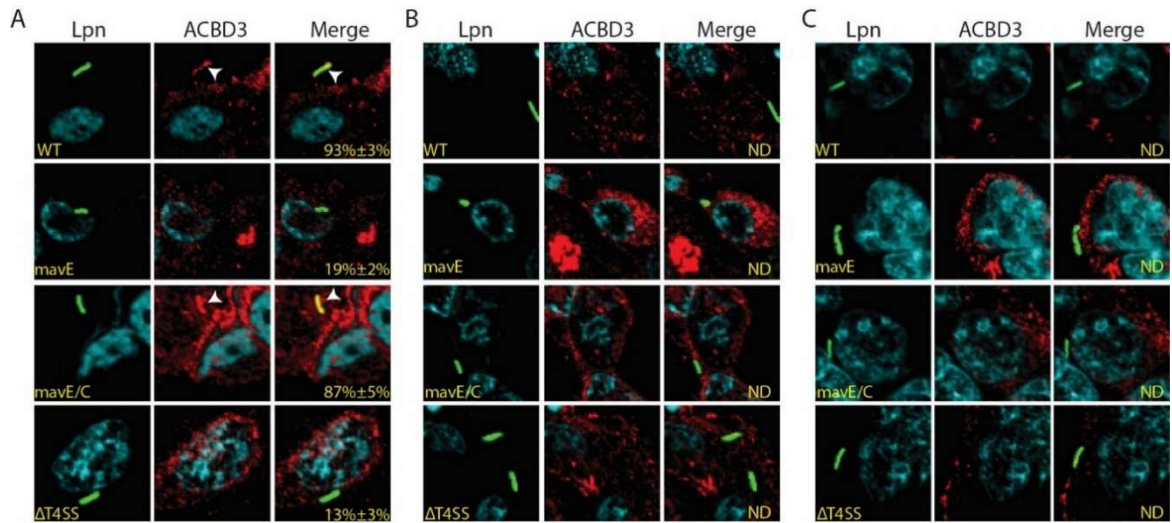


Figure 3-6: Localization of ACBD3 to the LCV during infection of HEK293T cells 1 hour post infection. Representative confocal microscopy images of Co-localization of the LCVs containing wild type, $\Delta T4SS$ mutant *L. pneumophila*, *mavE* mutant, or the complemented strain (*mavE/C*) labeled with anti-ACBD3 (red), DAPI (blue) and anti-*Legionella* (green). Quantification of co-localization with the LCV (indicated by arrowheads and yellow in color) is shown in merged images. ND indicates not detectable. **(A)** 1-Hour Infection of HEK293T cells **(B)** 1-hour Infection of HEK293T cells treated with non-targeting siRNA pool for 24 hours prior to infection. **(C)** 1-hour Infection of HEK293T cells treated with ACBD3 siRNA pool for 24 prior to infection. Results are representative of three independent experiments. A total of 100 infected cells for each replicate were counted for presence or absence of localization.

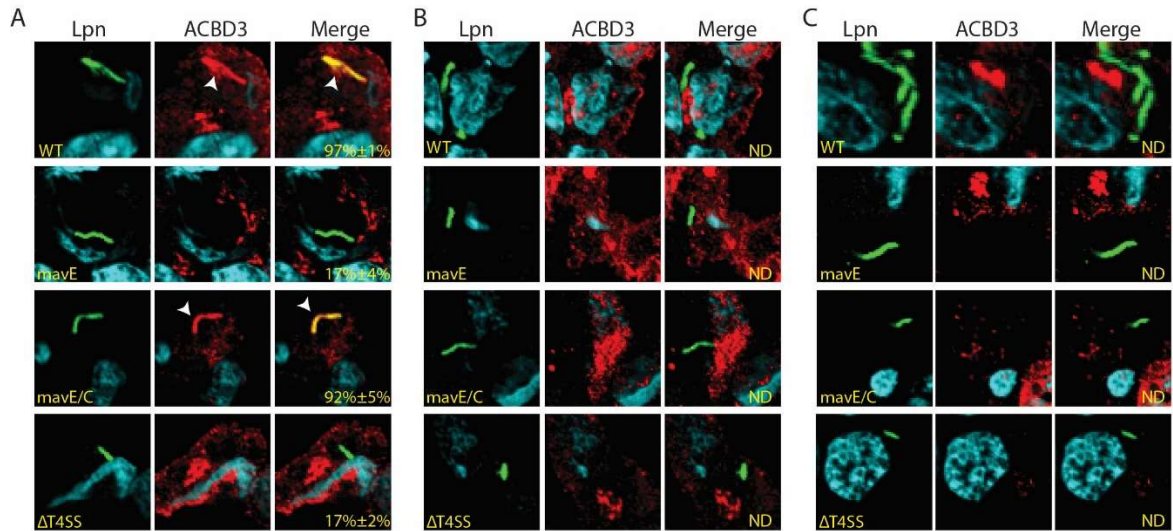


Figure 3-7: Localization of ACBD3 to the LCV during infection of HEK293T cells 10-hours post infection. Representative confocal microscopy images of Co-localization of the LCVs containing wild type, $\Delta T4SS$ mutant *L. pneumophila*, *mavE* mutant, or the complemented strain (*mavE/C*) labeled with anti-ACBD3 (red), DAPI (blue) and anti-*Legionella* (green). Quantification of co-localization with the LCV (indicated by arrowheads and yellow in color) is shown in merged images. ND indicates not detectable. **(A)** 10-hour Infection of HEK293T cells. **(B)** 10-hour Infection of HEK293T cells treated with non-targeting siRNA pool for 24 hours prior to infection. **(C)** 10-hour Infection of HEK293T cells treated with ACBD3 siRNA pool for 24 prior to infection. Results are representative of three independent experiments. A total of 100 infected cells for each replicate were counted for presence or absence of localization.

Role of MavE on intracellular replication of L. pneumophila in HEK293T cells

Since the *mavE* mutant was previously shown to be defective for intracellular growth in hMDMs and amoeba, we determined if the *mavE* mutant also showed attenuation in intracellular growth in HEK293T cells. The data showed that the *mavE* mutant did not exhibit a defective phenotype in HEK293T and grew similar to the WT strain. The translocation-deficient $\Delta T4SS$ mutant control failed to grow in HEK293T cells (Figure 3-8). These data indicate that HEK293T cells are not useful to determine the role of MavE-ACBD3 interaction in LCV biogenesis. This emphasizes the importance of our approach in using primary hMDMs throughout our studies.

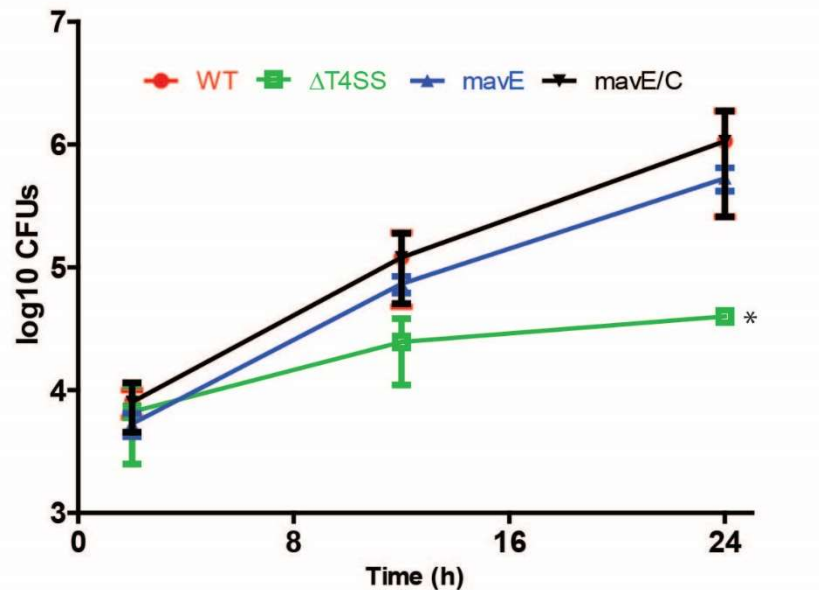


Figure 3-8: The *mavE* mutant is not attenuated within HEK293T cells. To determine intracellular replication of the WT strain, the *T4SS* mutant, the *mavE* mutant, and complemented *mavE* mutant (*mavE/C*), HEK293T cells were infected and number of CFUs was determined at 2, 12 and 24 h post-infection. Data points represent (mean CFUs \pm SD, n = 3) and are representative of three independent experiments. (Student *t*-test, * $p \leq 0.05$; ** $p \leq 0.01$; *** $p \leq 0.001$)

Discussion

Modulation of host cell processes is essential for the biogenesis of the LCV. The effector protein MavE potentially interacts with the host ACBD3 protein. ACBD3 maintains Golgi structure by interacting with giantin, affects transport between the ER and Golgi, and recruits PI4KB to the Golgi membrane, enhancing its enzymatic activity by increasing its local concentration [357, 370]. Protein transport from the ER to the Golgi compartments is mediated by small vesicles and requires a number of proteins, including coat protein complex (COPI and COPII) and GTPases ARF and Sar1p [371-373]. The effector protein, LotB, a *Legionella* deubiquitinase modulates the early secretory pathway by interacting with COPI vesicles when ectopically expressed [374]. The RalF effector functions as a GEF to recruit the ADP-ribosylation factor 1 (Arf1) to the LCV, enabling the GEF-like RalF effector to modulate membrane transport in the secretory pathway [243, 250]. Additionally, the DrrA/SidM effector preferentially recruits Rab1 and tethers ER-derived vesicles to the LCV, mediated by another *L. pneumophila* effector, LidA [166]. DrrA/SidM may compete with endogenous guanine nucleotide exchange factors (GEFs) to redirect Rab1 from its normal secretory intracellular localization to plasma membrane-derived vesicles [251]. The LepB effector accumulates on the LCV as DrrA/SidM and Rab1 cycle off and has been shown to function as a GTPase activating protein (GAP) for Rab1 (Figure 1-3) [196, 252]. The arsenal of effector proteins of *Legionella* employs multiple biochemical mechanisms to prevail over a diverse array of host cell processes. While MavE may not be the only effector protein to interact with ACBD3, localization of ACBD3 to the LCV is MavE dependent (Figure 3-3). MavE does harbor a eukaryotic NPxY motif that in eukaryotic cells binds with phosphotyrosine-binding domains present

on signaling and adaptor eukaryotic proteins. This motif could be responsible for binding/interaction with ACBD3. However, more studies are needed to determine the ability of various substitution mutants of MavE within the NPxY motif and its vicinity to interact with ACBD3.

Another peptide sequence fragment was identified unique to Isoform 2 of Ras-related protein Rab-8A was present in both biological repeats of MavE-BioID2. However, both samples had probabilities below the 95% confidence level (Table 2). While small GTPases Rabs are key regulators of intracellular membrane trafficking, further examination of this protein was not considered, because both biological repeats showed a confidence probability below 95%. Other host proteins identified were solely identified in only one biological repeat of MavE-BioID2 and further examination of MavE interaction with AP-1 Complex subunit beta and Arfaptin-2 should be performed. The AP-1 Complex subunit beta had a 100% probability and is a subunit of clathrin-associated adapter protein complex 1, playing a role in protein sorting in the late-Golgi/trans-Golgi network and/or endosomes [375]. Another biotinylated host-MavE interacting protein identified by mass spectrometry with a high probability of identification was Arfaptin-2. Arfaptin-2 plays a possible important function in vesicle biogenesis and is involved in autophagy by regulating the starvation-dependent trafficking of ARG9A vesicles which deliver PI4KB to membranes [376, 377].

Silencing of host protein ACBD3 in hMDMs proved to be exceptionally challenging. Another approach that can be used in the future is Magnetofection [378]. This method uses a magnetic field to concentrate the magnetic nanoparticles combined with gene vectors (siRNA) onto the cell surface. The cells take up the genetic material

naturally via endocytosis or pinocytosis, keeping membrane architecture and structure intact [378]. Co-localization of ACBD3 to the LCV was lost upon the silencing of ACBD3 and control siRNA in HEK293T cells in WT strain infected cells. DharmaFECT composition is proprietary and may compromise ACBD3 function via Golgi membrane permeabilization. Therefore, future studies using the Magnetofection method for transfecting hMDMs with ACBD3 RNAi may also avoid the possible impact of the DharmaFECT transfection reagent.

While the MavE effector is indispensable for intracellular replication of *L. pneumophila* in macrophages and amoeba, it is dispensable within the HEK293T cell line. While the HEK293 cells are useful in research and can be used for a variety of applications, they are not phagocytic cells and not naturally infected by *L. pneumophila*. Thus, *L. pneumophila* effectors may not have the same effect in transformed cell lines compared to primary cells. The use of hMDMs throughout most of the studies strengthens the rigor of our approach. We conclude that our data suggests MavE interacts with host protein ACBD3, but substantial follow up experiments need to be performed. We have developed a working model of the function of MavE during infection of hMDMs (Figure 3-9).

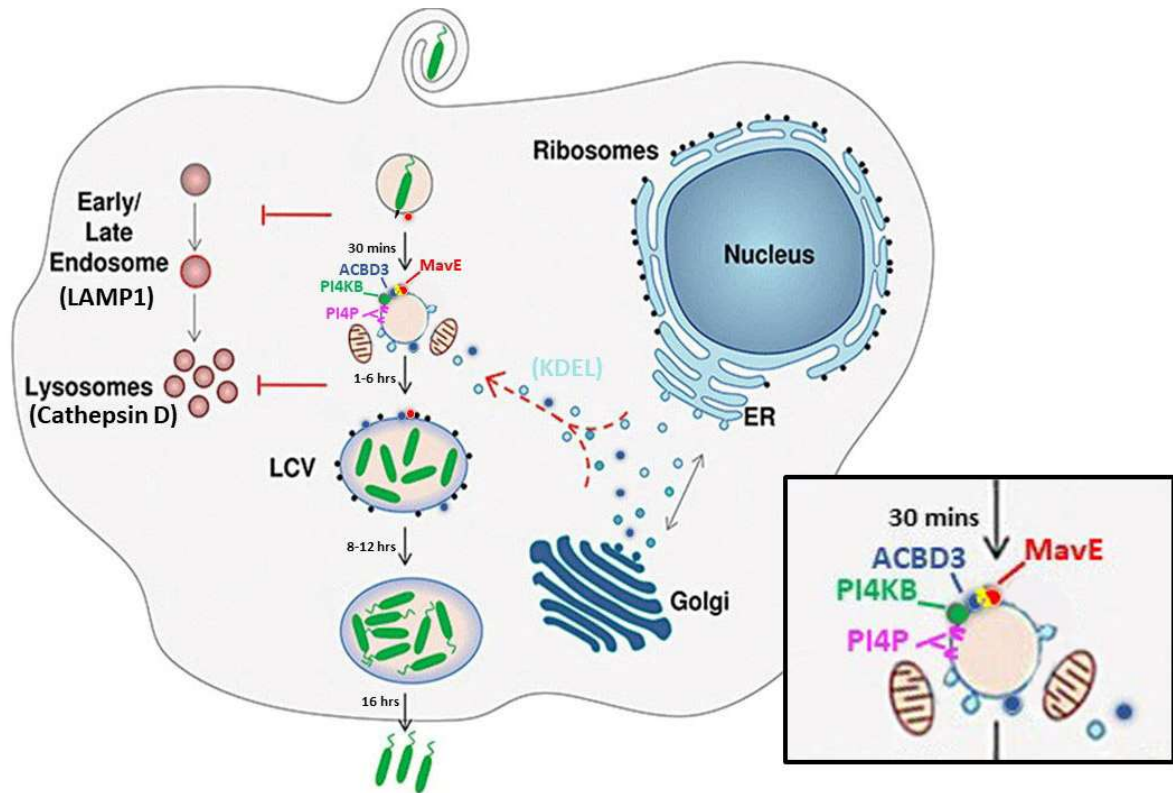


Figure 3-9. Working Model of MavE-ACBD3 Interaction in macrophages. MavE (red) is involved in the acquisition of ER-derived vesicles by the LCV and in evasion of lysosomal fusion. It is likely that both functions depend on the NPxY motif (yellow) located within the MavE structure. By mediating interactions with adaptor proteins, the NPxY motif of MavE may coordinate LCV trafficking through interaction with host adapter protein, ACBD3 (blue) and other *L. pneumophila* metaeffectors enabling ER remodeling and facilitating lysosomal evasion. ACBD3 recruits PI4KB and along with the PI4K2A enzyme, PI4KB synthesizes the phosphatidylinositol-4-phosphate (PI4P) lipid. *L. pneumophila* exploits PI4P to anchor secreted effector proteins to the LCV [362].

Materials and Methods

Cell lines

For infections of cell monolayers, *L. pneumophila* was grown in BCYE agar plates with appropriate antibiotic selection at 37°C for 3 days prior to use in infections, as described previously [337]. Human monocyte-derived macrophages (hMDMs) were isolated from healthy donors and cultured in RPMI 1640 (Corning Cellgro) as described previously [337, 338]. HEK293T cells (ATCC) were cultured in DMEM (Gibco) supplemented with 10% fetal bovine serum as previously described [337, 338]. All methods were carried out and approved in accordance with the University of Louisville Institutional Review Board guidelines and blood donors gave informed consent as required by the University of Louisville Institutional Review Board (IRB # 04.0358).

TABLE 3

Primers used in this study^a

| Primer ^b | Orientation ^c | Sequence |
|---|--------------------------|----------------------------|
| Primers used for cloning into the pacGFP1-C1 vector for eukaryotic expression | | |
| GFP mavE | F | GTCGACCTGACTCGATTCCATAATGC |
| GFP mavE | R | AAGCTTTTATGGTTTGTGCCAAAC |
| Primers used for cloning into the pmycBioID2-13x vector for eukaryotic expression | | |
| mycBioID2-MavE xhoI | F | ctcgagCTGACTCGATTCCATAATGC |
| mycBioID2-MavE kpnI | R | ggtaccTTATGGTTTGTGCCAAACA |

^aAll primers are 5'-phosphorylated.

^bKO, knockout.

^cF, forward; R, reverse.

To identify the Protein: Protein interactions of the MavE protein

We utilized a modified method derived from the previously reported BioID screens [367, 379-381]. Approximately 3×10^7 HEK293 cells were cultured as 80% confluent monolayers under normal conditions prior to transfection with either pBioID2 only, or pMavE-BioID2 (Table 3) and supplemented with 1 μ M biotin. After a 24-hour

transfection, the tissue culture cells were washed with 1xPBS, and whole cell lysates were generated via the addition of Lysis Buffer (50mM Tris, pH 7.6; 500mM NaCl; 0.4% Sodium Dodecyl Sulfate (SDS); 1mM DiThioThreitol (DTT); and 2.0% Triton X-100). The whole cell lysates were vortexed and frozen to ensure complete lysis, and the lysates were stored at -80°C until ready for further use. To confirm the BioID2 biotin ligase was function and labeling was specific we assessed the whole cell lysates using SDS-PAGE and Western Blotting techniques. Equal amounts of whole cell lysates were resolved via 8% SDS-PAGE and blotted to PVDF membranes. The blotted proteins were probed for protein biotinylation using streptavidin-HRP, or with anti-216 cMyc monoclonal antibodies to detect the individual expressed BioID2 fusion proteins.

Streptavidin-Biotinylated protein purification

Whole cell lysates were thawed on ice prior to being vigorously vortexed and clarified via centrifugation at 16,000xg for 5 minutes. The clarified whole cell lysates were transferred to a fresh microfuge tube and incubated with magnetic streptavidin beads for one hour at room temperature on a rotisserie mixer. After binding, the supernatant was removed and discarded, and the magnetic beads were washed 5 times with Lysis Buffer (50mM Tris, pH 7.6; 500mM NaCl; 0.4% Sodium Dodecyl Sulfate (SDS); 1mM DiThioThreitol (DTT); and 2.0% Triton X-100) to remove unbound proteins and nonspecific contaminants. The bound proteins were then released from the streptavidin resin via resuspension in 100µL 2x Laemmli buffer and a 15-minute incubation at 95°C. The eluted proteins were transferred to a fresh microfuge tube and precipitated with 25 µL 100% (w/v) TriChloroactic Acid (TCA). The samples were vortexed, and samples were incubated on ice for 10 minutes to allow complete

precipitation of the macromolecules in the solution. The precipitated proteins were pelleted via 5 minutes of centrifugation at 16,000xg at 4°C, and the supernatant was decanted into an appropriate waste container. The protein pellet was washed three times with ice cold acetone and again pelleted via 5 minutes of centrifugation at 16,000xg at 4°C. After the final wash, the pellet was dried by incubating the microfuge tube at 95°C for 5 minutes to drive off excess acetone. The dried proteins were stored at -80°C until mass spectrometry was performed.

Identification of MavE Interactions by Mass Spectrometry [382, 383]

8µL of LC-MS grade water (ThermoFisher Scientific, Waltham, MA, USA) and 2µL of 1M triethylammonium bicarbonate pH8.5 (Honeywell, Charlotte, NC, USA) were added to the dried purified protein samples. 2.5µL 25mM dithiothreitol (Sigma-Aldrich, St. Louis, MO, USA) in water was added, and the samples were incubated at 65°C for 30min. 2.5µL of 60mM iodoacetamide (Sigma-Aldrich) in water was added, and the samples were incubated at room temperature for 30min in the dark. 0.1µg of Pierce Trypsin, MS Grade (ThermoFisher) in 2.5µL water was added; the samples were incubated at 37°C for 30min. An additional 0.1µg trypsin was added, and the samples were incubated overnight at 37°C. After digestion, the samples were dried in a SpeedVac and stored at -80°C. The following protocol was used to prepare the samples for LC-MS analysis:

Cleanup with C18 PROTO™, 300Å Ultra MicroSpin Column

Solvents A=2% v/v acetonitrile / 0.1% v/v formic acid and B=80% v/v acetonitrile / 0.1% v/v formic acid were made and 100µL of solvent A used to dissolve the dried sample. The solution was placed a spin column with the adapter collar into a 2mL

microtube (empty this waste tube as needed). 100 μ L solvent B was added to the spin column and centrifuged at 110xg for 2min; this was repeated twice. The waste tube was emptied and 100 μ L solvent A was added to the spin column and centrifuged at 110xg for 2 mins and repeated twice. The liquid from the waste tube was transferred back into the column and sample is passed through the column for a second time. The waste tube was again emptied and 100 μ L of solvent A added, and centrifuge as above; repeat twice. The column was placed in a clean 2mL microtube and 100 μ L of solvent B added and centrifuged as above; this was repeated twice. The microtube was capped and frozen at -80°C for at least 30min. The eluate was dried in a SpeedVac (cap removed before drying), and the dried residue was dissolved in 20 μ L solution A. 2 μ L (1/10th) of each dissolved sample was analyzed on the Orbitrap Elite.

Liquid Chromatography

The columns used were an Acclaim PepMap 100 75 μ m x 2cm, nanoViper (C18, 3 μ m, 100Å) trap, and an Acclaim PepMap RSLC 75 μ m x 50cm, nanoViper (C18, 2 μ m, 100Å) separating column (ThermoFisher) heated at 50°C. An EASY-nLC 1000 UHPLC system (ThermoFisher) was used with solvents A = 2% v/v acetonitrile / 0.1% v/v formic acid and B = 80% v/v acetonitrile / 0.1% v/v formic acid. Following injection onto the trap, the sample was separated with a 165min linear gradient from 0% to 55% B at 250nL/min, followed by a 5min linear gradient from 55% to 95% B with a flow ramp from 250 to 300nL/min, and lastly a 10min wash with 95% B at 300nL/min. A 40mm stainless steel emitter (ThermoFisher) was coupled to the outlet of the separating column. A Nanospray Flex source (ThermoFisher) was used to position the end of the emitter near

the ion transfer capillary of the mass spectrometer. The ion transfer capillary temperature was set at 225°C, and the spray voltage at 1.75kV.

Data Acquisition

An Orbitrap Elite – ETD mass spectrometer (ThermoFisher) was used to collect data from the LC eluate. An Nth Order Double Play was created in Xcalibur v2.2 (ThermoFisher). Scan event one obtained an FTMS MS1 scan (normal mass range; 240,000 resolution, full scan type, positive polarity, profile data type) for the range 300-2000m/z. Scan event two obtained ITMS MS2 scans (normal mass range, rapid scan rate, centroid data type) on up to twenty peaks that had a minimum signal threshold of 5,000 counts from scan event one. The lock mass option was enabled (0% lock mass abundance) using the 371.101236m/z polysiloxane peak as an internal calibrant.

Data Analysis with Proteome Discoverer v2.4.0.305 and Scaffold Q+S v5.1.0

Proteome Discoverer v2.4.0.305 (ThermoFisher) was used to analyze the data. The UniprotKB reviewed reference canonical proteomes were concatenated from *Homo sapiens* (Proteome ID UP000005640) and *L. pneumophila* (Proteome ID UP000000609) for the Mascot v2.5.1 (Matrix Science Inc, Boston, MA, USA) and SequestHT searches. The enzyme specified was trypsin (maximum two missed cleavages with inhibition by Proline) with Carbamidomethyl(C) as a static modification and Oxidation(M), Biotin(K) as dynamic. Fragment tolerance was 1.0Da (monoisotopic) and parent tolerance was 50ppm (monoisotopic). A Target Decoy PSM Validator node was included in the Proteome Discoverer workflow.

Scaffold (version Scaffold_5.0.0, Proteome Software Inc., Portland, OR) was used to validate MS/MS based peptide and protein identifications. Peptide identifications

were accepted if they could be established at greater than 99.9% probability by the Scaffold Local FDR algorithm. Protein identifications were accepted if they could be established at greater than 99.9% probability and contained at least 1 identified peptide. Protein probabilities were assigned by the Protein Prophet algorithm [384] Proteins that contained similar peptides and could not be differentiated based on MS/MS analysis alone were grouped to satisfy the principles of parsimony. Proteins sharing significant peptide evidence were grouped into clusters. Proteins were annotated with GO terms from goa_human.gaf [385].

Transfection of HEK-293 cells (ATCC)

The *navE* gene was cloned into the mammalian expression vector, pAcGFP1-C1(Clontech). To generate the *navE*^{-9L¹⁰P/AA} allele, the wild type pAcGFP1-C1 *MavE* plasmid was used as a template for PCR based site directed mutagenesis (Table 3). HEK293T (ATCC) cells were grown to ~70% confluent and plated onto poly-L-lysine-treated 24 well plates. Following 24 h of incubation, HEK293T cell monolayers were transfected with ~2 µg of plasmid DNA/well by using polyethylenimine (Polysciences) and OptiMem (Gibco) for 24 h, following the manufacturer's recommendations (Roche) as previously described [341, 342, 386].

Antibodies and western blot analysis

Immunoprecipitated proteins were heated at 99°C for 5 minutes in 2x Laemmli sample buffer and loaded into mini-PROTEAN TGX precast gels separated by 10% SDS-PAGE (BioRad) and transferred onto a polyvinylidene difluoride (PVDF) (BioRad) membrane into the Trans-Blot Turbon Transfer System, by first wetting the nitrocellulose membrane in 1xTransfer Buffer for 2-3 minutes and then immersing in 100% ethanol for

2-3 minutes. Two ion reservoir stacks were also immersed in the transfer buffer for 2-3 minutes. One wetted stack was placed on the bottom of the cassette, serving as the bottom ion reservoir, the wetted PVDF membrane was placed on top of the wetted stack with the gel membrane directly on top. A second wetted transfer stack was placed on top of the gel and the cassette lid was closed and locked and transfer was initiated at 2.5A constant; up to 25V for mixed molecular weight. To perform antibody binding, the iBind Flex Solution Kit was used. The transferred PVDF membrane was immersed in 10mL of 1x iBind Flex solution and placed protein side down on the previously wetted iBind Flex card. The diluted 1° antibody was prepared and placed in row 1, 1x iBind Flex solution in row 2, diluted 2° antibody in row 3 and 1x iBind Flex solution placed in row 4. The iBind Flex device was closed and the device left undisturbed until the well of row 4 was empty. Rabbit polyclonal anti-ACBD3 (Invitrogen) was used at a dilution of 1:1000, Rabbit-HRP was used at a dilution of 1:5000 (ThermoFisher). To detect the blot proteins, Thermo Scientific SuperSignal West Femto was used as directed.

Intracellular replication in HEK293T

For infection of cell monolayers, *L. pneumophila* strains were grown in BYE broth with appropriate antibiotic selection, at 37 °C with shaking, to post-exponential phase (OD_{550nm} 2.1–2.2). HEK293T (ATCC) were cultured in DMEM supplemented with 10% fetal bovine serum, at 37 °C, as previously described [337]. The wild type strain; the isogenic mutants, *T4SS* and *mavE*; and complement *mavE/C* were grown to post-exponential phase in BYE broth at 37 °C with shaking prior to infection and used to infect HEK293T cells as previously described [337, 338]. A total of 1×10^5 host cells were plated in 96 well plates and infected with *L. pneumophila* at an MOI of 10. Plates

were centrifuged at $200 \times g$ (5 mins), to synchronize infection. After 1 h, cells were treated with gentamicin to kill extracellular bacteria, as previously described [337, 338]. Over a 24 h time course, host cells were lysed with sterile water. *L. pneumophila* CFUs were determined by plating serial dilutions onto BCYE agar.

RNAi Knockdown

Human ACBD3 (64746) siRNA SMARTpool targeting against four ACBD3 target sequences (Table 4) and scrambled non-targeting pool (Table 4) were resuspended per horizon resuspension protocol to obtain 250 μ L, 20 μ M Stock solutions. These stocks were then diluted to make 5 μ M siRNA working solutions using 1x siRNA buffer purchased from Horizon. For 96 wells/plate: In tube 1 mix 0.5 μ L of 5 μ M siRNA and 9.5 μ L serum-free medium (RPMI for hMDMs/DMEM for HEK293T); in tube 2 mix 0.5 μ L DharmaFECT reagent and 9.5 μ L serum-free medium. Gently mix the contents of each tube and incubate for 5 minutes at room temperature. Add the contents of tube 1 and tube 2, gently mix and incubate for 20 minutes at room temperature, then add 80 μ L of antibiotic-free complete medium (RPMI+10% FBS for hMDMs/DMEM+10% FBS for HEK293T) for a total volume of 100 μ L. Remove culture medium from 96-well plate and add 100 μ L transfection medium to each well. For 24wells/plate: In tube 1 mix 2.5 μ L of 5 μ M siRNA and 47.5 μ L serum-free medium (RPMI for hMDMs/DMEM for HEK293T); in tube 2 mix 2.5 μ L DharmaFECT reagent and 47.5 μ L serum-free medium. Gently mix the contents of each tube and incubate for 5 minutes at room temperature. Add the contents of tube 1 and tube 2, gently mix and incubate for 20 minutes at room temperature, then add 400 μ L of antibiotic-free complete medium (RPMI+10% FBS for hMDMs/DMEM+10% FBS for HEK293T) for a total volume of 500 μ L. Remove culture

medium from 24-well plate and add 500 μ L transfection medium to each well. Incubate cells at 37°C in 5% CO₂ for 24-48hours. Transfection optimization was performed to obtain the highest transfection efficiency by varying the volume of DharmaFECT reagent (0.5-2.5 μ L on 24 well plates).

TABLE 4

Dharmacon Product

| siRNA | Target Sequence |
|---|--|
| ON-TARGET plus Non-targeting Pool, 5nmol | |
| Catalog Item: D-001810-10-05 | UGGUUUACAUGUCGACUAA UGGUUUACAUGUUGUGUGA UGGUUUACAUGUUUCUGA UGGUUUACAUGUUUCCUA |
| ON-TARGET plus Human ACBD3 (64746) siRNA- SMARTpool, 5nmol | |
| Catalog Item: L-010799-01-0005 | GGAUGCAGAUUCCGUGAUU GCAACUGUACCAAGUAAUA GCAUAUGGGAAGUAACAUU GUAUAGAAACCAUGGAGUU |
| DharmaFECT 1 Transfection Reagent, 0.2mL | |
| Catalog Item: T-2001-01 | |

Confocal microscopy

Processing of infected cells for confocal microscopy was performed as we described previously [338]. Co-localization of the LCVs containing WT, Δ T4SS mutant, *mavE* mutant; and complement *mavE/C* were analyzed for confocal following 1hr infection in hMDMs and 1hr and 10hr infection in HEK293T cells. Cells were prepared using the same protocol for intracellular replication except 1 x 10⁵ host cells were plated on coverslips in 24 well plates. The monolayers were infected with *L. pneumophila* at an MOI of 10. Plates were centrifuged at 200 \times g (5 mins), to synchronize infection. After 1 h, cells were treated with gentamicin to kill extracellular bacteria, as previously

described [337, 338]. For all confocal experiments, cells were fixed in -20 °C methanol for 5 minutes and rinsed 3x in 10% PBS. For antibody labeling, goat anti-*L. pneumophila* was used at a dilution of 1:500 and detected by Alexa-Fluor 488-conjugated donkey anti-mouse IgG (1:1000) (Invitrogen, Carlsbad, CA) and rabbit polyclonal anti-ACBD3 (Invitrogen) was used at a dilution of 1:500 and detected by Alexa-Fluor 555-conjugated donkey anti-rabbit IgG (1:1000) (Invitrogen, Carlsbad, CA). For antibody labeling for localization, goat anti-*L. pneumophila* was used at a dilution of 1:750 and detected by detected by Alexa-Fluor 488-conjugated donkey anti-goat IgG (1:1000) (Invitrogen, Carlsbad, CA) rabbit polyclonal anti-ACBD3 (Invitrogen, Rockford, IL) was used at a dilution of 1:500 and detected by Alexa-Fluor 555-conjugated donkey anti-Rabbit IgG (Invitrogen, Carlsbad, CA), DAPI was used for all experiments at a 1:5000 dilution. An Olympus FV1000 laser scanning confocal microscope was used in house to examine cells as we described previously [298]. On average, 10–20 0.3 µm serial Z sections of each image were captured and stored for further analyses, using Adobe Photoshop CS3. A total of 100 infected cells for each replicate were counted for presence or absence of localization.

Statistical analysis

All experiments were performed at least three independent biological replicates, and the data shown are representatives of one experiment. To analyze for statistically significant differences between three sets of data, the two-tailed Student's *t*-test was used, and the *p*-value was obtained. (* indicates $p \leq 0.05$; ** indicates $p \leq 0.01$; *** indicates $p \leq 0.001$)

CHAPTER 4:
CONCLUSIONS AND FUTURE DIRECTIONS

The evolution of the pathogen to adapt to the intra-vacuolar environment of eukaryotic cells and inter-kingdom as well as inter-bacterial horizontal gene transfer has most likely shaped the long-term evolution of *L. pneumophila* with various protozoa as the natural hosts. The ability of *L. pneumophila* to replicate intracellularly and survive is totally dependent on interaction of the Dot/Icm translocated effectors with eukaryotic host target proteins. Biogenesis of the replicative LCV involves remodeling the *Legionella*-containing vacuole to an ER-derived LCV, that evades the endosomal-lysosomal degradation pathway [269]. It is important to note that the default endosomal-lysosomal degradation pathway is highly conserved throughout evolution, and the Dot/Icm secretion system is indispensable for LCV biogenesis in macrophages as well as amoeba. The data showing fusion of the vacuoles containing the *mavE* mutant with the lysosome illustrates that the effector MavE is required for biogenesis of the LCV into an ER-derived vacuole that evades lysosomal fusion [269]. Preliminary data suggests MavE interacts with the host protein ACBD3, which is involved in Golgi-to-ER traffic, but still needs to be confirmed. To further verify MavE-ACBD3 interaction, the reciprocal pulldown of tagged ACBD3 and immunoblotted with anti-MavE antibody needs to be performed.

Although many Dot/Icm-translocated effectors have been shown to directly regulate the early secretory system of the host cell, except for VipD, no *L. pneumophila* effector has ever been shown to be indispensable for evasion of the endosomal-lysosomal degradation pathway. The VipD effector of *L. pneumophila* localizes to early endosomes and interferes with endosomal trafficking through blocking interaction of Rab5 and Rab22 with EEA1 [253]. VipD binds to the endosomal regulator Rab5 and triggers the

hydrolytic phospholipase A1 activity of VipD, causing the removal of the lipid phosphatidylinositol 3-phosphate facilitating endosomal lysosomal evasion by *L. pneumophila* [254]. However, only deletion of *mavE* results in severe impairment of biogenesis of the LCV to an ER-derived vesicle that evades lysosomal fusion (Figure 2-4). We show that MavE is required for evasion of the default endosomal-lysosomal degradation pathway and plays a crucial early role in the biogenesis of the nascent LCV (Figure 2-6) [269]. It is not known whether ER-mediated remodeling or lysosomal evasion is executed first during LCV biogenesis. We speculate that it is likely that early and rapid MavE-mediated recruitment of ER-derived vesicles through MavE-ACBD3 interaction prevents traveling to the default endosomal-lysosomal pathway.

To identify inter-substrate physical interactions of effector-effector suppression pairs in *L. pneumophila* a yeast two-hybrid assay and LUMIER assay that detects direct protein-protein interactions showed MavE and the effector YlfA/LegC7 interact [191]. YlfA/LegC7 along with two other effectors (LegC2 & LegC3) assemble in a complex on the LCV and interact with ER-derived vesicles to initiate membrane fusion [190, 191, 266-268]. We attempted to reproduce this interaction by co-immunoprecipitation of tagged proteins of LegC2, LegC3 and LegC7 and MavE in HEK293T cells, along with the reciprocal tagged proteins. Unfortunately, LegC7 did not interact with MavE, and biological repeats did not reproduce this possible interaction between LegC7 and MavE. Our collaborators, Dr. Miroslaw Cygler and Dr. Kevin Voth, who resolved the crystal structure of MavE also tried to reproduce the LegC7 and MavE interaction *in vitro* using pulldown assays without success [387]. By performing the BioID2 proximity labeling

during infection of host cells, this should decipher possible interaction between LegC7 and MavE as previously published using a yeast two-hybrid assay and LUMIER assay.

Identification of MavE-interacting host proteins was determined by proximity-dependent cellular biotinylation of neighboring proteins during ectopic expression of MavE. While ACBD3 was not the sole protein identified by BioID2, it was the only one found in both biological repeats and in one of the biological repeats it had a 98% probability of identification (above the confidence level of 95%). ACBD3 recruits PI4KB to the Golgi apparatus and with the enzyme PI4K2A, synthesizes PI4P [355, 357-359]. PI4P is an essential lipid found in multiple membrane compartments of the Golgi, trans-Golgi network (TGN), plasma membrane, endocytic compartments, and the LCV [357, 362]. *L. pneumophila* exploits PI4P to anchor other injected effector proteins to the LCV to subvert host cell PI metabolism which is essential for establishment of the replicative LCV [362]. Determining if MavE interacts with PI4P or PI4KB could further expand our knowledge of the interaction of MavE with ACBD3 and ultimately provide a previously unknown link in vacuolar biogenesis of the LCV.

However, examination of MavE interaction with Arfaptin-2 and AP-1 Complex subunit beta should be performed as both were identified as having high probabilities of identification in one biological repeat. Identifying MavE-interacting host proteins BioID2 assay in both human and amoebal cells would be beneficial, as modulation of host cell functions and metaeffector activity could be different in various hosts. Again, determining the interactions of MavE with other proteins during infection of host cells by constructing a BioID2 plasmid that can be expressed in WT and the T4SS mutant *L.*

pneumophila, will clarify any potential MavE-interacting metaeffectors that modulate activity of the MavE effector, as function could vary between cell types.

The resolved crystal structure of MavE revealed an NPxY motif located on a poorly defined electron density loop with flexibility that may accommodate protein-protein interactions (Figure 2-8). Eukaryotic NPxY motifs (Asp-Pro-x-Tyr) are a conserved tyrosine phosphorylation motif that binds phosphotyrosine-binding domains (PTB) present on signaling and adaptor eukaryotic proteins [388]. Substitution of proline in the NPxY motif and substitution mutant aspartic acid within the predicted protease catalytic triad resulted in attenuation of *L. pneumophila* in hMDMs (Figure 2-9A). An additional substitution mutant H68A (Histidine) also showed attenuation in *A. polyphaga* (Figure 2-9B). Interestingly, both aspartic acid and histidine can be phosphorylated. Histidine phosphorylation is crucial in prokaryotes and accounts for roughly 6% of total phosphorylation in eukaryotes [389]. All substitution mutants in the NPxY were changed to alanine. Interestingly, changing the aliphatic proline to aliphatic alanine showed attenuation in both hMDMs and amoeba. However, the aromatic tyrosine, that is capable of being phosphorylated did not show attenuation.

In theory the tyrosine found within the NPxY motif may be phosphorylated during infection, but its substitution had no effect on the function of MavE and intracellular growth of *L. pneumophila*. This may indicate that the tyrosine residue within NPxY does not have an effect on MavE. Alternatively, tyrosines within close proximity of the NPxY motif may become phosphorylated. However, ACBD3 does not contain a PTB site, suggesting no role for the tyrosine residue within the NPxY motif in MavE-interaction with ACBD3. Future studies generating substitutions in the tyrosine

residues in close proximity to the NPxY motif to glutamic acid (E) would result in a negatively charged region, as previously reported as an analogous substitution for phosphotyrosine [390]. It would also be useful to determine if the expression of the already generated substitution mutants in the NPxY motif of MavE interact with ACBD3. Demonstrating if the NPxY motif or the tyrosine-based sorting motifs are responsible for the interaction of MavE and host protein ACBD3 and would further characterize the role of the NPxY motif of MavE in vacuolar biogenesis.

Additionally, protein phosphorylation is the most widespread type of post-translational modification affecting multiple cellular processes and plays a critical regulatory role in protein-protein interactions [391]. Protein kinases catalyze the transfer of γ -phosphate from ATP to specific potentially phosphorylatable residues including the structure of catalytic sites [391]. Determining if MavE or the NPxY substitution mutants are phosphorylated by ectopically expressing the constructs in HEK293T cells and immunoblotting with anti-phosphotyrosine antibody would selectively identify the tyrosine-phosphorylated peptides. To examine all residue phosphorylation of MavE, phosphorylation site mapping with tandem mass spectrometry would measure phosphorylated peptides within MavE, further identifying the protein's function.

Overall, we have identified a key effector utilized by *L. pneumophila* to remodel the LCV to an ER-derived vacuole and evade the default endosomal-lysosomal pathway (Figure 3-9). Importantly, this effector is required by *L. pneumophila* in both the natural amoebal hosts and the accidental host, the human macrophage, reflecting the high evolutionary conservation of the default endosomal-lysosomal pathway across eukaryotes.

REFERENCES

1. Henderson, R.B., A. , *Legionnaires' Disease*. Patient, 2017. **Chest and Lungs**.
2. Honigsbaum, M., *Legionnaires' disease: revisiting the puzzle of the century*. Lancet, 2016. **388**(10043): p. 456-7.
3. McDade, J.E., et al., *Legionnaires' disease: isolation of a bacterium and demonstration of its role in other respiratory disease*. N Engl J Med, 1977. **297**(22): p. 1197-203.
4. Brenner, D.J., A.G. Steigerwalt, and J.E. McDade, *Classification of the Legionnaires' disease bacterium: Legionella pneumophila, genus novum, species nova, of the family Legionellaceae, familia nova*. Ann Intern Med, 1979. **90**(4): p. 656-8.
5. Muder, R.R., V.L. Yu, and A.H. Woo, *Mode of transmission of Legionella pneumophila. A critical review*. Arch Intern Med, 1986. **146**(8): p. 1607-12.
6. *Legionnaires Disease History, Burden, and Trends*. Center for Disease Control and Prevention; Available from: <https://www.cdc.gov/legionella/about/history.html>.
7. Whiley, H. and R. Bentham, *Legionella longbeachae and legionellosis*. Emerg Infect Dis, 2011. **17**(4): p. 579-83.
8. Newton, H.J., et al., *Molecular pathogenesis of infections caused by Legionella pneumophila*. Clin Microbiol Rev, 2010. **23**(2): p. 274-98.
9. Beaute, J., P. Zucs, and B. de Jong, *Legionnaires disease in Europe, 2009-2010*. Euro Surveill, 2013. **18**(10): p. 20417.
10. Fields, B.S., R.F. Benson, and R.E. Besser, *Legionella and Legionnaires' disease: 25 years of investigation*. Clin Microbiol Rev, 2002. **15**(3): p. 506-26.
11. Yu, V.L., et al., *Distribution of Legionella species and serogroups isolated by culture in patients with sporadic community-acquired legionellosis: an international collaborative survey*. J Infect Dis, 2002. **186**(1): p. 127-8.
12. Palusinska-Szys, M., et al., *The Role of Legionella pneumophila Serogroup 1 Lipopolysaccharide in Host-Pathogen Interaction*. Front Microbiol, 2019. **10**: p. 2890.
13. Ricco, M., et al., *Epidemiology of Legionnaires' Disease in Italy, 2004-2019: A Summary of Available Evidence*. Microorganisms, 2021. **9**(11).
14. Castor, M.L., et al., *An outbreak of Pontiac fever with respiratory distress among workers performing high-pressure cleaning at a sugar-beet processing plant*. J Infect Dis, 2005. **191**(9): p. 1530-7.
15. Fields, B.S., et al., *Pontiac fever due to Legionella micdadei from a whirlpool spa: possible role of bacterial endotoxin*. J Infect Dis, 2001. **184**(10): p. 1289-92.

16. Burillo, A., M.L. Pedro-Botet, and E. Bouza, *Microbiology and Epidemiology of Legionnaire's Disease*. Infect Dis Clin North Am, 2017. **31**(1): p. 7-27.
17. Gump, D.W. and M. Keegan, *Pulmonary infections due to Legionella in immunocompromised patients*. Semin.Respir.Infect, 1986. **1**: p. 151-159.
18. Khweek, A.A. and A. Amer, *Replication of Legionella Pneumophila in Human Cells: Why are We Susceptible?* Front Microbiol, 2010. **1**: p. 133.
19. Bartlett, J.G., *Diagnostic tests for agents of community-acquired pneumonia*. Clin Infect Dis, 2011. **52 Suppl 4**: p. S296-304.
20. Graham, F.F., et al., *Review Global seroprevalence of legionellosis - a systematic review and meta-analysis*. Sci Rep, 2020. **10**(1): p. 7337.
21. Khodr, A., et al., *Molecular epidemiology, phylogeny and evolution of Legionella*. Infect Genet Evol, 2016. **43**: p. 108-22.
22. Musher, D.M., M.S. Abers, and J.G. Bartlett, *Evolving Understanding of the Causes of Pneumonia in Adults, With Special Attention to the Role of Pneumococcus*. Clin Infect Dis, 2017. **65**(10): p. 1736-1744.
23. Egan, J.R., et al., *Modeling Legionnaires' disease outbreaks: estimating the timing of an aerosolized release using symptom-onset dates*. Epidemiology, 2011. **22**(2): p. 188-98.
24. Marrie, T.J., J.R. Garay, and E. Weir, *Legionellosis: Why should I test and report?* CMAJ, 2010. **182**(14): p. 1538-42.
25. Dooling, K.L., et al., *Active Bacterial Core Surveillance for Legionellosis - United States, 2011-2013*. MMWR Morb Mortal Wkly Rep, 2015. **64**(42): p. 1190-3.
26. Granados, A., et al., *Pneumonia due to Legionella pneumophila and pneumococcal pneumonia: similarities and differences on presentation*. Eur Respir J, 1989. **2**(2): p. 130-4.
27. Kirby, B.D., et al., *Legionnaires' disease: report of sixty-five nosocomially acquired cases of review of the literature*. Medicine (Baltimore), 1980. **59**(3): p. 188-205.
28. Marston, B.J., H.B. Lipman, and R.F. Breiman, *Surveillance for Legionnaires' disease. Risk factors for morbidity and mortality*. Arch Intern Med, 1994. **154**(21): p. 2417-22.
29. Bopp, L.H., et al., *Activities of tigecycline and comparators against Legionella pneumophila and Legionella micdadei extracellularly and in human monocyte-derived macrophages*. Diagnostic Microbiology and Infectious Disease, 2011. **69**(1): p. 86-93.
30. Mandell, L.A., et al., *Infectious Diseases Society of America/American Thoracic Society Consensus Guidelines on the Management of Community-Acquired Pneumonia in Adults*. Clinical Infectious Diseases, 2007. **44**(Supplement_2): p. S27-S72.
31. Pedro-Botet, L. and V.L. Yu, *Legionella: macrolides or quinolones?* Clinical Microbiology and Infection, 2006. **12**: p. 25-30.
32. Kampitak, T., *Fever of unknown origin due to Legionnaires' disease: A diagnostic challenge*. Travel Med Infect Dis, 2018. **22**: p. 79.

33. Slawek, D., et al., *Tigecycline as a Second-Line Agent for Legionnaires' Disease in Severely Ill Patients*. *Open Forum Infect Dis*, 2017. **4**(4): p. ofx184.
34. Sivagnanam, S., et al., *Legionnaires' disease in transplant recipients: A 15-year retrospective study in a tertiary referral center*. *Transpl Infect Dis*, 2017. **19**(5).
35. Burillo, A., M.L. Pedro-Botet, and E. Bouza, *Microbiology and Epidemiology of Legionnaire's Disease*. *Infectious Disease Clinics of North America*, 2017. **31**(1): p. 7-27.
36. Phin, N., et al., *Epidemiology and clinical management of Legionnaires' disease*. *Lancet Infect Dis*, 2014. **14**(10): p. 1011-21.
37. Garrison, L.E., et al., *On-site availability of Legionella testing in acute care hospitals, United States*. *Infect Control Hosp Epidemiol*, 2014. **35**(7): p. 898-900.
38. Control, C.F.D. *Surveillance and Reporting 2018 2/7/2018*; Available from: <https://www.cdc.gov/legionella/surv-reporting.html>.
39. Cilloniz, C., et al., *Seasonality of pathogens causing community-acquired pneumonia*. *Respirology*, 2017. **22**(4): p. 778-785.
40. Cunha, B.A., J. Connolly, and E. Abruzzo, *Increase in pre-seasonal community-acquired Legionnaire's disease due to increased precipitation*. *Clin Microbiol Infect*, 2015. **21**(6): p. e45-6.
41. von Baum, H., et al., *Community-acquired Legionella pneumonia: new insights from the German competence network for community acquired pneumonia*. *Clin Infect Dis*, 2008. **46**(9): p. 1356-64.
42. Leland, D.S. and R.B. Kohler, *Evaluation of the L-CLONE Legionella pneumophila serogroup 1 urine antigen latex test*. *J.Clin.Microbiol.*, 1991. **29**: p. 2220-2223.
43. Mangiafico, J.A., K.W. Hedlund, and A.R. Knott, *Rapid and sensitive method for quantitation of Legionella pneumophila serogroup 1 antigen from human urine*. *J.Clin.Microbiol.*, 1981. **13**: p. 843-845.
44. Mao, H., *[Detection of Legionella antigens in the urine by a biotin-avidin enzyme-linked immunosorbent assay and coagglutination test]*. *Chung.Hua.Liu.Hsing.Ping.Hsueh.Tsa.Chih.*, 1988. **9**: p. 103-106.
45. Ratcliff, R.M., *Sequence-based identification of legionella*. *Methods Mol Biol*, 2013. **954**: p. 57-72.
46. Berendt, R.F., et al., *Dose-response of guinea pigs experimentally infected with aerosols of Legionella pneumophila*. *J.Infect.Dis.*, 1980. **141**: p. 186-192.
47. Davis, G.S., et al., *Legionnaires' pneumonia after aerosol exposure in guinea pigs and rats*. *Am.Rev.Respir.Dis.*, 1982. **126**: p. 1050-1057.
48. Hambleton, P., et al., *Survival of virulent Legionella pneumophila in aerosols*. *J.Hyg.(Lond)*, 1983. **90**: p. 451-460.
49. Muder, R.R., V.L. Yu, and A.H. Woo, *Mode of transmission of Legionella pneumophila. A critical review*. *Arch.Intern.Med.*, 1986. **146**: p. 1607-1612.
50. LeChevallier, M., *Monitoring distribution systems for Legionella pneumophila using Legiolert*. *AWWA Water Science*, 2019. **1**(1).
51. Correia, A.M., et al., *Probable Person-to-Person Transmission of Legionnaires' Disease*. *N Engl J Med*, 2016. **374**(5): p. 497-8.

52. Borges, V., et al., *Legionella pneumophila* strain associated with the first evidence of person-to-person transmission of Legionnaires' disease: a unique mosaic genetic backbone. *Scientific Reports*, 2016. **6**: p. 26261.
53. Yu, V.L., et al., *Lack of evidence for person-to-person transmission of Legionnaires' disease*. *J.Infect.Dis.*, 1983. **147**: p. 362.
54. Benedict, K.M., et al., *Surveillance for Waterborne Disease Outbreaks Associated with Drinking Water - United States, 2013-2014*. *MMWR Morb Mortal Wkly Rep*, 2017. **66**(44): p. 1216-1221.
55. Katz, S.M. and J.M. Hammel, *The effect of drying, heat, and pH on the survival of Legionella pneumophila*. *Ann Clin Lab Sci*, 1987. **17**(3): p. 150-6.
56. Biurrun, A., et al., *Treatment of a Legionella pneumophila -Colonized Water Distribution System Using Copper-Silver Ionization and Continuous Chlorination* •. Vol. 20. 1999. 426-8.
57. Darelid J, B.S., Jacobson K, Lofgren S, *The presence of a specific genotype of Legionella pneumophila serogroup 1 in a hospital and municipal water distribution system over a 12-year period* *Scand J Infect Dis*, 2004. **36**(6-7): p. 417-423.
58. Kusnetsov, J., et al., *Copper and silver ions more effective against legionellae than against mycobacteria in a hospital warm water system*. *Water Res*, 2001. **35**(17): p. 4217-25.
59. Muraca, P., J.E. Stout, and V.L. Yu, *Comparative assessment of chlorine, heat, ozone, and UV light for killing Legionella pneumophila within a model plumbing system*. *Appl.Environ.Microbiol.*, 1987. **53**: p. 447-453.
60. Ashbolt, N.J., *Environmental (Saprozoic) Pathogens of Engineered Water Systems: Understanding Their Ecology for Risk Assessment and Management*. *Pathogens*, 2015. **4**(2): p. 390-405.
61. Lau, H.Y. and N.J. Ashbolt, *The role of biofilms and protozoa in Legionella pathogenesis: implications for drinking water*. *J Appl Microbiol*, 2009. **107**(2): p. 368-78.
62. Garcia, M.T., et al., *Acanthamoeba polyphaga resuscitates viable non-culturable Legionella pneumophila after disinfection*. *Environ Microbiol*, 2007. **9**(5): p. 1267-77.
63. Fields, B.S., *The molecular ecology of legionellae*. *Trends Microbiol*, 1996. **4**(7): p. 286-90.
64. Breiman, R.F., et al., *Association of shower use with Legionnaires' disease: possible role of amoebae*. *JAMA*, 1990. **263**: p. 2924-2926.
65. Fields, B.S., et al., *Intracellular multiplication of Legionella pneumophila in amoebae isolated from hospital hot water tanks*. *Curr.Microbiol.*, 1989. **18**: p. 131-137.
66. Fields, B.S., et al., *Proliferation of Legionella pneumophila as an intracellular parasite of the ciliated protozoan Tetrahymena pyriformis*. *Appl.Environ.Microbiol.*, 1984. **47**: p. 467-471.

67. Hagele, S., et al., *Dictyostelium discoideum: a new host model system for intracellular pathogens of the genus Legionella*. Cell Microbiol, 2000. **2**(2): p. 165-71.
68. Newsome, A.L., et al., *Interactions between Naegleria fowleri and Legionella pneumophila*. Infect.Immun., 1985. **50**: p. 449-452.
69. Rowbotham, T.J., *Preliminary report on the pathogenicity of Legionella pneumophila for freshwater and soil amoebae*. J.Clin.Pathol., 1980. **33**: p. 1179-1183.
70. Rowbotham, T.J., *Current views on the relationships between amoebae, legionellae and man*. Isr.J.Med.Sci., 1986. **22**: p. 678-689.
71. Smith-Somerville, H.E., et al., *Survival of Legionella pneumophila in the cold-water ciliate Tetrahymena vorax*. Appl.Environ.Microbiol., 1991. **57**: p. 2742-2749.
72. Solomon, J.M., et al., *Intracellular growth of Legionella pneumophila in Dictyostelium discoideum, a system for genetic analysis of host-pathogen interactions*. Infect Immun, 2000. **68**(5): p. 2939-47.
73. Tyndall, R.L. and E.L. Domingue, *Cocultivation of Legionella pneumophila and free-living amoebae*. Appl.Environ.Microbiol., 1982. **44**: p. 954-959.
74. Kikuhara, H., et al., *Intracellular multiplication of Legionella pneumophila in Tetrahymena thermophila*. J UOEH, 1994. **16**(4): p. 263-75.
75. Tyson, J.Y., P. Vargas, and N.P. Cianciotto, *The novel Legionella pneumophila type II secretion substrate NttC contributes to infection of amoebae Hartmannella vermiformis and Willaertia magna*. Microbiology, 2014. **160**(Pt 12): p. 2732-2744.
76. Rasch, J., et al., *Legionella-protozoa-nematode interactions in aquatic biofilms and influence of Mip on Caenorhabditis elegans colonization*. International Journal of Medical Microbiology, 2016. **306**(6): p. 443-451.
77. Watanabe, K., et al., *Ciliate Paramecium is a natural reservoir of Legionella pneumophila*. Scientific Reports, 2016. **6**: p. 24322.
78. Scheikl, U., et al., *Free-living amoebae and their associated bacteria in Austrian cooling towers: a 1-year routine screening*. Parasitol Res, 2016. **115**(9): p. 3365-74.
79. Swanson, M.S. and B.K. Hammer, *Legionella pneumophila pathogenesis: a fateful journey from amoebae to macrophages*. Annu Rev Microbiol, 2000. **54**: p. 567-613.
80. Oliva, G., T. Sahr, and C. Buchrieser, *The Life Cycle of L. pneumophila: Cellular Differentiation Is Linked to Virulence and Metabolism*. Front Cell Infect Microbiol, 2018. **8**: p. 3.
81. Swanson, M.S. and I. Sturgill-Koszycki, *Exploitation of macrophages as a replication niche by Legionella pneumophila [see comments]*. Trends Microbiol, 2000. **8**(2): p. 47-9.
82. Cianciotto, N.P., *Pathogenicity of Legionella pneumophila*. Int J Med Microbiol, 2001. **291**(5): p. 331-43.

83. Molmeret, M., et al., *Amoebae as training grounds for intracellular bacterial pathogens*. Appl Environ Microbiol, 2005. **71**(1): p. 20-8.
84. Bouyer, S., et al., *Long-term survival of Legionella pneumophila associated with Acanthamoeba castellanii vesicles*. Environ Microbiol, 2007. **9**(5): p. 1341-4.
85. Abu Kwaik, Y., et al., *Invasion of protozoa by Legionella pneumophila and its role in bacterial ecology and pathogenesis*. Appl Environ Microbiol, 1998. **64**(9): p. 3127-33.
86. Price, C.T.D., et al., *Dot/Icm-Dependent Restriction of Legionella pneumophila within Neutrophils*. mBio, 2021. **12**(3): p. e0100821.
87. Ohno, A., et al., *Temperature-dependent parasitic relationship between Legionella pneumophila and a free-living amoeba (Acanthamoeba castellanii)*. Appl Environ Microbiol, 2008. **74**(14): p. 4585-8.
88. Kilvington, S. and J. Price, *Survival of Legionella pneumophila within cysts of Acanthamoeba polyphaga following chlorine exposure*. J Appl Bacteriol, 1990. **68**(5): p. 519-25.
89. Price, C., et al., *Paradoxical Pro-inflammatory Responses by Human Macrophages to an Amoebae Host-Adapted Legionella Effector*. Cell Host Microbe, 2020. **27**(4): p. 571-584 e7.
90. Rowbotham, T.J., *Isolation of Legionella pneumophila from clinical specimens via amoebae, and the interaction of those and other isolates with amoebae*. J Clin Pathol, 1983. **36**(9): p. 978-86.
91. Rowbotham, T.J., *Current views on the relationships between amoebae, legionellae and man*. Isr J Med Sci, 1986. **22**(9): p. 678-89.
92. Adeleke, A., et al., *Legionella-like amebal pathogens--phylogenetic status and possible role in respiratory disease*. Emerg Infect Dis, 1996. **2**(3): p. 225-30.
93. Marrie, T.J., et al., *Legionella-like and other amoebal pathogens as agents of community-acquired pneumonia*. Emerg Infect Dis, 2001. **7**(6): p. 1026-9.
94. Birtles, R.J., et al., *Phylogenetic diversity of intra-amoebal legionellae as revealed by 16S rRNA gene sequence comparison*. Microbiology (Reading), 1996. **142 (Pt 12)**: p. 3525-30.
95. Rowbotham, T.J., *Preliminary report on the pathogenicity of Legionella pneumophila for freshwater and soil amoebae*. J Clin Pathol, 1980. **33**(12): p. 1179-83.
96. Bruggemann, H., et al., *Virulence strategies for infecting phagocytes deduced from the in vivo transcriptional program of Legionella pneumophila*. Cell Microbiol, 2006. **8**(8): p. 1228-40.
97. Garduno, R.A., et al., *Intracellular growth of Legionella pneumophila gives rise to a differentiated form dissimilar to stationary-phase forms*. Infect Immun, 2002. **70**(11): p. 6273-83.
98. Greub, G. and D. Raoult, *Morphology of Legionella pneumophila according to their location within Hartmanella vermiformis*. Res Microbiol, 2003. **154**(9): p. 619-21.

99. Robertson, P., H. Abdelhady, and R.A. Garduno, *The many forms of a pleomorphic bacterial pathogen-the developmental network of Legionella pneumophila*. Front Microbiol, 2014. **5**: p. 670.
100. Faulkner, G. and R.A. Garduno, *Ultrastructural analysis of differentiation in Legionella pneumophila*. J Bacteriol, 2002. **184**(24): p. 7025-41.
101. Berk, S.G., et al., *Production of respirable vesicles containing live Legionella pneumophila cells by two Acanthamoeba spp.* Appl.Environ.Microbiol., 1998. **64**: p. 279-286.
102. Cirillo, J.D., L.S. Tompkins, and S. Falkow, *Growth of Legionella pneumophila in Acanthamoeba castellanii enhances invasion*. Infect.Immun., 1994. **62**: p. 3254-3261.
103. Byrne, B. and M.S. Swanson, *Expression of Legionella pneumophila virulence traits in response to growth conditions*. Infect Immun, 1998. **66**(7): p. 3029-34.
104. Hammer, B.K. and M.S. Swanson, *Co-ordination of legionella pneumophila virulence with entry into stationary phase by ppGpp*. Mol Microbiol, 1999. **33**(4): p. 721-31.
105. Pruckler, J.M., et al., *Association of flagellum expression and intracellular growth of Legionella pneumophila*. Infect Immun, 1995. **63**(12): p. 4928-32.
106. Abdel-Nour, M., et al., *Biofilms: the stronghold of Legionella pneumophila*. Int J Mol Sci, 2013. **14**(11): p. 21660-75.
107. Liu, R., et al., *Pyrosequencing analysis of eukaryotic and bacterial communities in faucet biofilms*. Sci Total Environ, 2012. **435-436**: p. 124-31.
108. Taylor, M., K. Ross, and R. Bentham, *Legionella, protozoa, and biofilms: interactions within complex microbial systems*. Microb Ecol, 2009. **58**(3): p. 538-47.
109. Emtiazi, F., et al., *Investigation of natural biofilms formed during the production of drinking water from surface water embankment filtration*. Water Res, 2004. **38**(5): p. 1197-206.
110. Dietersdorfer, E., et al., *Starved viable but non-culturable (VBNC) Legionella strains can infect and replicate in amoebae and human macrophages*. Water Res, 2018. **141**: p. 428-438.
111. Epalle, T., et al., *Viable but not culturable forms of Legionella pneumophila generated after heat shock treatment are infectious for macrophage-like and alveolar epithelial cells after resuscitation on Acanthamoeba polyphaga*. Microb Ecol, 2015. **69**(1): p. 215-24.
112. Molmeret, M., et al., *Amoebae as training grounds for intracellular bacterial pathogens*. Appl. Environ. Microbiol., 2005. **71**: p. 20-28.
113. Bozue, J.A. and W. Johnson, *Interaction of Legionella pneumophila with Acanthamoeba catellanii: uptake by coiling phagocytosis and inhibition of phagosome-lysosome fusion*. Infect.Immun., 1996. **64**: p. 668-673.
114. Horwitz, M.A., *Phagocytosis of the Legionnaires' disease bacterium (Legionella pneumophila) occurs by a novel mechanism: engulfment within a pseudopod coil*. Cell, 1984. **36**: p. 27-33.

115. Swanson, M.S. and I. Sturgill-Koszycki, *Exploitation of macrophages as a replication niche by Legionella pneumophila*. Trends Microbiol, 2000. **8**(2): p. 47-9.
116. Horwitz, M.A., *Formation of a novel phagosome by the Legionnaires' disease bacterium (Legionella pneumophila) in human monocytes*. J Exp Med, 1983. **158**(4): p. 1319-31.
117. Swanson, M.S. and R.R. Isberg, *Association of Legionella pneumophila with the macrophage endoplasmic reticulum*. Infect Immun, 1995. **63**(9): p. 3609-20.
118. Kitao, T., H. Nagai, and T. Kubori, *Divergence of Legionella Effectors Reversing Conventional and Unconventional Ubiquitination*. Frontiers in Cellular and Infection Microbiology, 2020. **10**(448).
119. Amer, A.O. and M.S. Swanson, *A phagosome of one's own: a microbial guide to life in the macrophage*. Curr Opin Microbiol, 2002. **5**(1): p. 56-61.
120. Molmeret, M., et al., *Cell biology of the intracellular infection by Legionella pneumophila*. Microbes Infect, 2004. **6**(1): p. 129-39.
121. Molmeret, M., et al., *Temporal and spatial trigger of post-exponential virulence-associated regulatory cascades by Legionella pneumophila after bacterial escape into the host cell cytosol*. Environ Microbiol, 2010. **12**(3): p. 704-15.
122. Molofsky, A.B. and M.S. Swanson, *Differentiate to thrive: lessons from the Legionella pneumophila life cycle*. Mol Microbiol, 2004. **53**(1): p. 29-40.
123. Rasis, M. and G. Segal, *The LetA-RsmYZ-CsrA regulatory cascade, together with RpoS and PmrA, post-transcriptionally regulates stationary phase activation of Legionella pneumophila Icm/Dot effectors*. Mol Microbiol, 2009.
124. Gao, L.-Y. and Y. Abu Kwaik, *Activation of caspase-3 in Legionella pneumophila-induced apoptosis in macrophages*. Infect.Immun., 1999. **67**(9): p. 4886-4894.
125. Gao, L.-Y. and Y. Abu Kwaik, *Apoptosis in macrophages and alveolar epithelial cells during early stages of infection by Legionella pneumophila and its role in cytopathogenicity*. Infect.Immun., 1999. **67**: p. 862-870.
126. Hägele, S., J. Hacker, and B.C. Brand, *Legionella pneumophila kills human phagocytes but not protozoan host cells by inducing apoptotic cell death*. FEMS Microbiol.Lett., 1998. **169**: p. 51-58.
127. Cianciotto, N.P., *Type II secretion: a protein secretion system for all seasons*. Trends Microbiol, 2005. **13**(12): p. 581-8.
128. Hales, L.M. and H.A. Shuman, *Legionella pneumophila contains a type II general secretion pathway required for growth in amoebae as well as for secretion of the Msp protease*. Infect.Immun., 1999. **67**: p. 3662-3666.
129. Hubber, A. and C.R. Roy, *Modulation of host cell function by Legionella pneumophila type IV effectors*. Annu Rev Cell Dev Biol, 2010. **26**: p. 261-83.
130. Ghosal, D., et al., *In vivo structure of the Legionella type II secretion system by electron cryotomography*. Nat Microbiol, 2019. **4**(12): p. 2101-2108.
131. Cianciotto, N.P. and R.C. White, *The Expanding Role of Type II Secretion in Bacterial Pathogenesis and Beyond*. Infection and Immunity, 2017.

132. Peabody, C.R., et al., *Type II protein secretion and its relationship to bacterial type IV pili and archaeal flagella*. Microbiology, 2003. **149**(Pt 11): p. 3051-72.
133. Tyson, J.Y., et al., *Multiple Legionella pneumophila Type II secretion substrates, including a novel protein, contribute to differential infection of the amoebae Acanthamoeba castellanii, Hartmannella vermiformis, and Naegleria lovaniensis*. Infect Immun, 2013. **81**(5): p. 1399-410.
134. Rossier, O., J. Dao, and N.P. Cianciotto, *The type II secretion system of Legionella pneumophila elaborates two aminopeptidases, as well as a metalloprotease that contributes to differential infection among protozoan hosts*. Appl Environ Microbiol, 2008. **74**(3): p. 753-61.
135. Rossier, O., S.R. Starckenburg, and N.P. Cianciotto, *Legionella pneumophila type II protein secretion promotes virulence in the A/J mouse model of Legionnaires' disease pneumonia*. Infect Immun, 2004. **72**(1): p. 310-21.
136. Söderberg, M.A., et al., *Importance of Type II Secretion for Survival of Legionella pneumophila in Tap Water and in Amoebae at Low Temperatures*. Applied and Environmental Microbiology, 2008. **74**(17): p. 5583.
137. White, R.C. and N.P. Cianciotto, *Type II Secretion Is Necessary for Optimal Association of the Legionella-Containing Vacuole with Macrophage Rab1B but Enhances Intracellular Replication Mainly by Rab1B-Independent Mechanisms*. Infection and Immunity, 2016. **84**(12): p. 3313-3327.
138. Cianciotto, N.P. and R.C. White, *Expanding Role of Type II Secretion in Bacterial Pathogenesis and Beyond*. Infect Immun, 2017. **85**(5).
139. Cianciotto, N.P., *Many substrates and functions of type II secretion: lessons learned from Legionella pneumophila*. Future Microbiol, 2009. **4**(7): p. 797-805.
140. DebRoy, S., et al., *Legionella pneumophila type II secretome reveals unique exoproteins and a chitinase that promotes bacterial persistence in the lung*. Proc Natl Acad Sci U S A, 2006. **103**(50): p. 19146-51.
141. Debroy, S., et al., *Legionella pneumophila Mip, a surface-exposed peptidylproline cis-trans-isomerase, promotes the presence of phospholipase C-like activity in culture supernatants*. Infect Immun, 2006. **74**(9): p. 5152-60.
142. White, R.C., et al., *Type II Secretion-Dependent Aminopeptidase LapA and Acyltransferase PlaC Are Redundant for Nutrient Acquisition during Legionella pneumophila Intracellular Infection of Amoebas*. mBio, 2018. **9**(2).
143. Rossier, O., J. Dao, and N.P. Cianciotto, *A type II secreted RNase of Legionella pneumophila facilitates optimal intracellular infection of Hartmannella vermiformis*. Microbiology (Reading, England), 2009. **155**(Pt 3): p. 882-890.
144. Söderberg, M.A. and N.P. Cianciotto, *A Legionella pneumophila Peptidyl-Prolyl cis-trans Isomerase Present in Culture Supernatants Is Necessary for Optimal Growth at Low Temperatures*. Applied and Environmental Microbiology, 2008. **74**(5): p. 1634-1638.
145. Duncan, C., et al., *Lcl of Legionella*

- pneumophila*; Is an Immunogenic GAG Binding Adhesin That Promotes Interactions with Lung Epithelial Cells and Plays a Crucial Role in Biofilm Formation. *Infection and Immunity*, 2011. **79**(6): p. 2168.
146. Duncan, C., et al., *Lcl of Legionella pneumophila is an immunogenic GAG binding adhesin that promotes interactions with lung epithelial cells and plays a crucial role in biofilm formation*. *Infect Immun*, 2011. **79**(6): p. 2168-81.
 147. Johnston, C.W., et al., *Informatic analysis reveals Legionella as a source of novel natural products*. *Synthetic and Systems Biotechnology*, 2016. **1**(2): p. 130-136.
 148. Stewart, C.R., D.M. Burnside, and N.P. Cianciotto, *The Surfactant of Legionella pneumophila Is Secreted in a TolC-Dependent Manner and Is Antagonistic toward Other Legionella Species*. *Journal of Bacteriology*, 2011. **193**(21): p. 5971.
 149. Stewart, C.R., O. Rossier, and N.P. Cianciotto, *Surface translocation by Legionella pneumophila: a form of sliding motility that is dependent upon type II protein secretion*. *J Bacteriol*, 2009. **191**(5): p. 1537-46.
 150. Stewart, C.R., D.M. Burnside, and N.P. Cianciotto, *The surfactant of Legionella pneumophila Is secreted in a TolC-dependent manner and is antagonistic toward other Legionella species*. *J Bacteriol*, 2011. **193**(21): p. 5971-84.
 151. McCoy-Simandle, K., et al., *Legionella pneumophila type II secretion dampens the cytokine response of infected macrophages and epithelia*. *Infect Immun*, 2011. **79**(5): p. 1984-97.
 152. Mallama, C.A., K. McCoy-Simandle, and N.P. Cianciotto, *The Type II Secretion System of Legionella pneumophila Dampens the MyD88 and Toll-Like Receptor 2 Signaling Pathway in Infected Human Macrophages*. *Infection and Immunity*, 2017. **85**(4).
 153. Truchan, H.K., et al., *Type II Secretion Substrates of Legionella pneumophila Translocate Out of the Pathogen-Occupied Vacuole via a Semipermeable Membrane*. *MBio*, 2017. **8**(3).
 154. White, R.C. and N.P. Cianciotto, *Type II Secretion Is Necessary for Optimal Association of the Legionella-Containing Vacuole with Macrophage Rab1B but Enhances Intracellular Replication Mainly by Rab1B-Independent Mechanisms*. *Infect Immun*, 2016. **84**(12): p. 3313-3327.
 155. Prashar, A. and M.R. Terebiznik, *Legionella pneumophila: homeward bound away from the phagosome*. *Curr Opin Microbiol*, 2015. **23**: p. 86-93.
 156. Bock, D., et al., *The Polar Legionella Icm/Dot T4SS Establishes Distinct Contact Sites with the Pathogen Vacuole Membrane*. *mBio*, 2021. **12**(5): p. e0218021.
 157. Andrews, H.L., J.P. Vogel, and R.R. Isberg, *Identification of linked Legionella pneumophila genes essential for intracellular growth and evasion of the endocytic pathway*. *Infect.Immun.*, 1998. **66**: p. 950-958.

158. Berger, K.H. and R.R. Isberg, *Two distinct defects in intracellular growth complemented by a single genetic locus in Legionella pneumophila*. Mol.Microbiol., 1993. **7**: p. 7-19.
159. Berger, K.H., J. Merriam, and R.R. Isberg, *Altered intracellular targeting properties associated with mutations in the Legionella pneumophila dotA gene*. Mol.Microbiol., 1994. **14**: p. 809-822.
160. Brand, B., A.B. Sadosky, and H.A. Shuman, *The Legionella pneumophila icm locus: a set of genes required for intracellular multiplication in human macrophages*. Mol.Microbiol., 1994. **14**: p. 797-808.
161. Purcell, M. and H.A. Shuman, *The Legionella pneumophila icmGCDJBF genes are required for killing of human macrophages*. Infect Immun, 1998. **66**: p. 2245-55.
162. Segal, G. and H.A. Shuman, *Characterization of a new region required for macrophage killing by Legionella pneumophila*. Infect Immun, 1997. **65**(12): p. 5057-66.
163. Vogel, J.P., et al., *Conjugative transfer by the virulence system of Legionella pneumophila*. Science, 1998. **279**: p. 873-876.
164. Nagai, H. and T. Kubori, *Type IVB Secretion Systems of Legionella and Other Gram-Negative Bacteria*. Front Microbiol, 2011. **2**: p. 136.
165. Sexton, J.A. and J.P. Vogel, *Type IVB secretion by intracellular pathogens*. Traffic, 2002. **3**(3): p. 178-85.
166. Ninio, S. and C.R. Roy, *Effector proteins translocated by Legionella pneumophila: strength in numbers*. Trends Microbiol, 2007. **15**(8): p. 372-80.
167. Schroeder, G.N. and H. Hilbi, *Molecular pathogenesis of Shigella spp.: controlling host cell signaling, invasion, and death by type III secretion*. Clin Microbiol Rev, 2008. **21**(1): p. 134-56.
168. Steele-Mortimer, O., *Infection of epithelial cells with Salmonella enterica*. Methods Mol Biol, 2008. **431**: p. 201-11.
169. Weber, S.S., C. Ragaz, and H. Hilbi, *Pathogen trafficking pathways and host phosphoinositide metabolism*. Mol Microbiol, 2009. **71**(6): p. 1341-52.
170. Green, E.R. and J. Meccas, *Bacterial Secretion Systems: An Overview*. Microbiol Spectr, 2016. **4**(1).
171. Filloux, A., A. Hachani, and S. Bleves, *The bacterial type VI secretion machine: yet another player for protein transport across membranes*. Microbiology, 2008. **154**(6): p. 1570-1583.
172. Steele-Mortimer, O., *The Salmonella-containing vacuole: moving with the times*. Curr Opin Microbiol, 2008. **11**(1): p. 38-45.
173. Jeong, K.C., et al., *Polar delivery of Legionella type IV secretion system substrates is essential for virulence*. Proc Natl Acad Sci U S A, 2017. **114**(30): p. 8077-8082.
174. Sutherland, M.C., et al., *The Legionella IcmSW complex directly interacts with DotL to mediate translocation of adaptor-dependent substrates*. PLoS Pathog, 2012. **8**(9): p. e1002910.
175. Meir, A., et al., *Legionella DotM structure reveals a role in effector recruiting to the Type 4B secretion system*. Nat Commun, 2018. **9**(1): p. 507.

176. Ninio, S., et al., *The Legionella lcmS-lcmW protein complex is important for Dot/lcm-mediated protein translocation*. Mol Microbiol, 2005. **55**(3): p. 912-26.
177. Vincent, C.D., et al., *Identification of the DotL coupling protein subcomplex of the Legionella Dot/lcm type IV secretion system*. Mol Microbiol, 2012. **85**(2): p. 378-91.
178. Cambronne, E.D. and C.R. Roy, *The Legionella pneumophila lcmSW complex interacts with multiple Dot/lcm effectors to facilitate type IV translocation*. PLoS Pathog, 2007. **3**(12): p. e188.
179. Vincent, C.D., et al., *Identification of the core transmembrane complex of the Legionella Dot/lcm type IV secretion system*. Mol Microbiol, 2006. **62**(5): p. 1278-91.
180. Buscher, B.A., et al., *The DotL protein, a member of the TraG-coupling protein family, is essential for Viability of Legionella pneumophila strain Lp02*. J Bacteriol, 2005. **187**(9): p. 2927-38.
181. Gomis-Ruth, F.X., et al., *Conjugative plasmid protein TrwB, an integral membrane type IV secretion system coupling protein. Detailed structural features and mapping of the active site cleft*. J Biol Chem, 2002. **277**(9): p. 7556-66.
182. Crabill, E., et al., *Dot/lcm-translocated proteins important for biogenesis of the Coxiella burnetii-containing vacuole identified by screening of an effector mutant sub-library*. Infection and immunity, 2018: p. IAI. 00758-17.
183. Burstein, D., et al., *Genomic analysis of 38 Legionella species identifies large and diverse effector repertoires*. Nat Genet, 2016. **48**(2): p. 167-75.
184. Gomez-Valero, L., et al., *More than 18,000 effectors in the Legionella genus genome provide multiple, independent combinations for replication in human cells*. Proceedings of the National Academy of Sciences, 2019. **116**(6): p. 2265-2273.
185. Lifshitz, Z., et al., *Computational modeling and experimental validation of the Legionella and Coxiella virulence-related type-IVB secretion signal*. Proc Natl Acad Sci U S A, 2013. **110**(8): p. E707-15.
186. Zhu, W., et al., *Comprehensive identification of protein substrates of the Dot/lcm type IV transporter of Legionella pneumophila*. PLoS One, 2011. **6**(3): p. e17638.
187. Nagai, H., et al., *A C-terminal translocation signal required for Dot/lcm-dependent delivery of the Legionella RalF protein to host cells*. Proc Natl Acad Sci U S A, 2005. **102**(3): p. 826-31.
188. Kubori, T., A. Hyakutake, and H. Nagai, *Legionella translocates an E3 ubiquitin ligase that has multiple U-boxes with distinct functions*. Mol Microbiol, 2008. **67**(6): p. 1307-19.
189. Burstein, D., et al., *Genome-scale identification of Legionella pneumophila effectors using a machine learning approach*. PLoS Pathog, 2009. **5**(7): p. e1000508.
190. Huang, L., et al., *The E Block motif is associated with Legionella pneumophila translocated substrates*. Cell Microbiol, 2011. **13**(2): p. 227-45.

191. Urbanus, M.L., et al., *Diverse mechanisms of metaeffector activity in an intracellular bacterial pathogen, Legionella pneumophila*. Mol Syst Biol, 2016. **12**(12): p. 893.
192. Kubori, T., et al., *Legionella metaeffector exploits host proteasome to temporally regulate cognate effector*. PLoS Pathog, 2010. **6**(12): p. e1001216.
193. Bruckert, W.M., C.T. Price, and Y. Abu Kwaik, *Rapid nutritional remodeling of the host cell upon attachment of Legionella pneumophila*. Infect Immun, 2014. **82**(1): p. 72-82.
194. Charpentier, X., et al., *Chemical genetics reveals bacterial and host cell functions critical for type IV effector translocation by Legionella pneumophila*. PLoS Pathog, 2009. **5**(7): p. e1000501.
195. Liu, Y., et al., *An in vivo gene deletion system for determining temporal requirement of bacterial virulence factors*. Proc Natl Acad Sci U S A, 2008. **105**(27): p. 9385-90.
196. Ingmundson, A., et al., *Legionella pneumophila proteins that regulate Rab1 membrane cycling*. Nature, 2007. **450**(7168): p. 365-9.
197. Neunuebel, M.R., et al., *De-AMPylation of the small GTPase Rab1 by the pathogen Legionella pneumophila*. Science, 2011. **333**(6041): p. 453-6.
198. Bardill, J.P., J.L. Miller, and J.P. Vogel, *IcmS-dependent translocation of SdeA into macrophages by the Legionella pneumophila type IV secretion system*. Mol Microbiol, 2005. **56**(1): p. 90-103.
199. Aurass, P., et al., *Life Stage-specific Proteomes of Legionella pneumophila Reveal a Highly Differential Abundance of Virulence-associated Dot/Icm effectors*. Mol Cell Proteomics, 2016. **15**(1): p. 177-200.
200. Gan, N., et al., *Legionella pneumophila regulates the activity of UBE2N by deamidase-mediated deubiquitination*. EMBO J, 2020. **39**(4): p. e102806.
201. Allombert, J., et al., *Deciphering Legionella effector delivery by Icm/Dot secretion system reveals a new role for c-di-GMP signaling*. J Mol Biol, 2021. **433**(13): p. 166985.
202. Luo, Z.Q. and R.R. Isberg, *Multiple substrates of the Legionella pneumophila Dot/Icm system identified by interbacterial protein transfer*. Proc Natl Acad Sci U S A, 2004. **101**(3): p. 841-6.
203. Isberg, R.R., T.J. O'Connor, and M. Heidtman, *The Legionella pneumophila replication vacuole: making a cosy niche inside host cells*. Nat Rev Microbiol, 2009. **7**(1): p. 13-24.
204. Ghosh, S. and T.J. O'Connor, *Beyond Paralogs: The Multiple Layers of Redundancy in Bacterial Pathogenesis*. Front Cell Infect Microbiol, 2017. **7**: p. 467.
205. O'Connor, T.J., et al., *Minimization of the Legionella pneumophila genome reveals chromosomal regions involved in host range expansion*. Proc Natl Acad Sci U S A, 2011. **108**(36): p. 14733-40.
206. Best, A. and Y. Abu Kwaik, *Evolution of the Arsenal of Legionella pneumophila Effectors To Modulate Protist Hosts*. mBio, 2018. **9**(5).

207. Kotewicz, K.M., et al., *A Single Legionella Effector Catalyzes a Multistep Ubiquitination Pathway to Rearrange Tubular Endoplasmic Reticulum for Replication*. *Cell Host Microbe*, 2017. **21**(2): p. 169-181.
208. Qiu, J., et al., *Ubiquitination independent of E1 and E2 enzymes by bacterial effectors*. *Nature*, 2016. **533**(7601): p. 120-4.
209. VanRheenen, S.M., et al., *Members of a Legionella pneumophila family of proteins with ExoU (phospholipase A) active sites are translocated to target cells*. *Infect Immun*, 2006. **74**(6): p. 3597-606.
210. Debnath Ghosal, Y.-W.C., Kwang Cheol Jeong, Joseph P. Vogel, Grant J. Jensen, *Molecular architecture of the Legionella Dot/Icm type IV secretion system*. preprint, 2018.
211. Gomez-Valero, L., et al., *More than 18,000 effectors in the Legionella genus genome provide multiple, independent combinations for replication in human cells*. *Proc Natl Acad Sci U S A*, 2019. **116**(6): p. 2265-2273.
212. Isaac, D.T., et al., *MavN is a Legionella pneumophila vacuole-associated protein required for efficient iron acquisition during intracellular growth*. *Proc Natl Acad Sci U S A*, 2015. **112**(37): p. E5208-17.
213. Christenson, E.T., et al., *The iron-regulated vacuolar Legionella pneumophila MavN protein is a transition-metal transporter*. *Proc Natl Acad Sci U S A*, 2019. **116**(36): p. 17775-17785.
214. Das, S., et al., *Genome plasticity as a paradigm of antibiotic resistance spread in ESKAPE pathogens*. *Environ Sci Pollut Res Int*, 2022.
215. Segal, G. and H.A. Shuman, *Legionella pneumophila utilizes the same genes to multiply within Acanthamoeba castellanii and human macrophages*. *Infect Immun*, 1999. **67**(5): p. 2117-24.
216. Stone, B.J. and Y.A. Kwaik, *Natural competence for DNA transformation by Legionella pneumophila and its association with expression of type IV pili*. *J Bacteriol*, 1999. **181**(5): p. 1395-402.
217. Cazalet, C., et al., *Evidence in the Legionella pneumophila genome for exploitation of host cell functions and high genome plasticity*. *Nat Genet*, 2004. **36**(11): p. 1165-73.
218. Franco, I.S., H.A. Shuman, and X. Charpentier, *The perplexing functions and surprising origins of Legionella pneumophila type IV secretion effectors*. *Cell Microbiol*, 2009. **11**(10): p. 1435-43.
219. Lurie-Weinberger, M.N., et al., *The origins of eukaryotic-like proteins in Legionella pneumophila*. *Int J Med Microbiol*, 2010. **300**(7): p. 470-81.
220. David, S., et al., *Multiple major disease-associated clones of Legionella pneumophila have emerged recently and independently*. *Genome Res*, 2016. **26**(11): p. 1555-1564.
221. Sanchez-Buso, L., et al., *Recombination drives genome evolution in outbreak-related Legionella pneumophila isolates*. *Nat Genet*, 2014. **46**(11): p. 1205-11.
222. David, S., et al., *Dynamics and impact of homologous recombination on the evolution of Legionella pneumophila*. *PLoS Genet*, 2017. **13**(6): p. e1006855.

223. Amaro, F., et al., *Diverse protist grazers select for virulence-related traits in Legionella*. ISME J, 2015. **9**(7): p. 1607-18.
224. Von Dwingelo, J., et al., *Interaction of the Ankyrin H Core Effector of Legionella with the Host LARP7 Component of the 7SK snRNP Complex*. mBio, 2019. **10**(4).
225. Hugoson, E., et al., *Host Adaptation in Legionellales Is 1.9 Ga, Coincident with Eukaryogenesis*. Mol Biol Evol, 2022. **39**(3).
226. Vieira, O.V., R.J. Botelho, and S. Grinstein, *Phagosome maturation: aging gracefully*. Biochem J, 2002. **366**(Pt 3): p. 689-704.
227. Kinchen, J.M. and K.S. Ravichandran, *Phagosome maturation: going through the acid test*. Nat Rev Mol Cell Biol, 2008. **9**(10): p. 781-95.
228. Pitt, A., et al., *Alterations in the protein composition of maturing phagosomes*. J Clin Invest, 1992. **90**(5): p. 1978-83.
229. Hybiske, K. and R.S. Stephens, *Mechanisms of Chlamydia trachomatis entry into nonphagocytic cells*. Infect Immun, 2007. **75**(8): p. 3925-34.
230. Mnich, M.E., R. van Dalen, and N.M. van Sorge, *C-Type Lectin Receptors in Host Defense Against Bacterial Pathogens*. Frontiers in Cellular and Infection Microbiology, 2020. **10**(309).
231. Do, H.T., et al., *Effectiveness of a Communication for Behavioral Impact (COMBI) Intervention to Reduce Salt Intake in a Vietnamese Province Based on Estimations From Spot Urine Samples*. J Clin Hypertens (Greenwich), 2016. **18**(11): p. 1135-1142.
232. Vaughn, B. and Y. Abu Kwaik, *Idiosyncratic Biogenesis of Intracellular Pathogens-Containing Vacuoles*. Front Cell Infect Microbiol, 2021. **11**: p. 722433.
233. Cakir, T., et al., *Novel Approaches for Systems Biology of Metabolism-Oriented Pathogen-Human Interactions: A Mini-Review*. Front Cell Infect Microbiol, 2020. **10**: p. 52.
234. Leseigneur, C., et al., *Emerging Evasion Mechanisms of Macrophage Defenses by Pathogenic Bacteria*. Front Cell Infect Microbiol, 2020. **10**: p. 577559.
235. Sachdeva, K. and V. Sundaramurthy, *The Interplay of Host Lysosomes and Intracellular Pathogens*. Frontiers in Cellular and Infection Microbiology, 2020. **10**(713).
236. Shau, H. and J.R. Dawson, *The role of the lysosome in natural killing: inhibition by lysosomotropic vital dyes*. Immunology, 1984. **53**(4): p. 745-51.
237. Bailo, N., et al., *Defective lysosome maturation and Legionella pneumophila replication in Dictyostelium cells mutant for the Arf GAP ACAP-A*. J Cell Sci, 2014. **127**(Pt 21): p. 4702-13.
238. Nuoffer, C., et al., *A GDP-bound of rab1 inhibits protein export from the endoplasmic reticulum and transport between Golgi compartments*. J Cell Biol, 1994. **125**(2): p. 225-37.
239. Wilson, B.S., et al., *A Rab1 mutant affecting guanine nucleotide exchange promotes disassembly of the Golgi apparatus*. J Cell Biol, 1994. **125**(3): p. 557-71.

240. Tisdale, E.J., et al., *GTP-binding mutants of rab1 and rab2 are potent inhibitors of vesicular transport from the endoplasmic reticulum to the Golgi complex*. J Cell Biol, 1992. **119**(4): p. 749-61.
241. Hay, J.C., et al., *Protein interactions regulating vesicle transport between the endoplasmic reticulum and Golgi apparatus in mammalian cells*. Cell, 1997. **89**(1): p. 149-58.
242. Xu, D., et al., *Subunit structure of a mammalian ER/Golgi SNARE complex*. J Biol Chem, 2000. **275**(50): p. 39631-9.
243. Nagai, H., et al., *A bacterial guanine nucleotide exchange factor activates ARF on Legionella phagosomes*. Science, 2002. **295**(5555): p. 679-82.
244. Derre, I. and R.R. Isberg, *Legionella pneumophila replication vacuole formation involves rapid recruitment of proteins of the early secretory system*. Infect Immun, 2004. **72**(5): p. 3048-53.
245. Kagan, J.C., et al., *Legionella subvert the functions of Rab1 and Sec22b to create a replicative organelle*. J Exp Med, 2004. **199**(9): p. 1201-11.
246. Aridor, M., et al., *Sequential coupling between COPII and COPI vesicle coats in endoplasmic reticulum to Golgi transport*. J Cell Biol, 1995. **131**(4): p. 875-93.
247. Scales, S.J., R. Pepperkok, and T.E. Kreis, *Visualization of ER-to-Golgi transport in living cells reveals a sequential mode of action for COPII and COPI*. Cell, 1997. **90**(6): p. 1137-48.
248. Duden, R., *ER-to-Golgi transport: COP I and COP II function (Review)*. Mol Membr Biol, 2003. **20**(3): p. 197-207.
249. Robinson, C.G. and C.R. Roy, *Attachment and fusion of endoplasmic reticulum with vacuoles containing Legionella pneumophila*. Cell Microbiol, 2006. **8**(5): p. 793-805.
250. Alix, E., et al., *The capping domain in RalF regulates effector functions*. PLoS Pathog, 2012. **8**(11): p. e1003012.
251. Murata, T., et al., *The Legionella pneumophila effector protein DrrA is a Rab1 guanine nucleotide-exchange factor*. Nat Cell Biol, 2006. **8**(9): p. 971-7.
252. Mishra, A.K., et al., *The Legionella pneumophila GTPase activating protein LepB accelerates Rab1 deactivation by a non-canonical hydrolytic mechanism*. J Biol Chem, 2013. **288**(33): p. 24000-11.
253. Ku, B., et al., *VipD of Legionella pneumophila targets activated Rab5 and Rab22 to interfere with endosomal trafficking in macrophages*. PLoS Pathog, 2012. **8**(12): p. e1003082.
254. Gaspar, A.H. and M.P. Machner, *VipD is a Rab5-activated phospholipase A1 that protects Legionella pneumophila from endosomal fusion*. Proc Natl Acad Sci U S A, 2014. **111**(12): p. 4560-5.
255. Wang, Y., et al., *Structural Insights into Non-canonical Ubiquitination Catalyzed by SidE*. Cell, 2018. **173**(5): p. 1231-1243 e16.
256. Hilbi, H. and A. Haas, *Secretive bacterial pathogens and the secretory pathway*. Traffic, 2012. **13**(9): p. 1187-97.

257. Tan, Y. and Z.Q. Luo, *Take it and release it: The use of the Rab1 small GTPase at a bacterium's will*. Cell Logist, 2011. **1**(4): p. 125-127.
258. Horwitz, M.A., *The Legionnaires' disease bacterium (Legionella pneumophila) inhibits phagosome-lysosome fusion in human monocytes*. J.Exp.Med., 1983. **158**: p. 2108-2126.
259. Pike, C.M., et al., *The Legionella effector RavD binds phosphatidylinositol-3-phosphate and helps suppress endolysosomal maturation of the Legionella-containing vacuole*. J Biol Chem, 2019. **294**(16): p. 6405-6415.
260. Ghosal, D., et al., *In situ structure of the Legionella Dot/Icm type IV secretion system by electron cryotomography*. EMBO Rep, 2017. **18**(5): p. 726-732.
261. Zink, S.D., et al., *The Dot/Icm type IV secretion system of Legionella pneumophila is essential for the induction of apoptosis in human macrophages*. Infect Immun, 2002. **70**(3): p. 1657-63.
262. Sol, A., et al., *Legionella pneumophila translocated translation inhibitors are required for bacterial-induced host cell cycle arrest*. Proc Natl Acad Sci U S A, 2019. **116**(8): p. 3221-3228.
263. Fromme, J.C. and N. Segev, *Regulation of vesicle trafficking: GTPases and friends*. Mol Biol Cell, 2014. **25**(6): p. 732.
264. Weber, M.M. and R. Faris, *Subversion of the Endocytic and Secretory Pathways by Bacterial Effector Proteins*. Front Cell Dev Biol, 2018. **6**: p. 1.
265. Tsai, A.Y., B.C. English, and R.M. Tsois, *Hostile Takeover: Hijacking of Endoplasmic Reticulum Function by T4SS and T3SS Effectors Creates a Niche for Intracellular Pathogens*. Microbiol Spectr, 2019. **7**(3).
266. Jahn, R. and R.H. Scheller, *SNAREs--engines for membrane fusion*. Nat Rev Mol Cell Biol, 2006. **7**(9): p. 631-43.
267. O'Brien, K.M., E.L. Lindsay, and V.J. Starai, *The Legionella pneumophila effector protein, LegC7, alters yeast endosomal trafficking*. PLoS One, 2015. **10**(2): p. e0116824.
268. Shi, X., et al., *Direct targeting of membrane fusion by SNARE mimicry: Convergent evolution of Legionella effectors*. Proc Natl Acad Sci U S A, 2016. **113**(31): p. 8807-12.
269. Vaughn, B., et al., *An Indispensable Role for the MavE Effector of Legionella pneumophila in Lysosomal Evasion*. mBio, 2021. **12**(1).
270. Leseigneur, C., et al., *Emerging Evasion Mechanisms of Macrophage Defenses by Pathogenic Bacteria*. Frontiers in Cellular and Infection Microbiology, 2020. **10**(538).
271. Thomas, D.R., et al., *Interfering with Autophagy: The Opposing Strategies Deployed by Legionella pneumophila and Coxiella burnetii Effector Proteins*. Frontiers in Cellular and Infection Microbiology, 2020. **10**(685).
272. Kubelkova, K. and A. Macela, *Innate Immune Recognition: An Issue More Complex Than Expected*. Frontiers in Cellular and Infection Microbiology, 2019. **9**(241).

273. Leipheimer, J., A.L.M. Bloom, and J.C. Panepinto, *Protein Kinases at the Intersection of Translation and Virulence*. *Frontiers in Cellular and Infection Microbiology*, 2019. **9**(318).
274. Wang, X., et al., *The Shigella Type III Secretion Effector IpaH4.5 Targets NLRP3 to Activate Inflammasome Signaling*. *Frontiers in Cellular and Infection Microbiology*, 2020. **10**(523).
275. Copenhaver, A.M., et al., *Alveolar macrophages and neutrophils are the primary reservoirs for Legionella pneumophila and mediate cytosolic surveillance of type IV secretion*. *Infect Immun*, 2014. **82**(10): p. 4325-36.
276. de Felipe, K.S., et al., *Legionella eukaryotic-like type IV substrates interfere with organelle trafficking*. *PLoS Pathog*, 2008. **4**(8): p. e1000117.
277. Bennett, T.L., et al., *LegC3, an effector protein from Legionella pneumophila, inhibits homotypic yeast vacuole fusion in vivo and in vitro*. *PLoS One*, 2013. **8**(2): p. e56798.
278. Richards, A.M., et al., *Cellular microbiology and molecular ecology of Legionella-amoeba interaction*. *Virulence*, 2013. **4**(4): p. 307-14.
279. Chakravarty, S. and E. Massé, *RNA-Dependent Regulation of Virulence in Pathogenic Bacteria*. *Frontiers in Cellular and Infection Microbiology*, 2019. **9**(337).
280. Joshi, A.D. and M.S. Swanson, *Secrets of a successful pathogen: legionella resistance to progression along the autophagic pathway*. *Front Microbiol*, 2011. **2**: p. 138.
281. Dong, N., et al., *Modulation of membrane phosphoinositide dynamics by the phosphatidylinositide 4-kinase activity of the Legionella LepB effector*. *Nat Microbiol*, 2016. **2**: p. 16236.
282. Lopez de Armentia, M.M., C. Amaya, and M.I. Colombo, *Rab GTPases and the Autophagy Pathway: Bacterial Targets for a Suitable Biogenesis and Trafficking of Their Own Vacuoles*. *Cells*, 2016. **5**(1).
283. Lee, H.J., et al., *Formation and Maturation of the Phagosome: A Key Mechanism in Innate Immunity against Intracellular Bacterial Infection*. *Microorganisms*, 2020. **8**(9).
284. Omotade, T.O. and C.R. Roy, *Manipulation of Host Cell Organelles by Intracellular Pathogens*. *Microbiol Spectr*, 2019. **7**(2).
285. Swart, A.L. and H. Hilbi, *Phosphoinositides and the Fate of Legionella in Phagocytes*. *Front Immunol*, 2020. **11**: p. 25.
286. Ensminger, A.W., *Legionella pneumophila, armed to the hilt: justifying the largest arsenal of effectors in the bacterial world*. *Curr Opin Microbiol*, 2016. **29**: p. 74-80.
287. Younes, S., et al., *Drosophila as a Model Organism in Host-Pathogen Interaction Studies*. *Frontiers in Cellular and Infection Microbiology*, 2020. **10**(214).
288. Li, P., et al., *Legionella pneumophila Infection Rewires the Acanthamoeba castellanii Transcriptome, Highlighting a Class of Sirtuin Genes*. *Frontiers in Cellular and Infection Microbiology*, 2020. **10**(428).

289. Altschul, S.F., et al., *Basic local alignment search tool*. J Mol Biol, 1990. **215**(3): p. 403-10.
290. Mount, D.W., *Using the Basic Local Alignment Search Tool (BLAST)*. CSH Protoc, 2007. **2007**: p. pdb top17.
291. Campodonico, E.M., L. Chesnel, and C.R. Roy, *A yeast genetic system for the identification and characterization of substrate proteins transferred into host cells by the Legionella pneumophila Dot/Icm system*. Mol Microbiol, 2005. **56**(4): p. 918-33.
292. Campodonico, E.M., C.R. Roy, and S. Ninio, *Legionella pneumophila Type IV Effectors YlfA and YlfB Are SNARE-Like Proteins that Form Homo- and Heteromeric Complexes and Enhance the Efficiency of Vacuole Remodeling*. PLoS One, 2016. **11**(7): p. e0159698.
293. Bonifacino, J.S. and L.M. Traub, *Signals for sorting of transmembrane proteins to endosomes and lysosomes*. Annu Rev Biochem, 2003. **72**: p. 395-447.
294. Uhlik, M.T., et al., *Structural and evolutionary division of phosphotyrosine binding (PTB) domains*. J Mol Biol, 2005. **345**(1): p. 1-20.
295. Pandey, K.N., *Functional roles of short sequence motifs in the endocytosis of membrane receptors*. Front Biosci (Landmark Ed), 2009. **14**: p. 5339-60.
296. Ghosal, D., et al., *Molecular architecture, polar targeting and biogenesis of the Legionella Dot/Icm T4SS*. Nat Microbiol, 2019. **4**(7): p. 1173-1182.
297. Price, C.T., et al., *Host proteasomal degradation generates amino acids essential for intracellular bacterial growth*. Science, 2011. **334**(6062): p. 1553-7.
298. Habyarimana, F., et al., *Role for the Ankyrin eukaryotic-like genes of Legionella pneumophila in parasitism of protozoan hosts and human macrophages*. Environ Microbiol, 2008. **10**(6): p. 1460-74.
299. Belyi, Y., et al., *Legionella pneumophila glucosyltransferase inhibits host elongation factor 1A*. Proc Natl Acad Sci U S A, 2006. **103**(45): p. 16953-8.
300. Holm, L., *DALI and the persistence of protein shape*. Protein Sci, 2020. **29**(1): p. 128-140.
301. Rajashankar, K., et al., *Structure of the functional domain of the major grass-pollen allergen Phlp 5b*. Acta Crystallogr D Biol Crystallogr, 2002. **58**(Pt 7): p. 1175-81.
302. Pechstein, J., et al., *The Coxiella burnetii T4SS Effector AnkF Is Important for Intracellular Replication*. Frontiers in Cellular and Infection Microbiology, 2020. **10**(695).
303. Hayward, R.J., et al., *Early Transcriptional Landscapes of Chlamydia trachomatis-Infected Epithelial Cells at Single Cell Resolution*. Frontiers in Cellular and Infection Microbiology, 2019. **9**(392).
304. Kunz, T.C., et al., *Detection of Chlamydia Developmental Forms and Secreted Effectors by Expansion Microscopy*. Frontiers in Cellular and Infection Microbiology, 2019. **9**(276).

305. Lou, L., et al., *Salmonella Pathogenicity Island 1 (SPI-1) and Its Complex Regulatory Network*. *Frontiers in Cellular and Infection Microbiology*, 2019. **9**(270).
306. Schesser Bartra, S., et al., *Chromosomally-Encoded Yersinia pestis Type III Secretion Effector Proteins Promote Infection in Cells and in Mice*. *Frontiers in Cellular and Infection Microbiology*, 2019. **9**(23).
307. Monjarás Feria, J. and M.A. Valvano, *An Overview of Anti-Eukaryotic T6SS Effectors*. *Frontiers in Cellular and Infection Microbiology*, 2020. **10**(617).
308. Maurin, M., *Francisella tularensis, Tularemia and Serological Diagnosis*. *Frontiers in Cellular and Infection Microbiology*, 2020. **10**(646).
309. Kamanova, J., *Bordetella Type III Secretion Injectosome and Effector Proteins*. *Frontiers in Cellular and Infection Microbiology*, 2020. **10**(466).
310. Çakır, T., et al., *Novel Approaches for Systems Biology of Metabolism-Oriented Pathogen-Human Interactions: A Mini-Review*. *Frontiers in Cellular and Infection Microbiology*, 2020. **10**(52).
311. Augenstreich, J. and V. Briken, *Host Cell Targets of Released Lipid and Secreted Protein Effectors of Mycobacterium tuberculosis*. *Frontiers in Cellular and Infection Microbiology*, 2020. **10**(618).
312. Mohareer, K., et al., *Mycobacterial Control of Host Mitochondria: Bioenergetic and Metabolic Changes Shaping Cell Fate and Infection Outcome*. *Frontiers in Cellular and Infection Microbiology*, 2020. **10**(457).
313. Green, R.S., et al., *Ehrlichia chaffeensis EplA Interaction With Host Cell Protein Disulfide Isomerase Promotes Infection*. *Frontiers in Cellular and Infection Microbiology*, 2020. **10**(500).
314. Gan, J., et al., *The Salmonella Effector SseK3 Targets Small Rab GTPases*. *Frontiers in Cellular and Infection Microbiology*, 2020. **10**(419).
315. Saha, S., P. Das, and S. BoseDasgupta, *"It Takes Two to Tango": Role of Neglected Macrophage Manipulators Coronin 1 and Protein Kinase G in Mycobacterial Pathogenesis*. *Frontiers in Cellular and Infection Microbiology*, 2020. **10**(546).
316. Mambu, J., et al., *Rck of Salmonella Typhimurium Delays the Host Cell Cycle to Facilitate Bacterial Invasion*. *Frontiers in Cellular and Infection Microbiology*, 2020. **10**(656).
317. Curto, P., et al., *Macrophages Infected by a Pathogen and a Non-pathogen Spotted Fever Group Rickettsia Reveal Differential Reprogramming Signatures Early in Infection*. *Frontiers in Cellular and Infection Microbiology*, 2019. **9**(97).
318. Curto, P., et al., *A Pathogen and a Non-pathogen Spotted Fever Group Rickettsia Trigger Differential Proteome Signatures in Macrophages*. *Frontiers in Cellular and Infection Microbiology*, 2019. **9**(43).
319. Maurya, R.K., S. Bharti, and M.Y. Krishnan, *Triacylglycerols: Fuelling the Hibernating Mycobacterium tuberculosis*. *Frontiers in Cellular and Infection Microbiology*, 2019. **8**(450).

320. Del Portillo, P., et al., *Hypoxia Is Not a Main Stress When Mycobacterium tuberculosis Is in a Dormancy-Like Long-Chain Fatty Acid Environment*. *Frontiers in Cellular and Infection Microbiology*, 2019. **8**(449).
321. Snäkä, T. and N. Fasel, *Behind the Scenes: Nod-Like Receptor X1 Controls Inflammation and Metabolism*. *Frontiers in Cellular and Infection Microbiology*, 2020. **10**(767).
322. Sherwood, R.K. and C.R. Roy, *Autophagy Evasion and Endoplasmic Reticulum Subversion: The Yin and Yang of Legionella Intracellular Infection*. *Annu Rev Microbiol*, 2016. **70**: p. 413-33.
323. Arora, S.K., et al., *Mycobacterium smegmatis Bacteria Expressing Mycobacterium tuberculosis-Specific Rv1954A Induce Macrophage Activation and Modulate the Immune Response*. *Frontiers in Cellular and Infection Microbiology*, 2020. **10**(543).
324. Garg, R., et al., *Mycobacterium tuberculosis Calcium Pump CtpF Modulates the Autophagosome in an mTOR-Dependent Manner*. *Frontiers in Cellular and Infection Microbiology*, 2020. **10**(461).
325. Tilney, L.G., et al., *How the parasitic bacterium Legionella pneumophila modifies its phagosome and transforms it into rough ER: implications for conversion of plasma membrane to the ER membrane*. *J Cell Sci*, 2001. **114**(Pt 24): p. 4637-50.
326. Shames, S.R., et al., *Multiple Legionella pneumophila effector virulence phenotypes revealed through high-throughput analysis of targeted mutant libraries*. *Proc Natl Acad Sci U S A*, 2017. **114**(48): p. E10446-E10454.
327. Steiner, B., et al., *ER remodeling by the large GTPase atlastin promotes vacuolar growth of Legionella pneumophila*. *EMBO Rep*, 2017. **18**(10): p. 1817-1836.
328. Sain, N., G. Tiwari, and D. Mohanty, *Understanding the molecular basis of substrate binding specificity of PTB domains*. *Sci Rep*, 2016. **6**: p. 31418.
329. Legate, K.R. and R. Fassler, *Mechanisms that regulate adaptor binding to beta-integrin cytoplasmic tails*. *J Cell Sci*, 2009. **122**(Pt 2): p. 187-98.
330. Smith, M.J., et al., *Screening for PTB domain binding partners and ligand specificity using proteome-derived NPXY peptide arrays*. *Mol Cell Biol*, 2006. **26**(22): p. 8461-74.
331. Jin, J., et al., *Eukaryotic protein domains as functional units of cellular evolution*. *Sci Signal*, 2009. **2**(98): p. ra76.
332. Clarke, M., et al., *Genome of Acanthamoeba castellanii highlights extensive lateral gene transfer and early evolution of tyrosine kinase signaling*. *Genome Biol*, 2013. **14**(2): p. R11.
333. Gebbie, L., et al., *Phg2, a kinase involved in adhesion and focal site modeling in Dictyostelium*. *Mol Biol Cell*, 2004. **15**(8): p. 3915-25.
334. Blankenship, E., et al., *Conformational flexibility in the catalytic triad revealed by the high-resolution crystal structure of Streptomyces erythraeus trypsin in an unliganded state*. *Acta Crystallogr D Biol Crystallogr*, 2014. **70**(Pt 3): p. 833-40.
335. Ge, J. and F. Shao, *Manipulation of host vesicular trafficking and innate immune defence by Legionella Dot/Icm effectors*. *Cell Microbiol*, 2011. **13**(12): p. 1870-80.

336. Chen, D.Q., S.S. Huang, and Y.J. Lu, *Efficient transformation of Legionella pneumophila by high-voltage electroporation*. Microbiol Res, 2006. **161**(3): p. 246-51.
337. Al-Khodor, S., et al., *A Dot/Icm-translocated ankyrin protein of Legionella pneumophila is required for intracellular proliferation within human macrophages and protozoa*. Mol Microbiol, 2008. **70**(4): p. 908-23.
338. Price, C.T., et al., *Molecular mimicry by an F-box effector of Legionella pneumophila hijacks a conserved polyubiquitination machinery within macrophages and protozoa*. PLoS Pathog, 2009. **5**(12): p. e1000704.
339. Stone, B.J. and Y. Abu Kwaik, *Expression of multiple pili by Legionella pneumophila: identification and characterization of a type IV pilin gene and its role in adherence to mammalian and protozoan cells*. Infect Immun, 1998. **66**(4): p. 1768-75.
340. Mousnier, A., et al., *A new method to determine in vivo interactomes reveals binding of the Legionella pneumophila effector PieE to multiple rab GTPases*. mBio, 2014. **5**(4).
341. Habyarimana, F., et al., *Molecular characterization of the Dot/Icm-translocated AnkH and AnkJ eukaryotic-like effectors of Legionella pneumophila*. Infect Immun, 2010. **78**(3): p. 1123-34.
342. Al-Quadani, T., C.T. Price, and Y. Abu Kwaik, *Exploitation of evolutionarily conserved amoeba and mammalian processes by Legionella*. Trends Microbiol, 2012. **20**(6): p. 299-306.
343. Santic, M., et al., *Host-dependent trigger of caspases and apoptosis by Legionella pneumophila*. Infect Immun, 2007. **75**(6): p. 2903-13.
344. Meunier, E. and P. Broz, *Quantification of Cytosolic vs. Vacuolar Salmonella in Primary Macrophages by Differential Permeabilization*. J Vis Exp, 2015(101): p. e52960.
345. Krogh, A., et al., *Predicting transmembrane protein topology with a hidden Markov model: application to complete genomes*. J Mol Biol, 2001. **305**(3): p. 567-80.
346. Stols, L., et al., *A new vector for high-throughput, ligation-independent cloning encoding a tobacco etch virus protease cleavage site*. Protein Expr Purif, 2002. **25**(1): p. 8-15.
347. Voth, K.A., et al., *The structure of Legionella effector protein LpnE provides insights into its interaction with Oculocerebrorenal syndrome of Lowe (OCRL) protein*. FEBS J, 2019. **286**(4): p. 710-725.
348. Grochulski, P., et al., *Beamline 08ID-1, the prime beamline of the Canadian Macromolecular Crystallography Facility*. J Synchrotron Radiat, 2011. **18**(Pt 4): p. 681-4.
349. Kabsch, W., *Xds*. Acta Crystallogr D Biol Crystallogr, 2010. **66**(Pt 2): p. 125-32.
350. Adams, P.D., et al., *The Phenix software for automated determination of macromolecular structures*. Methods, 2011. **55**(1): p. 94-106.

351. Park, J.M., S. Ghosh, and T.J. O'Connor, *Combinatorial selection in amoebal hosts drives the evolution of the human pathogen Legionella pneumophila*. Nat Microbiol, 2020. **5**(4): p. 599-609.
352. Steinert, M., *Pathogen-host interactions in Dictyostelium, Legionella, Mycobacterium and other pathogens*. Semin Cell Dev Biol, 2011. **22**(1): p. 70-6.
353. Tladen, A., et al., *The Legionella pneumophila response regulator LqsR promotes host cell interactions as an element of the virulence regulatory network controlled by RpoS and LetA*. Cell Microbiol, 2007. **9**(12): p. 2903-20.
354. Edwin E. Jeng, V.B., Nnejiuwa U. Ibe, Haley Gause, Lihua Jiang, Joanne Chan, Ruiqi Jian, David Jimenez-Morales, Erica Stevenson, Nevan J. Krogan, Danielle L. Swaney, Michael P. Snyder, Shaeri Mukherjee, Michael C. Bassik,, *Systematic Identification of Host Cell Regulators of Legionella pneumophila Pathogenesis Using a Genome-wide CRISPR Screen*. Cell Host & Microbe, 2019. **26**(4): p. 551-563.e6.
355. Fan, J., et al., *Acyl-coenzyme A binding domain containing 3 (ACBD3; PAP7; GCP60): an emerging signaling molecule*. Prog Lipid Res, 2010. **49**(3): p. 218-34.
356. Yu, X.J., M. Liu, and D.W. Holden, *Salmonella Effectors SseF and SseG Interact with Mammalian Protein ACBD3 (GCP60) To Anchor Salmonella-Containing Vacuoles at the Golgi Network*. mBio, 2016. **7**(4).
357. Klima, M., et al., *Structural insights and in vitro reconstitution of membrane targeting and activation of human PI4KB by the ACBD3 protein*. Sci Rep, 2016. **6**: p. 23641.
358. Boura, E. and R. Nencka, *Phosphatidylinositol 4-kinases: Function, structure, and inhibition*. Exp Cell Res, 2015. **337**(2): p. 136-45.
359. Baumlova, A., et al., *The crystal structure of the phosphatidylinositol 4-kinase I α* . EMBO Rep, 2014. **15**(10): p. 1085-92.
360. Sbodio, J.I., et al., *Golgi protein ACBD3 mediates neurotoxicity associated with Huntington's disease*. Cell Rep, 2013. **4**(5): p. 890-7.
361. Clayton, E.L., S. Minogue, and M.G. Waugh, *Mammalian phosphatidylinositol 4-kinases as modulators of membrane trafficking and lipid signaling networks*. Prog Lipid Res, 2013. **52**(3): p. 294-304.
362. Weber, S.S., et al., *Legionella pneumophila exploits PI(4)P to anchor secreted effector proteins to the replicative vacuole*. PLoS Pathog, 2006. **2**(5): p. e46.
363. Shinoda, Y., et al., *Acyl-CoA binding domain containing 3 (ACBD3) recruits the protein phosphatase PPM1L to ER-Golgi membrane contact sites*. FEBS Lett, 2012. **586**(19): p. 3024-9.
364. Wang, J., et al., *Functions of Sphingolipids in Pathogenesis During Host-Pathogen Interactions*. Front Microbiol, 2021. **12**: p. 701041.
365. Kunz, T.C. and V. Kozjak-Pavlovic, *Diverse Facets of Sphingolipid Involvement in Bacterial Infections*. Front Cell Dev Biol, 2019. **7**: p. 203.
366. Rolando, M., P. Escoll, and C. Buchrieser, *Legionella pneumophila restrains autophagy by modulating the host's sphingolipid metabolism*. Autophagy, 2016. **12**(6): p. 1053-4.

367. Kim, D.I., et al., *An improved smaller biotin ligase for BioID proximity labeling*. Mol Biol Cell, 2016. **27**(8): p. 1188-96.
368. Wu, Y.J., et al., *Identification of significant protein markers by mass spectrometry after co-treatment of cells with different drugs: An in vitro survey platform*. Rapid Commun Mass Spectrom, 2020. **34 Suppl 1**: p. e8582.
369. Herb, M., et al., *Highly Efficient Transfection of Primary Macrophages with In Vitro Transcribed mRNA*. J Vis Exp, 2019(153).
370. Sohda, M., et al., *Identification and characterization of a novel Golgi protein, GCP60, that interacts with the integral membrane protein giantin*. J Biol Chem, 2001. **276**(48): p. 45298-306.
371. Rothman, J.E. and L. Orci, *Molecular dissection of the secretory pathway*. Nature, 1992. **355**(6359): p. 409-15.
372. Rothman, J.E., *Mechanisms of intracellular protein transport*. Nature, 1994. **372**(6501): p. 55-63.
373. Jahn, R. and T.C. Sudhof, *Membrane fusion and exocytosis*. Annu Rev Biochem, 1999. **68**: p. 863-911.
374. Kitao, T., et al., *Legionella Manipulates Non-canonical SNARE Pairing Using a Bacterial Deubiquitinase*. Cell Rep, 2020. **32**(10): p. 108107.
375. *Ap1b1 - AP-1 complex subunit beta-1 - Mus musculus (Mouse) - Ap1b1 gene & protein*. 4/13/2022]; Available from: <https://www.uniprot.org/uniprot/O35643>.
376. *Arfp2 - Arfaptin-2 - Mus musculus (Mouse) - Arfp2 gene & protein*. 2/23/2022; Available from: <https://www.uniprot.org/uniprot/Q8K221>.
377. Judith, D., et al., *ATG9A shapes the forming autophagosome through Arfaptin 2 and phosphatidylinositol 4-kinase IIIbeta*. J Cell Biol, 2019. **218**(5): p. 1634-1652.
378. Fus-Kujawa, A., et al., *An Overview of Methods and Tools for Transfection of Eukaryotic Cells in vitro*. Front Bioeng Biotechnol, 2021. **9**: p. 701031.
379. Roux, K.J., D.I. Kim, and B. Burke, *BioID: a screen for protein-protein interactions*. Curr Protoc Protein Sci, 2013. **74**: p. 19 23 1-19 23 14.
380. Kim, D.I., S.C. Jensen, and K.J. Roux, *Identifying Protein-Protein Associations at the Nuclear Envelope with BioID*. Methods Mol Biol, 2016. **1411**: p. 133-46.
381. Roux, K.J., et al., *BioID: A Screen for Protein-Protein Interactions*. Curr Protoc Protein Sci, 2018. **91**: p. 19 23 1-19 23 15.
382. Larsen, C.P., et al., *LDL Receptor-Related Protein 2 (Megalin) as a Target Antigen in Human Kidney Anti-Brush Border Antibody Disease*. J Am Soc Nephrol, 2018. **29**(2): p. 644-653.
383. Landers, V.D., et al., *The Alphaviral Capsid Protein Inhibits IRAK1-Dependent TLR Signaling*. Viruses, 2021. **13**(3).
384. Nesvizhskii, A.I., et al., *A statistical model for identifying proteins by tandem mass spectrometry*. Anal Chem, 2003. **75**(17): p. 4646-58.
385. Ashburner, M., et al., *Gene ontology: tool for the unification of biology. The Gene Ontology Consortium*. Nat Genet, 2000. **25**(1): p. 25-9.

386. Al-Quadani, T., C. Price, and Y. Abu Kwaik, *Exploitation of evolutionarily conserved amoeba and mammalian processes by Legionella*. Trends Microbiol, 2012. **20**: p. 299-306, DOI: 10.1016/j.tim.2012.03.005.
387. Voth, K.A., *Structural Biology of Legionella pneumophila Effectors*. Vol. 1. 2019, Saskatchewan, Canada: College of Graduate and Postdoctoral Studies University of Saskatchewan. 187.
388. Rajala, R.V. and M.D. Chan, *Identification of a NPXY motif in growth factor receptor-bound protein 14 (Grb14) and its interaction with the phosphotyrosine-binding (PTB) domain of IRS-1*. Biochemistry, 2005. **44**(22): p. 7929-35.
389. Matthews, H.R., *Protein kinases and phosphatases that act on histidine, lysine, or arginine residues in eukaryotic proteins: a possible regulator of the mitogen-activated protein kinase cascade*. Pharmacol Ther, 1995. **67**(3): p. 323-50.
390. Qiu, Z., et al., *A Novel Mutation in an NPXY Motif of beta Integrin Reveals Phenotypes Similar to him-4/hemicentin*. Front Cell Dev Biol, 2019. **7**: p. 247.
391. Ubersax, J.A. and J.E. Ferrell, Jr., *Mechanisms of specificity in protein phosphorylation*. Nat Rev Mol Cell Biol, 2007. **8**(7): p. 530-41.

CURRICULUM VITAE

Bethany L. Vaughn
bethany.vaughn@louisville.edu
u Underwood, IN
812-621-7108

EDUCATION

- 08/2002-05/2006 Honors High School Diploma, South Ripley Jr. Sr. High School, Versailles, IN
- 08/2006-05/2011 Bachelor of Arts in Biology with a concentration in Environmental Biology and a concentration in Organismic Biology, An Associate of Arts in Chemistry, and an Associate of Arts in Spanish, Thomas More College, Crestview Hills, KY.
- 08/2016-8/2018 M.S. in Microbiology and Immunology, University of Louisville, Louisville, KY
- 08/2018-5/2022 Ph.D. in Microbiology and Immunology, University of Louisville, Louisville, KY
Principal Investigator: Yousef Abu Kwaik

ACADEMIC APPOINTMENTS

- 08/2018-05/2022 Graduate Research Assistant, Department of Microbiology and Immunology, University of Louisville, Louisville, KY

OTHER POSITIONS AND EMPLOYMENT

- 07/2008-05/2011 Research Assistant, Thomas More Biology Field Station, California, KY
- 05/2012-01/2014 Office Manager for Geotechnical & Environmental Drilling Services
Hoosier Drilling Contractors, Inc. Madison, IN
- 02/2015-04/2018 Histotechnologist, Norton Healthcare/CPA Lab, Louisville, KY
- 08/2017-Present Pathology Assistant, Pediatrics and Perinatal Pathology Associates,
Louisville, KY

BOARD CERTIFICATIONS

- 2016-Present ASCP Certified Histotechnologist (HTL)

PROFESSIONAL MEMBERSHIPS

| | |
|--------------|--|
| 2009-2011 | Member of Tri Beta, Biological Honor Society |
| 2015-Present | Member of the Kentucky Society for Histotechnology |
| 2015-2017 | Member of the National Society of Histotechnology |
| 2018-Present | Member of the Kentucky Academy of Science |
| 2016-Present | Microbiology and Immunology Student Organization |

LABORATORY INSTRUMENTAL EXPERIENCE

| | |
|--------------|---|
| 2007-2011 | Inductively Coupled Plasma Atomic Emission Spectrometry (ICPAES), Electrofishing, Seining |
| 2009-2011 | Gas Chromatography (GC), Infrared Spectrometry (IR), Nuclear Magnetic Resonance (NMR), High Pressure Liquid Chromatography (HPLC), Citric Voltammetry (CV), and Gas Chromatography Mass Spectrometry (GCMS) |
| 2015-2018 | Leica Bond III (Immunohistochemistry), Dako Artisan (Histochemical Special Stains) |
| 2016-Present | Confocal Microscopy, Transmission Electron Microscopy (TEM) |

HONORS AND AWARDS

| | |
|-----------|---|
| 2010-2011 | Dean's List, Thomas More College, Crestview Hills, KY |
| 2022 | Graduate Dean's Citation, Microbiology & Immunology, University of Louisville, Louisville, KY |

COMMITTEE ASSIGNMENTS AND ADMINISTRATIVE SERVICES

| | |
|-----------|---|
| 2010-2011 | President of Tri Beta, Thomas More College, Crestview Hills, KY |
|-----------|---|

EDUCATIONAL ACTIVITIES

LECTURES/PRIMARY INSTRUCTION

| | |
|-----------|---|
| 2008-2011 | Instructor for Chemistry and Biology in Tutoring Center, Thomas More College, Crestview Hills, KY |
| 2010 | Thomas More College STEM summer institute instructor |

OUTREACH

| | |
|----------------|---|
| 2006-2007 | Big Brother/Big Sister Program Thomas More College, Crestview Hills, KY |
| 2009-2011 | Newport Aquarium Husbandry Department Volunteer, Newport, KY |
| 2010 | Cincinnati Regional Science and Engineering Fair Judge, Crestview Hills, KY |
| 2009,2010,2011 | Habitat for Humanity, Eastern KY & Fort Lauderdale, FL |

ABSTRACTS AND PRESENTATIONS

POSTERS

1. **Vaughn, Bethany**, Wetzel, William C. (2009) Analysis of Hair by Inductively Coupled Plasma-Atomic Emission Spectrometry *Federation of Analytical Chemistry & Spectroscopy Societies (FACSS) Annual Conference*. Louisville, KY
2. **Vaughn, Bethany**, Wetzel, William C. (2010) Analysis of Hair by Inductively Coupled Plasma-Atomic Emission Spectrometry, *Beta Beta Beta Biological Honor Society/Southern Association of Biologists Annual Conference*. Raleigh, NC
3. **Vaughn, Bethany**, Wetzel, William C. (2010) Analysis of Hair by Inductively Coupled Plasma-Atomic Emission Spectrometry, *Thomas More College Research Consortium*, Crestview Hills, KY

ABSTRACTS

1. **Vaughn, Bethany**, Wetzel, William C. (2009) Analysis of Hair by Inductively Coupled Plasma-Atomic Emission Spectrometry, Thomas More College, Crestview Hills, KY.

PUBLICATIONS

PEER-REVIEWED

1. ***Vaughn B**, Voth K, Price CT, Jones S, Ozanic M, Santic M, Cygler M, Abu Kwaik Y. An Indispensable Role for the MavE Effector of *Legionella pneumophila* in Lysosomal Evasion. *mBio*. 2021 Feb 9;12(1):e03458-20. doi: 10.1128/mBio.03458-20. PMID: 33563829; PMCID: PMC7885109.
2. **Vaughn B**, Abu Kwaik Y. Idiosyncratic Biogenesis of Intracellular Pathogens-Containing Vacuoles. *Front Cell Infect Microbiol*. 2021 Nov 11;11:722433. doi: 10.3389/fcimb.2021.722433. PMID: 34858868; PMCID: PMC8632064.

*Editor's Pick, Microbial Pathogenesis Research Article

TRAININGS

Biosafety Training, Radiation Safety, Formaldehyde Training, Process of Fixation and the Nature of Fixatives, Tissue Identification, Recombinant DNA Guidelines, HIPPA (Health Insurance Portability and Accountability Act), Blood-Borne Pathogen Training, Biohazard and Laboratory Safety Training